İSTANBUL TECHNICAL UNIVERSITY ★ INSTITUTE OF SCIENCE AND TECHNOLOGY

EFFECT OF DIESEL COMBUSTION PROCESS TO VEHICLE INTERIOR SOUND QUALITY

M.Sc. Thesis by

Caner SEVGİNER, B.Sc.

Department : Mechanical Engineering

Programme: Automotive Engineering

JUNE 2007

İSTANBUL TECHNICAL UNIVERSITY ★ INSTITUTE OF SCIENCE AND TECHNOLOGY

EFFECT OF DIESEL COMBUSTION PROCESS TO VEHICLE INTERIOR SOUND QUALITY

M.Sc. Thesis by

Caner SEVGİNER, B.Sc.

(503031005)

Date of submission : 7 May 2007

Date of defence examination: 13 June 2007

Supervisor (Chairman): Prof. Dr. Ahmet GÜNEY

Members of the Examining Committee Prof.Dr. Murat EREKE (İ.T.Ü.)

Prof.Dr. Orhan DENİZ (Y.T.Ü.)

JUNE 2007

İSTANBUL TEKNİK ÜNİVERSİTESİ ★ FEN BİLİMLERİ ENSTİTÜSÜ

DİZEL YANMA PROSESİNİN ARAÇ İÇİ SES KALİTESİNE ETKİSİ

YÜKSEK LİSANS TEZİ

Mak. Müh. Caner SEVGİNER
(503031005)

Tezin Enstitüye Verildiği Tarih : 7 Mayıs 2007
Tezin Savunulduğu Tarih : 13 Haziran 2007

Tez Danışmanı : Prof.Dr. Ahmet GÜNEY
Diğer Jüri Üyeleri Prof.Dr. Murat EREKE (İ.T.Ü.)
Prof.Dr. Orhan DENİZ (Y.T.Ü.)

HAZİRAN 2007

ACKNOWLEDGEMENT

I would like to express my gratitude to all those who gave me the possibility to complete this thesis. I am deeply indebted to my advisor Professor Ahmet GÜNEY for his guidance during all phases of this study.

I would also like to thank all my friends and colleagues for their help and support. I have furthermore to thank Ford OTOSAN NVH team for supporting me with brilliant ideas and M. Yedikel for his eagerness and stimulating support.

I wish to say many thanks to my family, my brother and my friends for all their patience and encouragement at every phase of my studies. Especially, I would like to give my special thanks to Hülya who was always beside me in difficult times along the way.

May 2007 Caner Sevginer

TABLE OF CONTENTS

ACRONYMS

NVH	: Noise Vibration and Harshness
ADC	: Analog to Digital Converter
FFT	: Fast Fourier Transform
FIR	: Finite Impulse Response
IIR	: Infinite Impulse Response
DFT	: Discrete Fourier Transform
SI	: Standard International
ERB	: Equivalent Rectangular Bandwidths
DC	: Direct Current
RMS	: Root Mean Square
EGR	: Exhaust Gas Recirculation
TDC	: Top Dead Center
BMEP	: Brake Mean Effective Pressure
WOT	: Wide Open Throttle
ECU	: Engine Control Unit
SPL	: Sound Pressure Level
EO	: Engine Order
BP	: Band-Pass
LP	: Low-Pass
CA	: Crankshaft Angle
ISVR	: Institue of Sound and Vibration Research
B&K	: Bruel & Kjaer

LIST OF TABLES

LIST OF FIGURES

Page No

LIST OF SYMBOLS

α	: Scaling factor
B	: One-sided baseband bandwidth
cal	: Calibration factor of roughness
$CWT_S(t,\alpha)$	: Wavelet transform
Δf	: Frequency bandwidth
ΔL	: Perceived masking depth
Δt	: Time segment
f	: Frequency
f_c	: Center frequency
f_l	: Lower frequency limit
f_{mod}	: Modulation frequency
f_s	: Sampling rate
f_u	: Upper frequency limit
K_N	: Scaling factors of different sharpness scales
m_i^*	: Modulation depth
N	: Specific loudness
$p(\alpha)$	: Cylinder pressure function in crankshaft angle domain
$p(\omega)$	: Cylinder pressure spectrum function
S	: Sharpness
S_i	: Spectral lines
tu	: Tonality unit
x(t)	: Continous time signal
X(T)	: Continous fourier transform of a signal
ω	: Wavelength
W_A	: A-Weighting function
z	: Critical bands in Bark scale

EFFECT OF DIESEL COMBUSTION PROCESS

TO VEHICLE INTERIOR SOUND QUALITY

SUMMARY

This study aims to identify the impulsiveness due to diesel combustion process and its effect over interior sound quality. Importance of choosing the best analysis method is presented with a case study in a five cylinder engine. Further studies were focused on using frequency modulation analysis more comprehensive to determine the root cause of the issue. For this purpose, a basic engine model is developed with Simulink and a simple design of experiment has been performed by manipulating the excitation parameters of each cylinder. In the following sections, the findings of artificial sound generation study has been correlated with the measurement of cylinder pressures simultaneously with a near-field microphone.

First step of the studies emphasize the frequency modulation analysis as the most proper method for discriminating impulsive content in a sound. Other metrics fail to differentiate subjective differences between good and bad diesel impulsiveness.

Second step, covers the sound generation study, which utilizes the frequency modulation analysis for determining the error state in the engine. The Simulink model used in this study contains five impulse signal generators, in order to seperately introduce different parameter setups for each cylinder. The combustion pressures, combustion excitation spectrums and ignition delays are manipulated to find an identical frequency modulation analysis result with the real life measurements.

Final step includes the confirmation of previous step with the analysis of cylinder pressures and further examination of the acquired data. Briefly, the higher excitation of first cylinder is pointed out as the root cause. The relationship between combustion pressure spectrum and radiated noise is examined in details.

In this study, the opportunities with artificial sound generation is highlighted. The sound generation with an improved engine model will be a useful tool for engineers for checking possible error states in the noise source as it is in this case.

DİZEL YANMA PROSESİNİN

ARAÇ İÇİ SES KALİTESİNE ETKİSİ

ÖZET

Bu çalışmada dizel motorun kendine has yanma özelliklerinden kaynaklanan vuruntulu çalışma sesi ve bu sesin araç içi ses kalitesine etkisi incelenmiştir. Uygun analiz metodunu seçiminin taşıdığı önem, beş silindirli bir motorda yapılan örnek çalışmayla gösterilmiştir. Daha sonraki çalışmalarda frekans modülasyon analizi, sorunun ana sebebini bulmakta etkin bir şekilde kullanılmıştır. Bu amaçla, basit bir içten yanmalı motor modeli Simulink programı kullanılarak oluşturulmuş ve tahrik parametreleri değiştirilerek elde edilen sonuçlar irdelenmiştir. İlerleyen bölümlerde bu tip bir yapay ses üretiminden elde edilen sonuçların gerçek bir motordan silindir basıncı ile eşzamanlı yakın mesafe mikrofon kayıtları aracılığıyla korelasyonu sağlanmıştır.

Çalışmaların ilk ayağını frekans modülasyon analizinin bir ses içindeki belirli bir rutinde tekrarlayan bileşenlerin ayırdedilmesindeki başarısı ivurgulanmıştır. Kullanlan diğer metrikler iyi ile kötü dizel vuruntusu arasındaki farkı ortaya çıkarmakta başarısız olmaktadırlar.

Bir sonraki adımda ise yapay ses üretimi sayesinde frekans modülasyon analizinin yanma prosesindeki hata çeşidini ortaya çıkarması hedeflenmiştir. Bu amaçla, beş ayrı silindirin yerini alan sinyal üreteçleri farklı yanma parametrelerini oluşturabilmek için modele eklenmiştir. Yanma basınç seviyeleri, frekans spektrumu ve tutuşma gecikmelerinde farklı değerler kullanılarak gerçek hayattakine benzer bir diyagram elde edilmesi sağlanmıştır.

Son olarak modellenen beş silindirli motordan silindir basınçları ve yakın alan mikrofonları ile veri toplanmış ve bir önceki adımdaki sonuçların doğrulanması amaçlanmıştır. Özetle ilk silindirdeki yüksek basınç seviyesi ve farklı frekans spektrumunun sorunu ortaya çıkardığı görülmüştür.

Bu çalışmada yapay ses üretimi sayesinde ortaya çıkan fırsatlar gösterilmiştir. Daha gelişmiş bir model ile araştırmacıların olası hataları ortaya çıkarması mümkündür.

1. INTRODUCTION

Diesel engines are becoming the main preference of passenger car customers with its superior fuel economy and flexible drive provided by the high torque delivered even in relatively lower engine speeds. Recent technological development is focused on improving the significant common complaints as smell, smoke and noise emissions over the last two decades. Introduction of high pressure fuel injection, turbocharging and successful injection management led diesel engines to achieve legal targets and marketing demands for exhaust emissions; however the impulsive and rough character of diesel noise is still well behind the gasoline engine levels. Moreover, noise refinement is becoming essential not only for the passenger cars, but also for the commercial vehicles due to the extensive usage in urban areas and increasing in-vehicle working hours spent. For this reason, the challenge in front of the automotive industry is to reach satisfactory interior and exterior sound quality levels without any compromises from weight and cost perspectives. Consequently, instead of applying acoustic treatment on the noise transfer path, efforts are driven towards a decrease in the excitation from noise source, which includes the combustion process inside the chamber as well as all other mechanical noises in this case.

March et al. (2005b) classifies the key diesel engine associated Powertrain NVH issues as combustion noise, turbocharger related noises, transmission rattle, booming noise and contact vibration. Among these issues, mainly combustion noise reflects the distinct impulsive character of diesel engines. Efficient and robust sealing of body, optimisation of acoustic trim pack to attenuate problem frequency range and maximising the absorption material and shields inside and around the engine bay is proposed to have acceptable performance for interior and exterior noise (March et al., 2005a). However such actions will bring an additional cost with assembly and timing difficulties for the vehicle production line.

In current high speed direct injection diesel engines, time available after the top dead centre to complete the combustion is very short. Accordingly, use of high pressure injection systems is necessary to rapidly mix the fuel with air charge.

However, this high injection rate usually extends throughout the injection period. As a result, more fuel than needed to initiate ignition is injected into the combustion chamber between the start of ignition and start of fuel injection. At ignition, the fuel injected and intimately mixed with the air charge during the ignition delay burns almost instantaneously. The heat release during this process is so quickly that the cylinder pressure rises rapidly and this sudden pressure rise generates a harsh combustion knock. Introduction of pilot injection in direct injection diesel engines resulted in producing a gradual combustion pressure increase instead of this sudden rise (Russell and Haworth, 1985).

In June 1997, Bosch introduced the Common Rail Injection System for mass production of passenger car direct injection diesel engines. Thus, precise control over injection pressure, quantity and timing is availed for almost all operating conditions. Advantages of this system are shorter ignition delay of the main injection and reduction of rise and peaks in highest cylinder pressure achieved (Flaig et al. 1999). State of the art systems are able to perform two pilot and after injections at certain engine speeds. Various studies have been performed to optimise the quantity and timing of these injections for less noise and better sound quality without compromising from exhaust emissions and fuel economy. See for example Badami et al. (2002), Mallamo et al. (2002) and Russell et al. (2000).

Due to the more restricted legal noise emission limits and increasing sales of diesel powered vehicles, combustion noise of these engines has been widely investigated in recent years. On the other hand, application of traditional Fourier transforms had brought difficulties because of the poor resolution in both time and frequency domain at the same analysis segment. For this reason, studies focused on post-processing the signals by means of a time-frequency technique, named as the Wigner distribution or the wavelet transform (Desantes et al. 2001). Being located in both frequency and time domains brought various advantages, mainly providing information about the localization of the energy content. In summary, wavelet transform analysis offered a new approach to study combustion process, which has a short, impulsive and non-stationary nature (Villaroel and Agren, 1997).

Even though the legal limits don’t take the impulsive character of diesel combustion into account, increasing demands push manufacturers to introduce more refined vehicles to the market. Numerous studies have been performed to quantify the annoyance created by diesel engines in addition to the previous knowledge of disturbing mechanical noises in gasoline engines. These studies include correlation

of subjective evaluation to objective measurements, usually post-processed to represent psychoacoustic metrics (Hussain et al., 1991). In addition to the real world in-vehicle measurements, in some investigations, artificial recordings have been generated as well to decrease the test timing and also to rank the combustion noise parameters that affect the human perception most (Hastings, 2004). Champagne and Shiau (1997) includes the semantic differences between nations in their study to give a better direction for further developments. This study is a good indicator for showing how important it is to define an NVH problem.

The aim of this study is to define diesel combustion related noises in a commercial vehicle and present the effects to the interior sound quality. Furthermore, simultaneous cylinder pressure data and engine bay noise recordings have been acquired to exhibit the interactions between combustion chamber and the radiated noise. Finally, possible root causes and potential solutions are discussed in details.

2. FUNDAMENTALS OF ACOUSTIC SIGNAL PROCESSING

The acoustic engineers need to use proper signal processing techniques in order to understand the physics of a sound generating mechanism. Since the sound is not always a perfect continous periodic signal, it is necessary to observe changes in the time domain as well as the frequency domain. In this chapter, the basics of transition process between time and frequency domains will be summarised. In addition, advantages and disadvantages of different methods will be pointed out for investigation of diesel combustion noise phenomena.

2.1 Digital Signal Processing

Acoustic signals are usually digitized and studied in one of the following domains: time domain (one-dimensional signals), spatial domain (multidimensional signals), frequency domain, autocorrelation domain, and wavelet domains. The domain in which the signal to be processed and studied is chosen with the knowledge from previous experiences and education, or even by trying different possibilities. This choice should be best in representing the essential characteristics of the signal. For instance, a sequence of samples from a measuring device, which is usually microphones for acoustic signals, produces a time or spatial domain representation, whereas a discrete Fourier transform produces the frequency domain information.

2.1.1 Signal Sampling and Nyquist-Shannon Theorem

Sampling of a signal is usually carried out in two stages, discretization and quantization. In the discretization stage, the space of signals is divided into equivalence classes and discretization is carried out by replacing the signal with representative signal of the corresponding equivalence class. In case of acoustic signals, this represents the voltage as the microphone's input and sound pressure level as the output. In the quantization stage the representative signal values are approximated by values from a finite set (Pharr and Humphreys, 2004).

2.1.1.1. Nyquist-Shannon Theorem

To ensure that a sampled analog signal can be exactly reconstructed the Nyquist-Shannon sampling theorem must be satisfied (Nyquist, 1928). Shortly, the sampling frequency must be greater than twice the bandwidth of the signal. This concept can be formalized in equation (2.1). Let $x(t)$ represent a continuous-time signal and $X(f)$ be the continuous Fourier transform of that signal:

$$X(f) = \int_{-\infty}^{\infty} x(t).e^{-2\pi ift}.dt \quad \textbf{(2.1)}$$

The signal $x(t)$ is bandlimited to a one-sided baseband bandwidth B if:

$$X(f) = 0 \text{ for all } |f| > B \quad \textbf{(2.2)}$$

Then the condition for exact reconstructability from samples at a uniform sampling rate f_s (in samples per unit time) is**:**

$$f_s > 2B \quad \textbf{(2.3)}$$

or equivalently**:**

$$B < \frac{f_s}{2} \quad \textbf{(2.4)}$$

$2B$ is called the Nyquist rate and is a property of the bandlimited signal, while $f_s / 2$ is called the Nyquist frequency and is a property of this sampling system. Basically, the theorem states that

> ***"Exact reconstruction of a continuous-time based signal from its samples is possible if the signal is bandlimited and the sampling frequency is greater than twice the signal bandwidth***."

The schematic of an acoustic signal is shown in Figure 2.1. Since the audible range of human beings is between 20-20kHz the sampling rate for acoustic studies are usually above 40kHz, and the most used values are 44.1 kHz 48kHz.

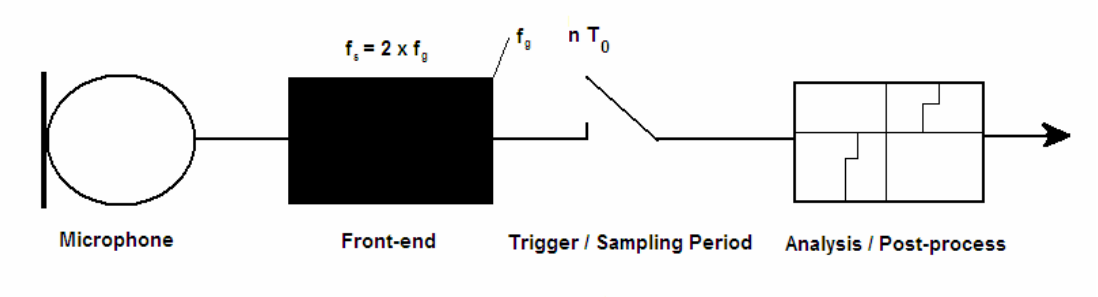

Figure 2.1 : Schematic view of an acoustic signal acquusition

2.1.1.2. Anti-aliasing

If Nyquist criterion is violated, a phenomenon known as aliasing occurs. Figure 2.2 shows a properly sampled signal and an undersampled signal. In the undersampled case, an aliased signal occurs, which appears to be at a lower frequency than the actual signal (Pharr and Humphreys, 2004).

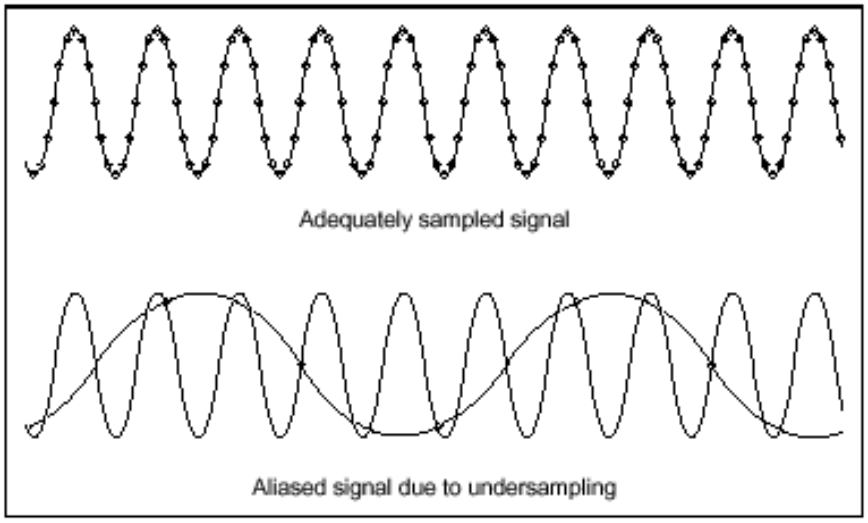

Figure 2.2 : Adequate and inadequate signal sampling

When the Nyquist criterion is violated, frequency components above half the sampling frequency appear as frequency components below half the sampling frequency, resulting in an erroneous representation of the signal. For example, a component at frequency greater than the nyquist frequency appears in the frequency equal to the difference between sampling rate and the real frequency of the component.

Figure 2.3 shows the alias frequencies that appear when the signal with real components at 25, 70, 160, and 510 Hz is sampled at 100 Hz. Alias frequencies of high frequency signals appear at 10, 30, and 40 Hz.

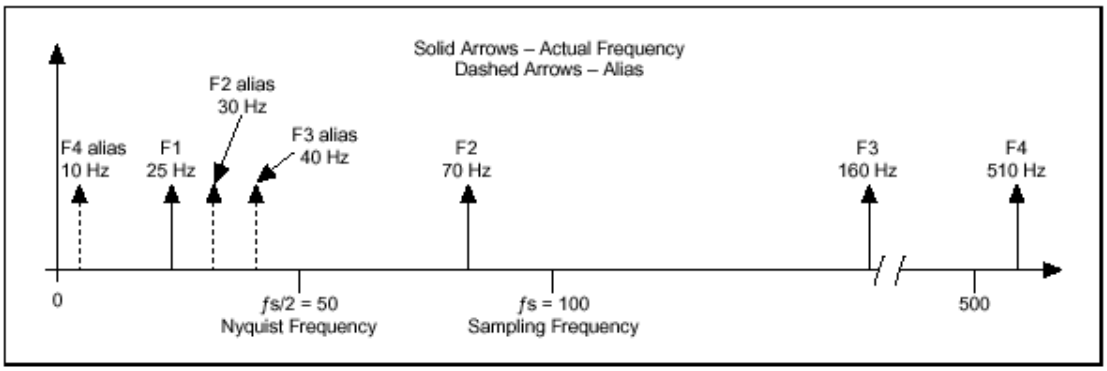

Figure 2.3 : Alias frequencies resulting from sampling a signal at 100 Hz containing frequency components greater than or equal to 50 Hz

Before a signal is digitized, aliasing can be prevented by using antialiasing filters to attenuate the frequency components at and above half the sampling frequency to a level below the dynamic range of the analog-to-digital converter (ADC). For instance, if the digital converter has a full-scale range of 80 dB, then the frequency components at and above half the sampling rate must be attenuated to 80 dB below of the full scale.

2.1.1.3. Windowing Functions

For high accuracy in spectral measurement, it is not sufficient to use proper signal acquisition techniques because of the spectral leakage. Spectral leakage is the result of an assumption in the FFT algorithm that the time record is exactly repeated throughout all time and that signals contained in a time record are thus periodic at intervals that correspond to the length of the time record. If the time record has a non-integral number of cycles, this assumption is violated and spectral leakage occurs.

In order to guarantee that an integral number of cycles are always acquired, two methods can be used. One case is to sample synchronously with respect to the signal that is being measure in order to take an integral number of cycles. Second method is to capture a transient signal that fits entirely into the time record. In most cases, however, the measured signal is unknown and it's a continuous event which means it is present before, during, and after the acquisition. Therefore it is not

possible to guarantee that an integral number of cycles is sampled. Spectral leakage distorts the measurement in such a way that energy from a given frequency component is spread over adjacent frequency lines or bins. In order to prevent this, windows are used to eliminate the effects of performing an FFT over a non-integral number of cycles. In Figure 2.4 an example of spectral leakage is shown. Spectral leakage can obscure adjacent frequency peaks. Using a Hanning window prevents leakages.

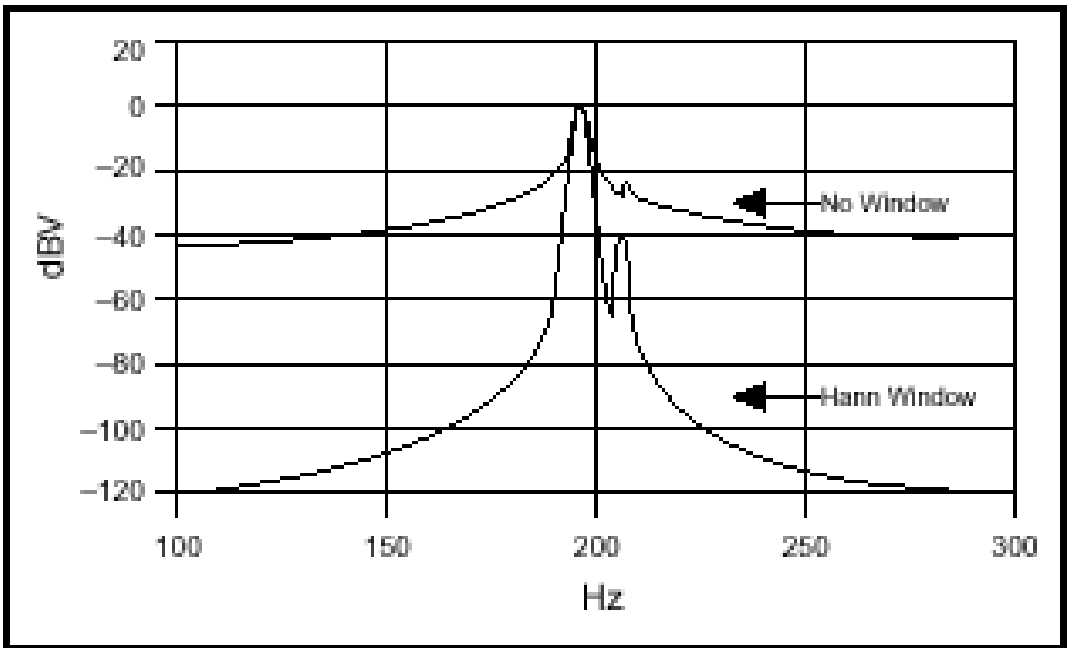

Figure 2.4 : Spectral leakage obscuring adjacent frequency components

Each window has its own characteristics, and different windows are used for different applications. In general, the Hanning window is satisfactory in 95% of cases. It has good frequency resolution and reduced spectral leakage. If transient signals such as impact and response signals are being investigated, it is better not to use the spectral windows since these windows can attenuate important information at the beginning of the sample block. The Exponential window is useful for analysing transient response signals because it damps the end of the signal, ensuring that the signal fully decays by the end of the sample block. Selecting a window function is not a simple task. Table 2.1 gives brief information about the most common windows and the applications that they are used for. Again, experience is the most important factor when choosing a proper window for the application.

Table 3.1 : Window Choices Based on Signal Content

Signal Content	Window
Sine wave or combination of sine waves	Hanning
Sine wave (amplitude accuracy is important)	Flat Top
Narrowband random signal (vibration data)	Hanning
Broadband random (white noise)	Uniform
Closely spaced sine waves	Uniform, Hamming
Excitation signals (Hammer blow)	Force
Response signals	Exponential
Unknown content	Hanning

2.1.2 Time and Space Domains

The most common processing approach in the time or space domain is enhancement of the input signal through a method called filtering. Filtering generally consists of some transformation of a number of surrounding samples around the current sample of the input or output signal. There are various ways to characterize filters; for example as linear filters, finite impulse response (FIR) filters or, infinite impulse response (IIR) filters, eg.

Most filters can be described in frequency domain by their transfer functions. A filter may also be described as a difference equation, a collection of zeroes and poles or, if it is an FIR filter, an impulse response or step response.

2.1.3 Frequency Domain

Fourier transform is usually used to convert signals from time or space domain to the frequency domain. The Fourier transform converts the signal information to a

magnitude and phase component for all frequency range. Sometimes, the Fourier transform is converted to the power spectrum, which is the magnitude of each frequency component squared. As a result the phase information is removed from the data, however the magnitude scale is more emphasized. This way, higher frequencies may better be emphasized (Wikipedia, 2006).

There are some commonly used frequency domain transformations. For example, the cepstrum is calculated by an inverse Fourier transform of the logarithmized DFT spectrum. The term cepstrum is an inversion of the word spectrum. Accordingly, the time axis resulting from the transformation of the frequency axis is called quefrency (inversion of frequency).This emphasizes the frequency components with smaller magnitude while retaining the order of magnitudes of frequency components. (Head Artemis Documentation, 2006)

2.2 Methods for Transformation between Time and Frequency Domains

Fourier transform is a certain linear operator that maps functions to other functions. Briefly, the Fourier transform decomposes a function into a continuous spectrum of its frequency components, and the inverse transform synthesizes a function from its spectrum of frequency components. An example can be the relationship between a series of pure notes representing the frequency components and a musical chord representing the function itself (Wikipedia, 2006).

2.2.1 Fourier Transform

Suppose x(t) is a complex-valued Lebesgue integrable function. The Fourier transform to the frequency domain, ω, is given by the function:

$$X(w) = \frac{1}{\sqrt{2\pi}} \int_{-\infty}^{\infty} x(t) e^{-iwt} dt \qquad \textbf{(2.5)}$$

When the independent variable t represents time (with SI unit of seconds), the transform variable ω represents angular frequency (in radians per second).

However, when the subsutition of wavelength and frequency in equation 2.6 is performed, the equation becomes equation 2.7:

$$w = 2\pi f \tag{2.6}$$

$$X(f) = \int_{-\infty}^{\infty} x(t) e^{-i 2\pi f t} \, dt \tag{2.7}$$

and the inverse transform is:

$$x(t) = \int_{-\infty}^{\infty} X(f) e^{i 2\pi f t} \, df \tag{2.8}$$

As a result, the signal in time domain can be expressed with respect to frequency (Wikipedia, 2006).

2.2.1.1. Fast Fourier Transform and Power Spectrum

The Fast Fourier Transform (FFT) and the power spectrum are the most preferred tools for converting signals from time to frequency domain. The basic functions for FFT-based signal analysis are the FFT, the Power Spectrum, and the Cross Power Spectrum. Using these functions as building blocks, additional algorythms to rank and compare different sounds is possible. By having the frequency spectrum of a noise other functions can be derived, such as frequency response, impulse response, coherence, amplitude spectrum, and phase spectrum. Moreover, weighting functions or sound quality metrics are all based on the frequency spectra. In summary, frequency spectrum of a noise should be determined in order to supply desired information about the character of a sound.

FFTs and the Power Spectrum are useful for measuring the frequency content of stationary or transient signals. FFTs produce the average frequency content of a signal over the entire time that the signal was acquired. For this reason, FFTs should be used for stationary signal analysis or in cases where only the average energy at each frequency line is needed.

The Fast Fourier Transform (FFT) is an efficient algorithm to compute the discrete Fourier transform (DFT) and its inverse. Let x_0, ..., x_{N-1} be complex numbers. The DFT is defined by the formula (2.9):

$$X_k = \sum_{n=0}^{N-1} x_n e^{-\frac{2\pi i}{N} n} k \quad \text{where} \quad k = 0,\ldots,N-1. \qquad \textbf{(2.9)}$$

Evaluating these sums directly would take N^2 arithmetical operations. On the other hand, an FFT is an algorithm to compute the same result in only N. log N operations. In general, such algorithms depend upon the factorization of N, but (contrary to popular misconception) there are N x log N FFTs for all N.

2.2.1.2. Power Spectrum Density

The power spectrum returns an array that contains the two-sided power spectrum of a time-domain signal. The array values are proportional to the amplitude squared of each frequency component making up the time-domain signal. (Wikipedia, 2006).

Because of noise-level scaling with Δf, spectra for noise measurement are often displayed in a normalized format called power or amplitude spectral density. The power or amplitude spectrum is normalised in this way to the spectrum that would be measured by a 1 Hz-wide square filter, a convention for noise-level measurements. The level at each frequency line then reads as if it were measured through a 1 Hz filter centered at that frequency line.

The spectral density format is appropriate for random or noise signals but inappropriate for discrete frequency components, because the latter theoretically have zero bandwidth (Randall and Tech, 1979).

2.2.2 Wavelet Analysis

Wavelet analysis is particularly advantageous when investigating short, transient signals, for instance, a few stroke cycles of a combustion engine. Transient means that the signal is characterized by rapid, non-periodic changes.

In wavelet analysis, in comparison to a comparable analysis of FFT over a time period, frequency resolution is better at low frequencies and time resolution is better at higher frequencies. For this reason, wavelet analysis results are on the whole more accurate and tell us more than results from a comparable FFT analysis.

Wavelet transform is achieved from a large number of bandpass filters (as in 1/n octave filters), which cover the band under analysis. The particularity of this

transform is that the bandwidth Δf of these filters is in proportion to their center frequency f .

The wavelet transform can be thought of as a filter bank analysis. The filter bank consists of bandpass filters of constant relative bandwidth (Constant Q analysis), i.e. filter bandwidth is a function of center frequency.

In the case of logarithmic scaling, the transfer functions are at equal intervals. The wavelet transform is a simplification of Constant Q analysis: all impulse responses of the filter bank are defined as scaled and are expanded or compressed versions of the same prototype $h(t)$:

$$h_\alpha(t) = \frac{1}{\sqrt{|\alpha|}} h\left(\frac{t}{\alpha}\right) \qquad \textbf{(2.10)}$$

where α is the scaling factor. The constant $1/\sqrt{\alpha}$ is applied for normalization of energy. This results in the definition of the wavelet transform which is applied to the signal $s(t)$:

$$CWT_s(t,\alpha) = \int s(\tau) h_\alpha^*(\tau - t) d\tau = s(t) \times h_\alpha^*(-t) = s(t) \times \tilde{h}_\alpha(t) \qquad \textbf{(2.11)}$$

The prototype $h(t)$ is designated basis wavelet. The principle applies to any bandpass function $h(t)$ (Rioul and Vetterli, 1991).

2.2.3 Comparison of FFT and Wavelet

Ahead of FFT analysis, the time signal is subdivided into n time segments of length $\Delta t = n/f_S$ (f_S = sampling frequency). An FFT analysis is then calculated for each time signal segment. So increasing the quantity of n for a constant period of time will lead to examination of larger time segments in the analysis, resulting in poor time resolution. On the other hand, decreasing the quantity of n will bring higher time resolution. But this time, it will lead to larger frequency bandwidths to be summed up together which makes harder to focus on a particular narrow band issue. For this reason, usage of FFT for analysing a signal is limited either with frequency or time resolution.

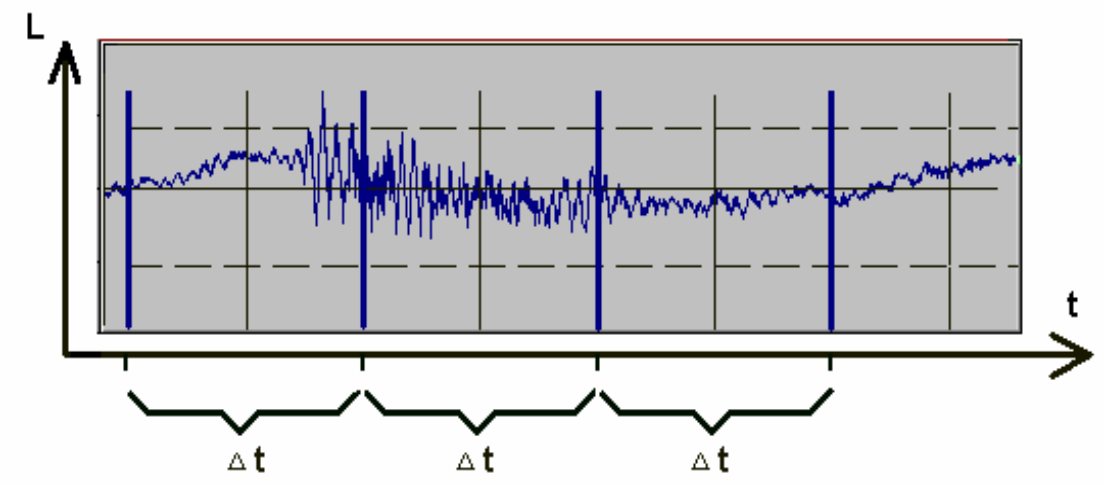

Figure 2.5 : Example of a time signal which is divided into three Δt segments

For example, for a data set having 48 kHz sampling rate, an FFT analysis with a spectrum size of 8192 will result in a frequency resolution of 5,859375 Hz and a time resolution of 0.1706 seconds. As the spectrum size increases, a better frequency resolution is achieved. However increasing time steps degrade the time resolution of the analysis. These limitations are surpassed with the wavelet analysis since it is a windowing technique with variable-sized regions. Figure 2.6 shows the windowing difference between wavelet spectrum and FFTs with large and small spectrum size.

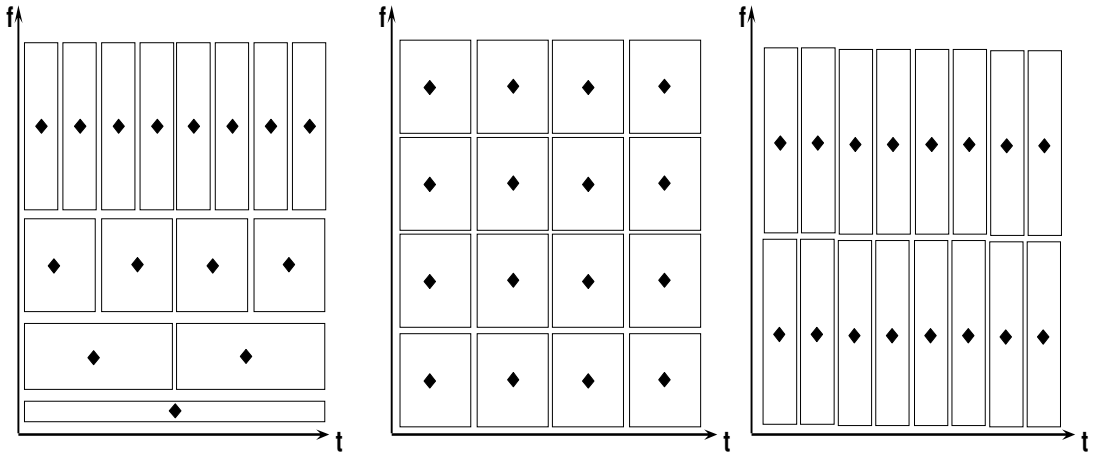

Figure 2.6 : Scheme of windowing methods of wavelet(a), FFT with a small spectrum size (b) and FFT with a large spectrum size (c).

Figure 2.7 shows the diagrams of same sound sample with three different analyses. The event consists of repeating excitations for all frequency range between 2nd and 3rd seconds. Afterwards, a tonal component is present in the data at 250 Hz. Lower

FFT spectrum size results in a very high time resolution, each excitation can be separated from the others in time domain. However the exact frequency of the repeated excitations and the tonal noise are not displayed very well. On the other hand with a higher spectrum size, it is possible to detect the 250Hz tonal component with high accuracy. But, Wavelet transform is able to reach the desired time and frequency resolution within the same analysis.

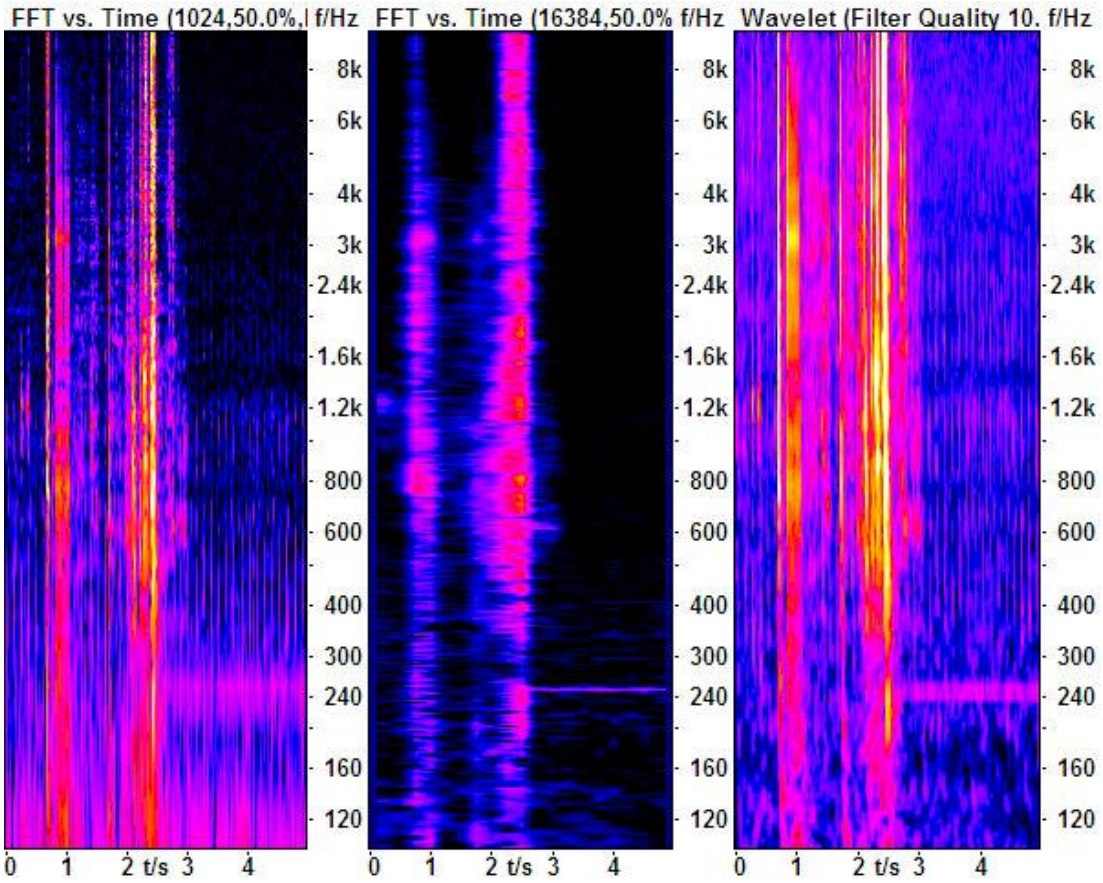

Figure 2.7 : A transient signal analysed with three different methods. FFT with 1k spectrum size, FFT with 16k spectrum size and wavelet function.

2.3 Ranking Sounds According to Human Perception: Psychoacoustics

The area of human hearing and human perception of sound is investigated under the branch Psychoacoustics. Due to the complicated structure of human hearing system, it is not sufficient to quantify the complete character of a sound by only its dynamic pressure levels. Often, the perception is affected by the frequency, bandwidth, period and the modulation of the noise. Therefore, many different frequency scales and sound quality metrics are introduced for quantifying sounds with different characteristics (Zwicker and Fastl, 1999).

Engineering acoustics, as previously mentioned, deals with a variety of areas of application, such as infra sound, ultra sound, underwater acoustics and etc. However, in the acoustical design of the environments or equipments, which are directly intended to the use of humans, the important parameter is the way human ear hears. When dealing with subjective perception of acoustics and also acoustic signal processing, it is essential to have knowledge on how ears hear.

2.3.1 Basic Auditory Process

The hearing system performs a spectrographic analysis of any auditory stimulus. The cochlea can be regarded as a bank of filters. The filters closest to the cochlear base respond maximally to the highest frequencies and those closest to its apex respond maximally to the lowest.

In order to understand the perception of pitch, it is also necessary to consider the facts that are given by the harmonic structure of many sounds, such as the voiced sounds of speech (Pickles, 1988). We learn early in our lives where the partials of such sounds are to be expected, since we are exposed predominantly to harmonic sounds already in utero. This knowledge enables us to judge musical pitch intervals, and it explains why the fundamental pitch of a harmonic sound is not necessarily altered when the lowest partial is removed.

The perceived pitch of a sinusoidal tone is not strictly given by its frequency, but it is also marginally influenced by its intensity level: An increase in level produces a slightly more extreme sensation of pitch.

2.3.2 Frequency Scales

It is often convenient to measure just frequencies when pitch perception is studied. Thus, the pitch of a sound may be specified by the frequency of a pure tone whose pitch is judged to be the same as the pitch of that sound, but auditory scales of frequency representation are required in models of auditory perception. In order to scale sounds according to the human perception, frequency spectrum is divided into bands such as octaves and bark scale.

2.3.2.1. Octave and 1/3 Octave Band Filters

In octave band analysis, each band covers a specific range of frequencies while excluding the other. In $1/n^{th}$ octave band analysis, the defining parameters are the

upper, lower and the centre frequencies of each band. The relation between these parameters is shown in equation 2.12, 2.13 and 2.14 (Randall and Tech, 1987).

$$f_c = \sqrt{f_l . f_u} \quad \textbf{(2.12)}$$

$$f_u = 2^{\frac{1}{n}} . f_l \quad \textbf{(2.13)}$$

where, n defines the octave band interval of interest.

$$\Delta f = f_u - f_l \quad \textbf{(2.14)}$$

Third octave bands are a useful approximation to critical bands for mid to high frequencies. The human auditory system consists of a whole series of critical bands, each filtering out a specific portion of the audio spectrum. Which sounds are audible, and which are masked (hidden) by other sounds can be better understood by working with critical bands. For this reason, many sound quality metrics begin by putting the measured spectrum into critical bandwidths. In the low frequency range third octave bands are grouped together to give an approximation to critical bandwidths. Equations below and table 2.2 give an understanding about how the frequency bandwidths change for the 1 octave scale and 1/3rd octave scale.

Octave Bandwidth:

$$f_c = \sqrt{2} f_l \quad \textbf{(2.15a)}$$

$$f_u = 2 f_l \quad \textbf{(2.16a)}$$

$$\Delta f = f_u - f_l = f_l = f_c / \sqrt{2} \quad \textbf{(2.17a)}$$

Third-octave Bandwidth:

$$f_c = \sqrt[6]{2} f_l = 1.12 f_l \quad \textbf{(2.15b)}$$

$$f_u = \sqrt[3]{2} f_l = 1.26 f_l \quad \textbf{(2.16b)}$$

$$\Delta f = 0.26 f_l \qquad \textbf{(2.17b)}$$

Table 3.2 : Center Frequencies and Bandwidths for the Preferred Octave and 1/3 Octave Bands.

Center Frequency (Hz)		10 log (Bandwidth)	
Octave	1/3 Octave	Octave	1/3 Octave
16	10	10,5	3,6
	12,5		4,6
	16		5,7
	20		6,6
31,5	25	13,4	7,6
	31,5		8,6
	40		9,7
63	50	16,5	10,6
	63		11,6
	80		12,7
125	100	19,5	13,6
	125		14,6
	160		15,7
250	200	22,5	16,7
	250		17,6
	315		18,6
500	400	25,5	19,7
	500		20,6
	630		21,6
1000	800	28,5	22,7
	1000		23,6
	1250		24,6
2000	1600	31,5	25,7
	2000		26,7
	2500		27,6
4000	3150	34,5	28,6
	4000		29,7
	5000		30,6
8000	6300	37,5	31,6
	8000		32,7

2.3.2.2. Bark Scale

In psychoacoustics the bark scale is often used instead of octave scale to quantify frequency (for example when calculating loudness). This quantity is based on critical bandwidths and is therefore a subjective representation of frequency; a better representation than the frequency in Hertz. Though it may not be an exact representation of exactly what happens in the ear. Indeed, there are other methods which model the frequency scaling of the auditory system e.g. Equivalent

Rectangular Bandwidths (ERBs). However, it is widely accepted that the bark scale is a useful starting point when trying to model how an individual may perceive a sound.

A formula for converting frequency values, f (in Hz) into bark values, z (in Bark) is given in equation 2.18 (Zwicker and Fastl, 1999):

$$z = 13\tan^{-1}\left(\frac{0.76f}{1000}\right) + 3.5\tan^{-1}\left(\frac{f}{7500}\right)^2 \quad \textbf{(2.18)}$$

Aures (1984) defines inverse conversion from bark scale to frequency scale is shown in equation 2.19:

$$f = \left(2{,}841 * e^{0.219z} + 100\right) * z - 32 * e^{-0.15*(5-z)^2} \quad \textbf{(2.19)}$$

2.3.3 Weighting Functions and Psychoacoustic Metrics

Since the human perception is frequency dependant, sounds in daily life are also quantified according to their frequency contents. For this reason, there are a large number of metrics and weighting functions, some of which are well defined and others which are not. Very few have been standardized and the usefulness of a particular metric is dependant on the nature of the sound being tested. In general, the weighting functions are used for legal restrictions to define the threshold of a noise source acting in a rural area such as pass-by noise of a road vehicle or turbine noise of an aircraft.

Manufacturers who undertake sound quality testing involving the use of sound quality metrics often develop their own metrics (the definitions of which are often not generally available), as well as making use of more well known ones. The choice of which sound quality metrics to apply is specific to individual appliance. Individual metrics do not give an indication of the sound quality as a whole and indeed for many appliances no metrics may currently exist to adequately quantify the subjective impression.

The standardized weighting functions and widely used sound quality metrics such as loudness, sharpness, tonality, roughness and fluctuation strength will be briefly explained in sub-sections.

2.3.3.1. Weighting Functions

Weighting networks have been introduced in acoustic signal processing in order to conduct correct evaluation of the measured data. This enables engineers to correctly determine the existence of a noise problem, or to achieve realistic noise development in many areas of application.

In acoustic signal processing, several weighting networks have been defined based on the sensitivity of human ear in different frequencies and sound intensity levels. The use of one of the weighting networks labelled as A, B, C and D depends on the place of the noise of interest in ear sensitivity map. The weighting filters, in other words, have certain attenuation levels, which are approximated based on the frequency response of human ear. Choice of a weighting filter strongly depends on the area of application. In vehicle NVH development, A and B weighting are the most commonly used filters; however, in applications where high noise levels are subject to consideration, such as air craft jet engine noise, C and D weighting filters are used.

A-weighting is the most widely used metric of environmental noise and it is expressed as dB(A) (Kinsler,1982). The attenuation character of the A-weighting filters is based on the fact that human ear is not as sensitive to low frequencies as it is to relatively high frequencies. 1 kHz is the reference value in all filters and does not apply any reduction to the sound of interest. The A-weighting curve follows the 40 phon equal loudness curve. Equal-loudness contours were first measured by Fletcher and Munson using headphones (1933). In their study, listeners were presented with pure tones at various frequencies and over 10 dB increments in stimulus intensity. For each frequency and intensity, the listener was also presented with a reference tone at 1000 Hz. The reference tone was adjusted until it was perceived to be of the same loudness as the test tone. Loudness, being a psychological quantity, is difficult to measure, so Fletcher and Munson averaged their results over many test subjects to derive reasonable averages. Plot showing the standardized ISO226:1993 and Fletcher-Munson equal loudness contours is presented in Figure 2.8.

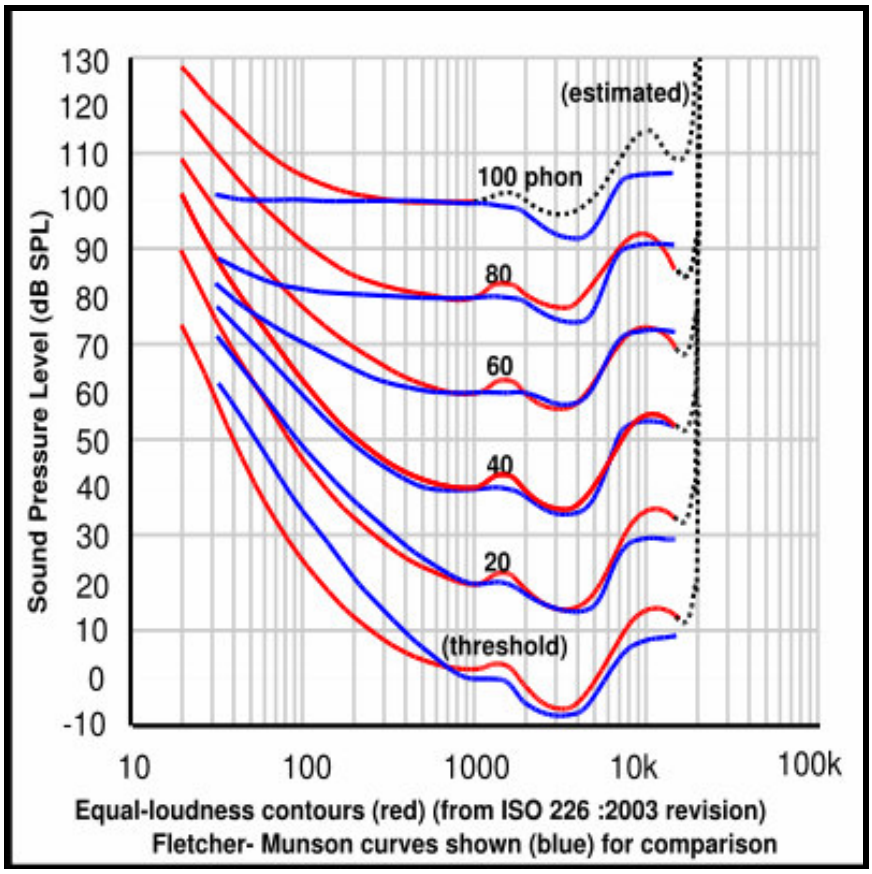

Figure 2.8 : Equal loudness contours (Wikipedia, 2006)

An approximate calculation of the A-weighting as a function of frequency is given in equation 2.14.

$$W_A = 10\log\left[\frac{1.562339 f^4}{(f^2+107.65265^2)(f^2+737.86223^2)}\right] + 10\log\left[\frac{2.24288*10^{16} f^4}{\left(f^2+20.598997^2\right)^2 (f^2+12194.22^2)2}\right] \quad \textbf{(2.20)}$$

The A-weighting function is standardized in EN 60651. Other weightings such as B and C-weighting is intended to be used in measurement of relatively louder noises. Therefore the attenuation in low frequencies is decreased with respect to the A-weighting. On the other hand, D-weighting is used to assess aircraft noise according to IEC 537 regulations. In figure 2.9, the attenuation characteristics of the A, B, C and D weighting filters are presented. B and C weighting is more focused on low frequencies whereas D weighting mostly emphasizes the frequency range between 1 and 5 kHz.

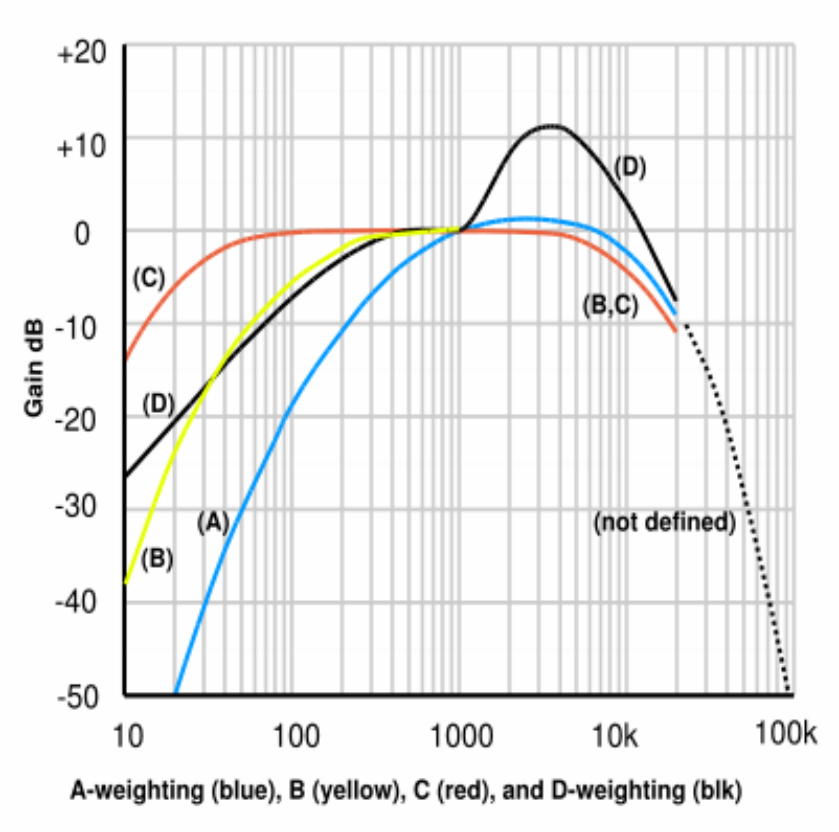

Figure 2.9 : Frequency response functions of A, B, C and D weighting filters.

2.3.3.2. Loudness

Loudness term is used to define the effect of energy content of a sound on the ear as a perceptual measure. Decibel (dB) scale of sound pressure level is used to quantify the power of a sound and it is logarithmic. Doubling the sound power of a sound leads to an increase of 3dB instead of doubling on the decibel scale. However, the perceived loudness is also dependent on the frequency content of a sound. For instance, a very low frequency sound such as a 20Hz tone at 40dB would be perceived to be quieter for a person with normal hearing capabilities than a 1 kHz tone at 40dB. Loudness metrics is used in automotive industry for examining sound quality, measuring car interior noise, engine noise, exhaust noise etc. It has also been used in research to quantify the sound quality of some domestic appliances, vacuum cleaners, or refrigerator noise.

A definition for the loudness of tones can be constructed from the results of experimental studies. Zwicker and Fastl (1990) defines the loudness level of a sound as 'the sound pressure level of a 1 kHz tone in a plane wave and frontal incident that is as loud as the sound; its unit is phon.' As a result, a sound that is as

loud as a 1kHz tone with a sound pressure level of 40dB is said to have a loudness level of 40 phon. This principle can be used to define the loudness of tones by comparing them with an equivalently loud 1 kHz tone. BS ISO 226 (2003) makes use of this idea of a loudness level and constructs equal loudness contours.

However, loudness level calculation of more complex sounds requires further details since two tones less than one critical bandwidth apart will not be heard as two separate sounds. Instead the sounds will partially mask each other, making loudness summation a more complex process. Third octave bands can be used as an approximation to these critical bands. However, a better measure of the perceived loudness can be derived by proper application of the critical bandwidths

A specific loudness can be calculated from the dB level for each third octave band using the assumption that a relative change in loudness is proportional to a relative change in intensity (Zwicker and Fastl, 1990). So values of specific loudness (N') in sone per Bark can be calculated using a power law. Masking curves can then be constructed around these levels representing the effect of critical bands. The final value for loudness (N) is then calculated as the integral under the curve and is presented in sones. The critical band rate is represented as z in this equation.

$$N = \int_{0}^{24\,Bark} N' dz \qquad \textbf{(2.21)}$$

However, the validity of this method has been questioned for impulsive sounds shorter than 200ms duration because of dependence of subjective loudness on duration for short bursts of sound (Blommer et al. 1996).

2.3.3.3. Sharpness

Sound signals whose spectral components are chiefly located in the higher frequency range are heard by the human as sharp or shrilling. Sharpness has been introduced as a unit for this sensation. In other words, sharpness is a measure of the high frequency content of a sound. Crucial to sharpness is the peak of the area below the spectrum envelope. The further this peak shifts towards the higher frequencies, the sharper the perception of the signal gets.

When the high frequency content of a sound is important for determining the quality of a product, sharpness can be a useful measure. It has been used to partially

quantify sound quality in examples such as measuring engine noise, and some domestic appliances such as vacuum cleaners and hair dryers. It has also been used in the calculation of a sensory pleasantness metric and an unbiased annoyance metric (Zwicker and Fastl, 1990).

Zwicker and Fastl (1990) define a sound of sharpness of 1 acum as a narrow band noise that is one critical band wide at centre frequency of 1 kHz having a level of 60dB. However, sharpness metric has not been standardized yet. Consequently there are several methods to calculate the metric including: Von Bismarck's method, Aures' method and Zwicker & Fastl's method. The latter is in the process of being implemented as a DIN standard. Equations 2.22, 2.23 and 2.24 show the calculation methods of different approaches.

Sharpness according to Zwicker and Fastl's method:

$$S = 0.11 \frac{\int_0^{24Bark} n'(z).z.g(z)dz}{N} \qquad \textbf{(2.22a)}$$

$$g(z) = \begin{cases} 1 & (z \le 15.8Bark) \\ 0.85 + 0.15e^{0.42(z-15.8} & (z > 15.8Bark) \end{cases} \qquad \textbf{(2.22b)}$$

Sharpness according to Aures' method:

$$S = K_1 \frac{\int_0^{24Bark} n'(z).e^{0.171z}dz}{\ln(\frac{N}{20}+1)} \qquad \textbf{(2.23)}$$

Sharpness according to Von Bismarck's method:

$$S = K_2 \frac{\int_0^{24Bark} n'(z).z.g(z)dz}{N} \qquad \textbf{(2.24a)}$$

$$g(z) = \begin{cases} 1 & (z < 14Bark) \\ 1 + 0.003.(z-14)^3 & (z \geq 14Bark) \end{cases} \quad \textbf{(2.24b)}$$

In equations 2.23 and 2.24 K_N represents scaling factors.

Besides the different weighting curves for the specific loudness shown in Figure 2.10, there is a difference in the denominator. Whereas the DIN and v. Bismarck formulas give the same results for different total loudness values as long as the specific loudness distribution is the same, Aures' formula will give higher sharpness values with increasing total loudness.

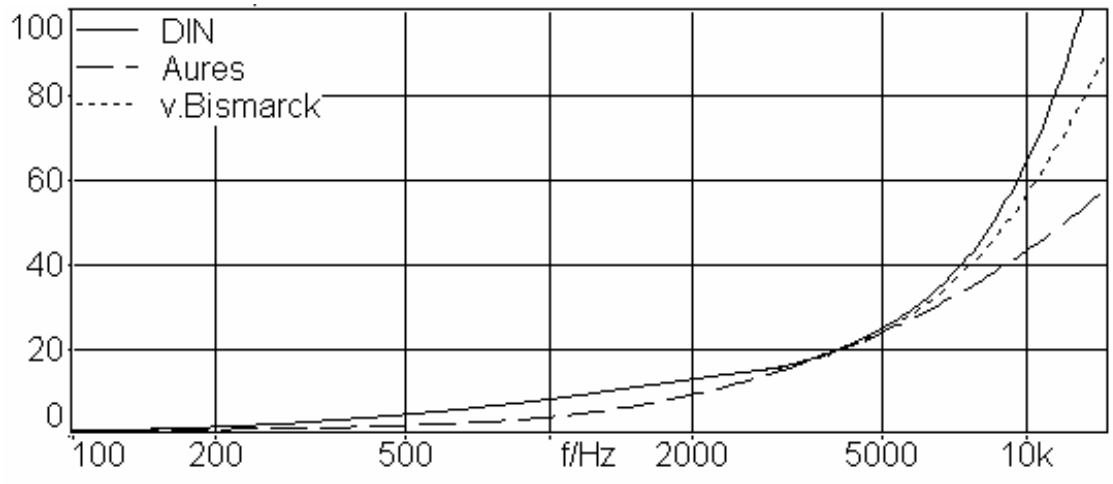

Figure 2.10 : Weighting curves for different sharpness methods.

2.3.3.4. Tonality

Tonality is a measure of the proportion of tonal components in the spectrum of a signal and allows a distinction between tones and noises. Tones consist mainly of tonal components which show in the spectrum as pronounced peaks. White noise and broadband noises have no or little tonality (Head Acoustics 2006).

Calculation of tonality is achieved via short time spectra, via an FFT of 4096 points and a Hanning window. In the first pass, a search is made for spectral lines S_i which are larger than both their respective neighbours $S_i \pm 1$. Only the lines which are at least 7 dB larger than the lines $S_i \pm 2$ and $S_i \pm 3$ are taken into account. The seven-line groups with the indexes i-3 to i+3 found in this way as pure tones are removed from the spectrum.

Only up to a single tonal component per critical band is taken into account. A search is then made for narrowband noise in the remaining spectrum of bandwidth smaller than the critical bandwidth at this location. This is because such signals also create an impression of tonality, although only to a small extent.

The remaining level is calculated for the tonal components thus found. Level of the components are determined by post processing with the substraction of the resting threshold, noise power in each critical band which is given by the power of the remaining spectral lines after subtraction of the tonal components and the excitation level resulting at this position from the other tonal components. The tonality unit is tu and the reference value 1 tu equals the sine tone of 1 kHz with a level of 60 dB.

2.3.3.5. Roughness

Roughness is a complex effect which quantifies the subjective perception of rapid (15-300 Hz) amplitude modulation of a sound. The unit of measure is the asper and one asper is defined as the roughness produced by a 1 kHz tone of 60dB which is 100% amplitude modulated at 70Hz (Zwicker and Fastl, 1990). For a tone with a frequency of 1 kHz or above, the maximal roughness is found to be at a modulating frequency of 70Hz. For the carrier frequencies below 1 kHz, maximal roughness is found to be at increasingly lower modulation frequencies.

In order to begin constructing a model for roughness, a sound containing an amplitude modulated tone with a rapidly changing loudness level should be described. The concept of subjective duration should be clarified before to understand the effect on the ear. Usually the duration of a sound refers to the objective duration, and for sounds greater than 300 ms in length, this is adequate as the objective measurement and subjective perception are the same. However, as the duration of a sound gets shorter and goes below 300 ms a different subjective effect changes the perception. Sounds of shorter durations are perceived to be longer than the objective measurement. For example, a sound of duration 10ms may be subjectively perceived to be 20 ms long and this has important consequences for the subjective perception of temporarily varying sounds, such as rough sounds. The modulated tone mentioned above includes rapidly changing loudness, with respect to the capability of human ear perception. Therefore, the total loudness change that a human ear can differentiate is lower than that of real sound. Figure 2.11 describes the difference between real sound wave and the perception.

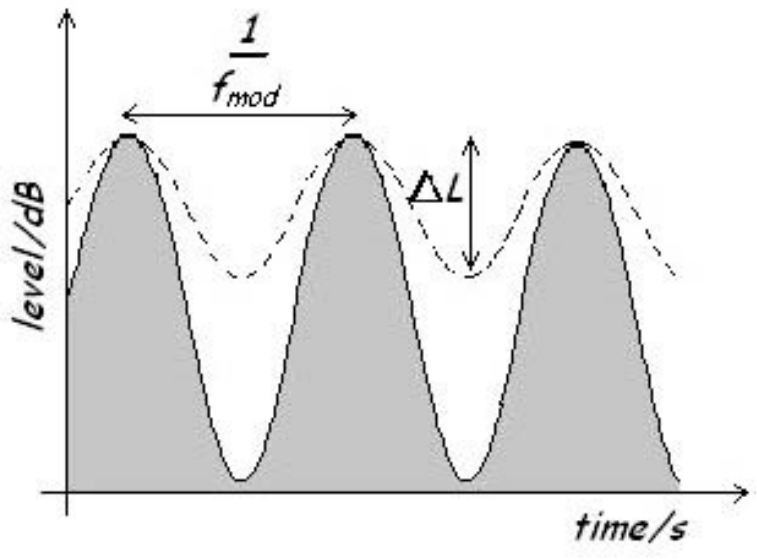

Figure 2.11 : The effect of subjective duration on rapid amplitude modulated noise: (i) the modulation depth (unbroken line) and (ii) the perceived masking depth (dashed line).

As a result of findings above, the roughness of a sound can be evaluated from the following equation:

$$R = cal * \int_{0}^{24\,Bark} f_{\mathrm{mod}} . \Delta L . dz \qquad \textbf{(2.25)}$$

In this equation cal stands for calibration factor, f_{mod} is the frequency modulation and ΔL is the perceived masking depth (Zwicker and Fastl, 1990).

Because of the difficulty in accurate quantification, the roughness metric has not yet been standardised and there are several proposed methods of calculation. In another method, which is proposed by Aures, calculation of generalised modulation depths m_i^* is performed. First the signal is filtered into 24 individual 1 Bark wide bands, and then the envelope of each filtered signal is multiplied by an appropriate weighting function in the frequency domain that gives maximal values at 70 Hz (in accordance with the behaviour of roughness). Then after conversion back to the time domain the RMS value of the each resulting time function is divided by the DC value of each original filtered signal to give 24 generalised modulation depths m_i^*. These generalised modulation depths m_i^* are then each multiplied by a value $g(z_i)$

where z_i is the Bark band of the signal. Each resulting value $g(z_i)^* m_i^*$ is equivalent to $f_{\mathrm{mod}} * \Delta L$ for a particular Bark band so the equation 2.26 is derived.

$$R = cal.\sum_{i=0}^{24} g(z_i).m_i^* \qquad \textbf{(2.26)}$$

Systematic investigations have revealed that roughness depends on centre or modulation frequency and degree of modulation. On the other hand, level dependency is very low for roughness perception.

2.3.3.6. Fluctuation Strength

Fluctuation strength is similar in principle to roughness except it quantifies subjective perception of slower amplitude modulation of a sound, which is up to 20 Hz. The sensation of fluctuation strength persists up to 20Hz, and after this point the sensation of roughness takes over. There is a fuzzy border at the change over of the two sensations when it is difficult to precisely quantify one or the other.

The unit of measure for fluctuation strength is the vacil. One vacil is defined as the fluctuation strength produced by a 1000Hz tone of 60dB which is 100% amplitude modulated at 4Hz. Maximal values are found to occur at a modulation frequency of 4 Hz. Fastl and Zwicker (1990) gives equation 2.27, which shows the variation of fluctuation strength F with masking depth ΔL, and modulation frequency f_{mod}.

$$F = \frac{0.008.\int_0^{24\,Bark} \Delta L.dz}{(f_{\mathrm{mod}}/4) + (4/f_{\mathrm{mod}})} \qquad \textbf{(2.27)}$$

It is important to note that ΔL represents the masking depth. This is not the same as the modulation depth, since short term memory effects rather than post masking effects.

3. DIESEL ENGINE SOUND CHARACTERISTICS

In diesel engines, combustion starts with compression ignition, in which fuel ignites as it is injected into the air in combustion chamber. The threshold for initial flame formation is reached by compressing and increasing the temperatures high enough to cause ignition. For this reason, the design is optimised to work with higher compression ratios and higher combustion pressures with respect to petrol engines. Because of this sudden pressure rise restraint, diesel engines have an impulsive characteristic, which has also been reflected to their sound emitions.

3.1 Noise Radiation Sources in a Diesel Engine

In an internal combustion noise engine, the radiated noise consists of three main groups: mechanical noise, combustion noise and accessory noise (Ford Internal Documents, 2005).

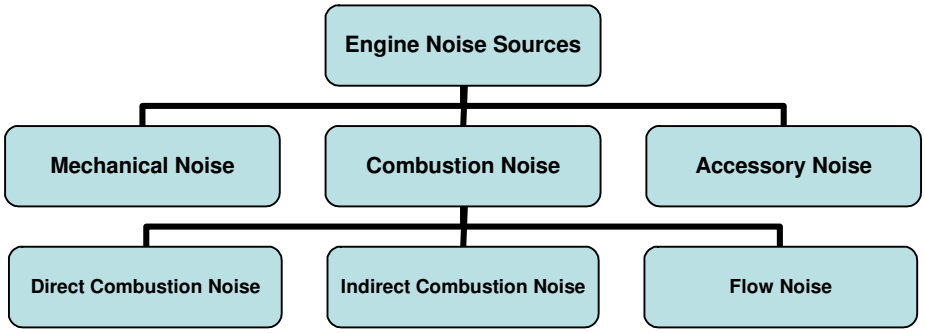

Figure 3.1 : Scheme showing the contributors of engine radiated noise

3.1.1 Mechanical noise sources

Mechanical noise sources in an engine include the moving parts except the crankshaft and pistons which are more proper to be discussed under combustion noise. However, usually the noise source is mainly affected by engine speed and it is independent from combustion process. In other words, the noise does not change with increasing or decreasing load in the engine. According to this description main

mechanical noise sources are valvetrain, oil pump, fuel pump and the chain(s) driving these components.

Noise generating mechanisms for these components are most commonly whining issues due to chain and sprocket interaction. In addition, mechanical impacts in valvetrain should be considered, since it can be an indicator of failures in the system. Mechanical impacts can be between camshaft and the valves and the valves and the cylinder head. Valve seat, tappet to cylinder head and valve spring supports are other mechanisms. All these problems occur due to impact excitation, force excitation, longitudinal vibrations of the spring and secondary movement of the tappet.

Other issues include noises due to bearing failures, camshaft modes excited by engine firing frequencies and noises related to pumping of fuel.

3.1.2 Combustion Noise Sources

Combustion noise sources can be investigated under threee subdivisions: direct combustion noise, indirect combustion noise and flow noise.

3.1.2.1 Direct Combustion Noise

Excitation of direct combustion noise is the pressure rise inside the chamber, which is continously applied on the piston walls every cycle. This excitation on the combustion chamber walls are transfered as vibrations to the outer surfaces of engine through the block. Finally, the airborne noise is produced from these vibrating surfaces. Figure 3.2 illustrates this mechanism (Ford Internal Docs, 2005).

As mentioned before, diesel engine compression ratios are higher with respect to the petrol engines in order to support self ignition. As a result, higher pressure peak levels are reached in diesel engines.Moreover, the timing is not sufficient to reach these high levels without high pressure rise rates. Consequently, the combustion noise of diesel engines are relatively higher.

The shape of cylinder pressure frequency spectrum can be described with Föller's estimation (Gowindswamy and Tomazic, 2004). Each element derived from the amplitude in time domain affects different sections of frequency domain. As shown in figure 3.3, the maximum pressure level and the total pressure level created in one cycle affects the low frequency content of the spectrum. On the other hand, the first

derivative of pressure defines the shape of spectrum between 250Hz and 1kHz. Finally, higher frequency content is related to second derivative of pressure level. Minimization of all these components will result in a reduced combustion noise for all frequency range, shown in equation 3.1.

$$|p(w)| = MIN\left\{\int|p(\alpha)|;\frac{1}{w}(p_{\max}-p_{\min});\frac{1}{w^2}\sum\left(\left(\frac{dp}{d\alpha}\right)_{\max}-\left(\frac{dp}{d\alpha}\right)_{\min}\right);\frac{1}{w^3}\sum\left(\left(\frac{d^2p}{d\alpha^2}\right)_{\max}-\left(\frac{d^2p}{d\alpha^2}\right)\right)_{\min}\right\} \quad \textbf{(3.1)}$$

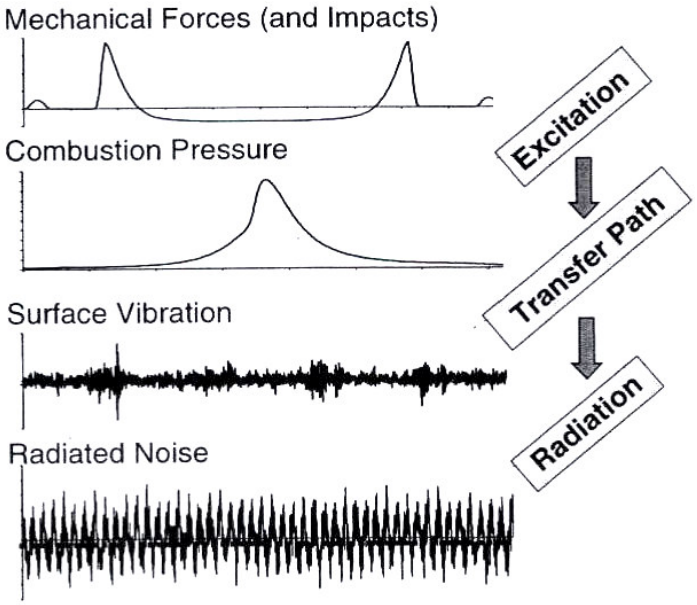

Figure 3.2 : Combustion noise transfer mechanism

Structure attenuation should be considered in order to have a better understanding about the generation of direct combustion noise. The noise generated in the combustion chamber is attenuated in the engine structure and transforms into airborne noise by panel radiation of engine outer surfaces.

The structural attenuation of engine is a function of frequency (Russell and Haworth, 1985). For the low frequencies, the response of the engine is controlled by the stiffness. The radiation efficiencies of the sump and thin section covers and panels which make up the surface of most engines tend to be low. Above 200 Hz, and below 1 kHz inline engines have flexural resonances of the crankcase and cylinder block, which can radiate sound in response to the cylinder pressure excitation, but this excitation is not particularly well coupled to these modes of vibration. Between 1kHz and 5kHz the cast panels and the covers over the valve gear and the first crankcase panel mode is closely coupled to the cylinder pressure excitation via the

connecting rod and crankshaft vibration. Also for the same frequency range, there is a longitudinal mode of the piston, connecting rod and crankshaft which increases the structure response. For the higher frequencies than 5kHz, sound is efficiently radiated by the cast aluminium covers and small thin-section cast iron areas, particularly those of the cylinder head and block. The cylinder head motion, rising over each cylinder as it fires, tends to transmit vibration to the normal modes in the components attached to it which have a wavelength of approximately twice the cylinder pitch dimension. However the cylinder head route for transmitting vibration is very much stiffer than the piston connecting-rod route, resulting in decreasing structure response beyond 5kHz.

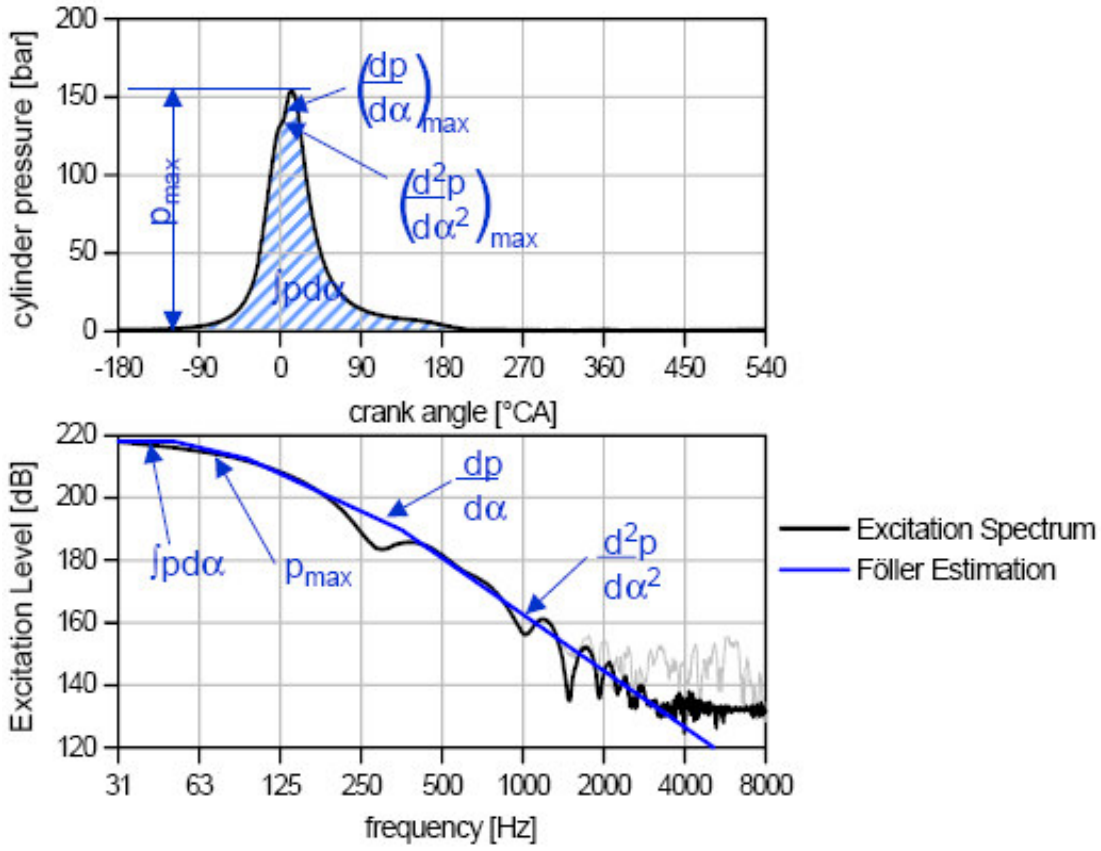

Figure 3.3 : Cylinder pressure excitation and Föller estimation (Gowindswamy and Tomazic, 2004).

Many engines have identical material and construction designs in their structures. Consequently, similar structural attenuation function characteristics are achieved with experimental studies. Optimisation of structure for the concern frequencies could yield a good engineering solution for the direct combustion noise.

The direct combustion noise radiation of an engine can be estimated with the availability of structural attenuation and cylinder pressure diagrams. The target values of combustion pressure development for various engine speeds and loads can be determined from this estimation.

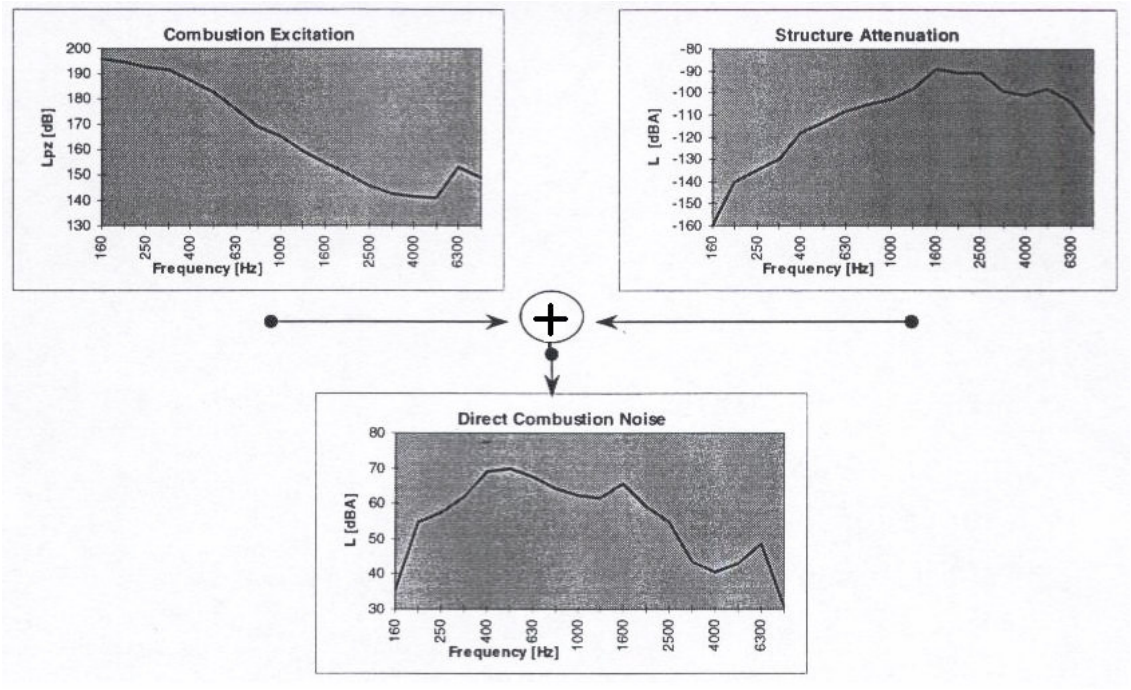

Figure 3.4 : Calculation of direct combustion noise by combustion exictation and structure attenuation (Ford Internal Documents, 2005).

3.1.2.2 Indirect Combustion Noise

All mechanical impacts due to the excitation inside the combustion chamber are regarded as indirect combustion noises. Piston to cylinder wall, piston to connecting rod impacts and crankshaft bearings are the main sources of indirect combustion noise (Ford Internal Documents, 2005).

Piston noise is often complained under cold condition if no optimisation has been done. This is related to high oil viscosity in low temperatures. The most common piston impact types are top land impact, skirt impact and piston pin impact.

Top land impact is caused by the change of direction of piston movement at the top dead center. When the piston is moving upwards it sweeps over the surface on the connecting rod side. When the direction is changed, due to the conical side shape, top corner of the piston hits to the cylinder liner. Usual operating conditions are

medium engine speed range and low load conditions. The emitted noise is characterized as rattling around 2-8kHz range.

Skirt impact happens 10-20^{o} after the top dead center, mainly because of the rotational oscillation of the piston inside the skirt. This impact produces croaking noise between 1-2kHz. Low engine speed and low to medium engine load is the worst case for skirt impacts.

The forces acting on the piston top surface are created by the compression of air and combustion processes. Piston pin impacts happen because of this increasing force in reverse direction at the connection point around 25-40 degrees before the top dead center. Usual indicators are tickering noise in 2-3kHz frequency range from idling to 1500rpm with no load.

In order to avoid these phenomena in cranktrain, following designs should be considered: opimization of piston-liner clearence, piston coating to minimize clearence, reduced piston liner deformation, oil supply of the skirt, stiff crankshaft, optimized main bearing radial and axial clearance, decopling of vibration modes of crankshaft and crankcase, and acoustically tuned crank damper.

3.1.2.3 Flow Noise

The noise generated from the gas motion to and from the combustion chamber is regarded as flow noise.

The charge of the clean air to the engine needs to be provided so that the cool air can be sustained free of huge pulsations. Therefore, the clean air intake is usually placed to the front side of the engine bay to utilize the air flow coming to the front of a moving vehicle. This point acts as a monopole sound source since the pulsation of each cylinder and also the flow noise inside the system is radiated through with the propogation of the sound waves in reverse direction of the flow. For this reason, a muffler volume is used to decrease the pulsation in the flow. Other silencers such as helmholtz resonators and quarterwave tubes are inserted as well to avoid particular resonances in the system. Volume of the intake manifold itself and the runners to the cylinders has a huge affect on the order contents and broadband content of the flow noise. The wall thickness of the connecting hoses, intake manifold and the intake air-filter box can be important since the noise can also be radiated from these regions. Plastic intake manifolds are a good example for this problem.

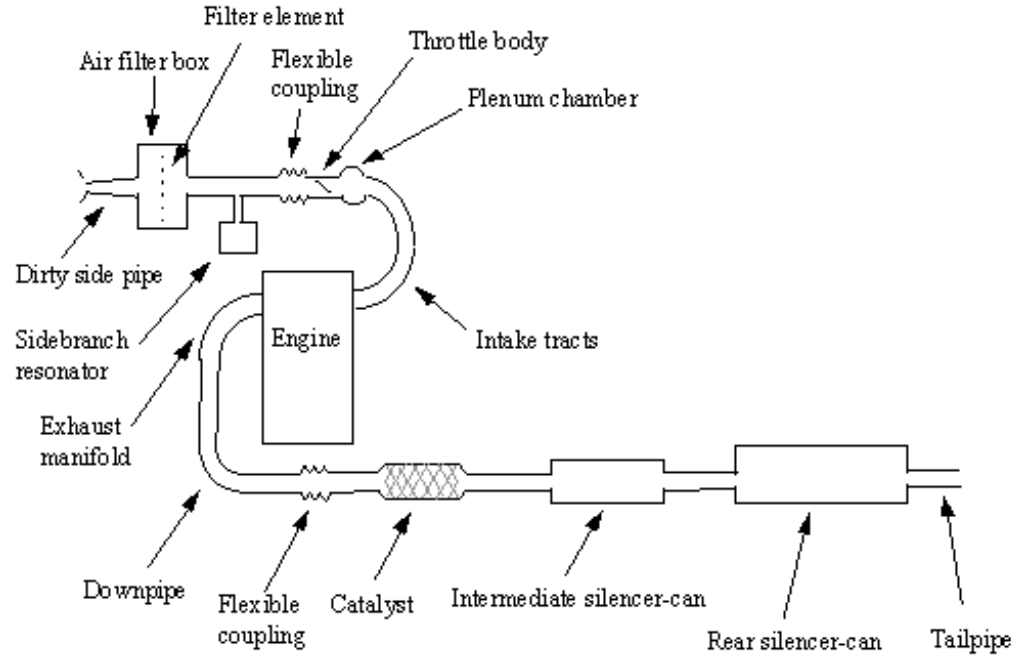

Figure 3.5 : Scheme showing the elements of intake and exhaust systems.

Exhaust system is used in a car to discharge the burnt gases from the combustion chamber. The discharge of the gases is moved as much as possible far away from the passenger compartment to avoid any noise complaints. The other attribute of the exhaust system is to convert or keep the harmful gases in the vehicle.

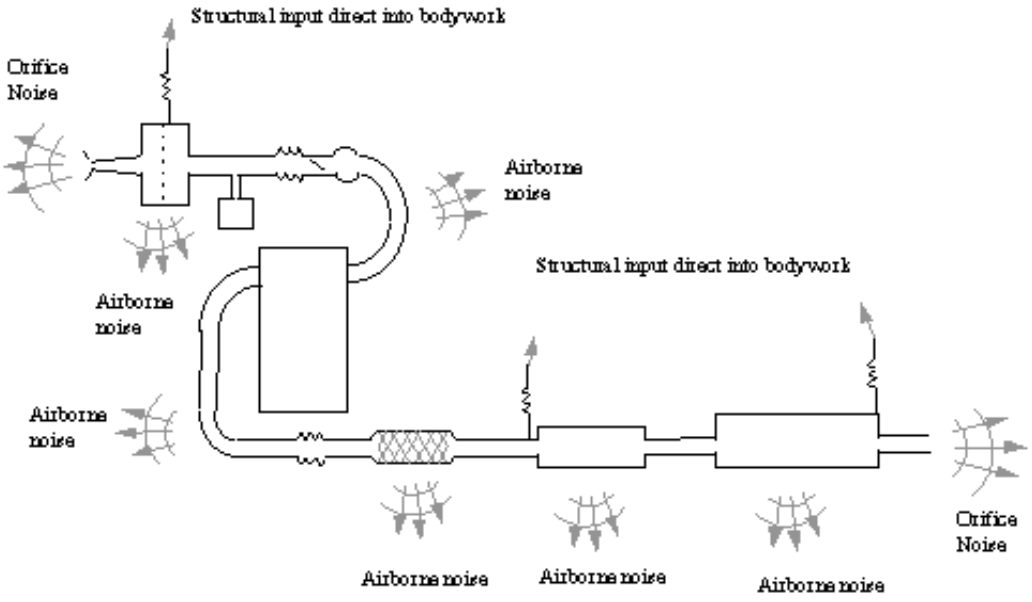

Figure 3.6 : Scheme showing noise radiation paths from intake and exhaust systems

3.1.3 Accessory Noise

Accessory components are connected to the engine via a belt or chain to provide energy to these systems. They use mechanical energy for pumping and electric generation such as cooling fluid pump, power assisted steering pump, vacuum pump, alternator and air conditioning compressor.

Beside the mechanical noise created by the rotational motion of the component, other elements such as pulleys, sprockets, belt and chain is a noise source as well. For instance, the alternator has its own cooling fans, which can create bladepass noise concerns. On the other hand, the pumps can have more complicated issues due to the pulsation they create in the pipes, which are usually connected to body without any damping applications. Moreover, the brackets attaching these components to the engine body can effect the radiated noise and vibration since the resonances and modes of these components can behave like an amplifier for the inputs from the engine.

3.2 Parameters Affecting the Combustion Noise

The combustion noise character and amplitude in diesel engines can be affected by various factors. For instance, fuel injection parameters and exhaust gas recirculation (EGR) rate will directly affect the ignition delay and have a huge impact on the combustion noise whereas secondary factors such as charge air temperature and fluctuations in fuel injection system will also have minor effects.

3.2.1 Effect of Injection Parameters

Modern fuel injection systems like Common Rail Fuel Injection System allows precise and flexible control over the injection quantity and timing, providing higher level of pressure at the same time. This precise control is able to perform multiple injections in a combustion cycle, enabling a smoother pressure build-up and balanced rate of heat release for lower emissions. State-of-the-art systems are able to perform two pilot, one main and an after injection in one cycle (Badami et al., 2002).

Studies of Mallamo et al. (2002) and Badami et al. (2002) summarizes the parametric fuel injection investigations for common rail and conventional high pressure fuel injection systems. Common practice is to apply various injection

timings and come up to a point where satisfactory levels are reached from both emissions and radiated noise point of view.

Methodology of Mallamo et al. (2002) includes five steps for injection timing optimisation. The first step includes the alignment of the start of main injection timing within six iterations. Afterwards appropriate first pilot injection timing is chosen among five increments between 30^o and 90^o. Then, the main injection realigned again to comply with the addition of a pilot injection. For the next step, a second pilot injection is introduced to the system, optimised in five points varying between 20^o and 40^o. Finally, a proper timing for after injection is chosen between the two best parameter settings from previous results.

According to this study, in case of only one single main injection, the combustion noise decreases as the start of fuel injection gets closer to the top dead center. It is reasonable since the late injection forms shorter ignition delay, and therefore provides lower peak pressure and pressure rise levels with the combustion of less amount of injected fuel. Addition of a pilot injection drastically lowers the combustion noise, creating up to a 6 dB difference at 30^o before top dead center. When a pilot injection is added to the cycle, the effect of start of main injection timing changes as well, descending to a level as it gets further from TDC, then increasing again after 8^o. But the variation of the radiated noise levels are within 2dB band for different start of main injection values. Inserting a second pilot injection to the process, results in at least 2 dB decrease in measured combustion noise levels. On the other hand, introduction of an after injection causes slightly higher radiated noise values. The produced power is kept constant for all of the iterations mentioned above.

Badami et al. (2002) shows again that pilot-pilot-main strategy can be more effective in reducing combustion noise and fuel consumption than the corresponding double injection strategy with a disadvantage of higher emission values to be faced.

As seen from the examples above, pilot injection is a very effective method to reduce the combustion noise from a diesel engine. It is a matter of optimizing the injection strategy and quantities for various cases. But squeezed development timings restricts a perfect optimisation for every operating point of the engine. Therefore, initially, responsible engineer investigates the effect of pilot injection in certain hot points where a trade-off between emissions, fuel economy and noise radiation is needed. Because of the legal requirements, the priority is to reach emission targets. Other critical points can be, highway cruise operating load-speed

range and concern regions where noise complaints found to be unacceptable with regards to development targets. Parameters for remaining operating points can be determined through previous experience and with the insight from studied operating conditions.

3.2.2 Effect of Charge Air Temperature

Heating the charge air temperature of a diesel engine is a method to improve cold startability in low temperatures. In cold climates, where the ambient temperature is lower than 0^{o}, apart from the diffuculties of startability and drivability, the low temperature air charged inside the combustion chamber increases the ignition delay. As a result, the steepness of pressure trace increases with higher quantity of fuel burning spontaneously. Figure 3.7 shows the effect of charge air heating on radiated noise levels for a 1.4 liter 4 cylinder direct injection diesel engine.

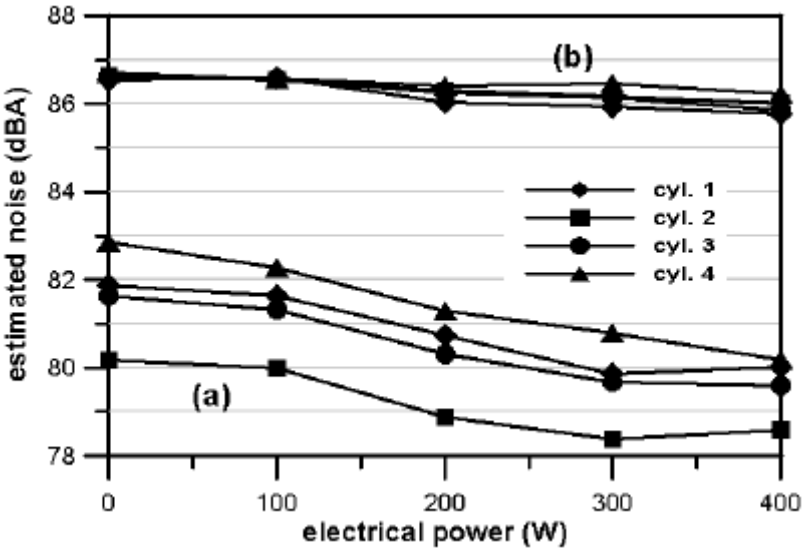

Figure 3.7 : Estimated combustion noise levels for different electric power supplied to the air charge heater (a) cold engine (b) hot engine (Payri et al., 2006)

3.2.3 Secondary Influence Factors

Another factor that affects combustion noise is the irregularities of the combustion due to injection rate modulation, cycle to cycle and/or cylinder to cylinder combustion variation. These irregularities cause a degradation in sound quality of radiated noise, since the noise characteristics changes within a period of time.

These variations are caused by two kinds of source: Fluctuations caused by the preceding cycle (residual unburned gas, partial burn or misfire) and fluctuations in the same cycle (variations of in–cylinder flow and turbulence, fluctuations in injection system) (Gazon and Blaisot, 2006). Following statements are the results of this study:

- Cyclic fluctuations are always larger for low engine speeds and low brake mean effective pressures (BMEP).
- The fact that the compression stroke does not induce significant fluctuations, leads to the result that the fluctuations of cylinder pressure are only due to the combustion process.
- With regards to the standard deviations in time, the fluctuations of ignition delay are higher at low speed.
- On the same cylinder, correlations are found between the maximum of pressure rise, the maximum of the rate of heat release and the combustion noise.
- Correlations on cylinder-to-cylinder fluctuations at low engine speed are found compliant with cylinder ignition order. This could be due to a mechanical or EGR effect.

3.2.4 Differences between Steady State and Transient Conditions

Usual driving cycle of a customer includes a moderate acceleration after a period of cruising in highway speed for taking over. Experiences show that, the generated combustion noise during this maneuver is higher than in steady state loadings. The reason of this have been investigated by Shu et al. (2005, 2006) and testing procedures have been developed.

In transient conditions, the diesel engine noise exhibits 1~6 dB higher combustion noise levels than in steady state conditions for 1000-2200 rpm range. The reason for this difference is explained in this way: In low load and at low rotational speed the ignition delay is shortened in transient conditions compared with that in steady conditions. But combustible fuel injection quantity of the shortened ignition delay in transient conditions is larger than that in steady conditions causing more noise in transient. In addition, the amplitude of high frequency oscillation of combustion

pressure in transient conditions is larger than that in steady conditions. However, as the rotational speed increases, the trend of combustion noise difference tends to decrease and after a certain point, steady condition combustion noise is higher than that of steady conditions.

The differences between the combustion chamber's wall temperature, needle lift and injection pressure in transient and those in steady conditions influence the ignition delay and the combustible fuel injection quantity in ignition delay, which causes the differences of dynamic load and high frequency oscillation of combustion pressure in the two conditions, which further results in the difference between the combustion noises in transient and steady conditions.

3.3 Transfer Paths of Diesel Combustion Noise

The noise of the diesel engine is transfered to the passenger compartment through two main paths: structureborne and airborne. Noise transfer path analyses show that the frequencies below 250Hz is usually structureborne. On the other hand, the airborne content dominates the frequency range above 800Hz. The band between 250 Hz and 800 Hz is a mix of structureborne and airborne sounds in a vehicle (March et al., 2005a).

Structureborne noise of diesel engine is transfered to the body from the mounts of the powerplant, hangers of exhaust system, bearing brackets of driveshaft, and the suspension attachment points of axle that drives the vehicle. Powerplant is attached to the body with damper components at these points. These are the mounts of powerplant, rubber bush in the leaf spring front and rear eyes, lower arm, knockle on the damper i.e. These rubber components provide sufficient isolation between the body and the powertrain in higher frequencies than their natural frequencies. As a result, only lower frequency range excitations are transfered through these attachment points.

Transfer of airborne noise happens through the transmission loss of body frontal area, the dash panel and the floor pan. In order to decrease airborne noise transfer, four aspects must considered in the body design:

- Engine Compartment Absorption: The absorption in the engine bay decreases the reverberation and thus prevents redirection of sound wave to the dash panel or floor pan.

- Body & Insulator Blocking: Sheet metal panels have a transparency against the sound wave. This transparency can be decreased by adding additional layers and absorbing materials. A treatment like this will also create a damping of the sheet metal to avoid high frequency resonances.

- Pass-thru Sealing: Sealing of gaps in body or components such as pipes going through the dash panel will improve the noise reduction levels of the body. In case of a gap in dash panel, all remaining acoustical treatment would be useless.

- Interior Absorption: Interior absorption decreases the reverberation in the passenger compartment providing a lower perception of engine noise.

3.4 Methodologies for Quantification of Diesel Combustion Noise

Seperation of combustion noise from other masking effects and quantification with respect to human perceptions have been an issue for researchers. This section will provide information about methods that have been applied in various studies.

It has been preferred to consider only the overall level of radiated noise for quick check of optimization of noise, emissions and fuel economy parameters. However, for a detailed investigation, frequency content characteristics, sound quality properties and excitation mechanism needs to be investigated. Simultaneous measurement of noise and in cylinder pressure with snychronous monitoring of fuel injection system variables, driving conditions, operation temperature from various locations and piston location will provide a better understanding of the issue.

3.4.1 Investigation of Time-Frequency Spectra

Frequency spectrum is a good indicator to build up correlations between in-cylinder and noise recordings, or even the measured acceleration levels. The concern regions are the range where human perception is determined to be higher and where high peaks of modulated noise are detected.

Chiatti and Chiavola (2004) compares in-cylinder pressure crank angle traces of one cylinder diesel engines equipped with high pressure displacement fuel pump. The traces of different injection advances are investigated for high frequency pressure oscillations. For the processing of the data, authors rely on mean frequency trends

to comment on the measurements. In figure 3.8, the results from an operation point is shown for two different injection advances. When the pressure trace oscillates at peak pressure, the mean of the frequency content moves to higher values.

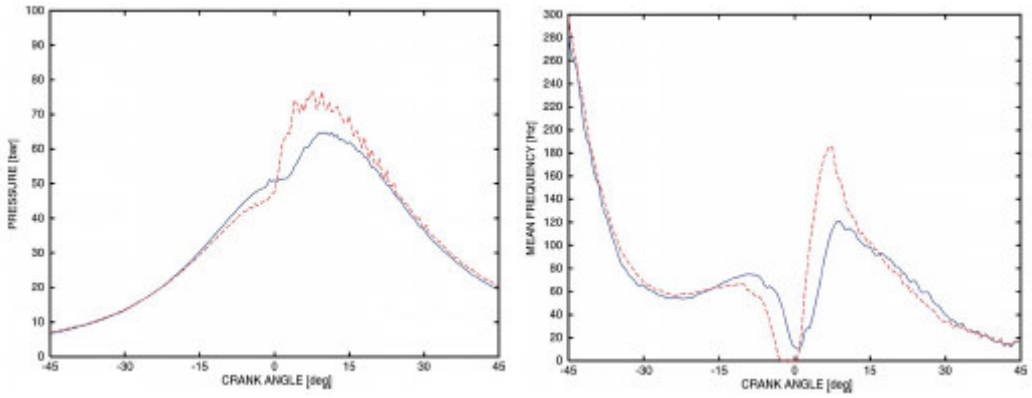

(a) (b)

Figure 3.8 : In cylinder pressure trace and mean frequency trends for a one cylinder diesel engine. (3600 rpm, solid lines: 18.5^{o} , dashed lines 20.3^{o} inection advance) (Chiatti and Chiavola, 2004).

Increasing concern in construction of more general wavelets to form bases for square-integrable functions and development of faster processors availed the application of these techniques to signal processing. Being located in two domains is an advantage in many cases: the primary one being that wavelet transform analysis can provide information on the localization of energy content in time and frequency. Small frequency changes in the Fourier transform yields a change everywhere in the time domain (Villarroel and Agren, 1997).

Villarroel and Agren (1997), Desantes et al. (2001), Scholl and Blommer (2005) and Yajima and Nakashima (1997) uses wavelet transform for quantifying diesel combustion noise. The study of Villarroel and Agren show the effectiveness of wavelet technique in pointing out the time fluctuations of each frequency component. The experimental results also show that the detection of combustion noise and piston slap can be successfully improved by using wavelet transform analysis instead of Fourier transform. The vibroacoustic complexity of an engine with complicated structure and multiple sources of vibration such as pistons, valves and gears makes it difficult to identify the effects of individual sources.

Yajima and Nakashima (1997) invesitgates the effect of pilot injection combustion in low and high speed ranges. It has been determined in this investigation that pilot injection is less effective in higher speeds since the diffusion combustion is

dominant. Wavelet analysis has been used here to differentiate the amplitudes of premixed combustion and diffusion combustion.

Scholl and Blommer (2005) uses wavelet transforms to investigate a technique to reduce the impulsive character in noise recordings. Shift-Invariant Discrete Wavelet Transform provides a measure of the energy content of sound signal as a function of frequency and time. With the help of this function, the coefficients with high energy content are removed and replaced with an average value. The inverse function is applied again to reconstruct the sound recording. A similar process was performed with Fourier transformation. The measurement of reconstructed and original recordings show very promising results with the wavelet impulsiveness removal.

Desantes et al. (2001) compares with and without pilot injection conditions for high and low speed range in high and low load operating points for each case. The coherence between changes in cylinder pressure and radiated noise spectrum have been investigated for these various conditions.

3.4.2 Sound Quality Metrics and Correlation with Subjective Evaluations

A relation between the objective measurement and subjective evaluation is needed to understand the likes and dislikes of people. Because of the complicated structure of diesel noise, it is becoming necessary to use a method to combine various metrics and come to a conclusion in this way.

Russell et al. (1987) uses real world recordings of diesel engines and resimulate the condition to the subjects. The recordings used in this subjective evaluation is reconstructed by adding amplified sounds from near-field microphones. Moreover, the subjects are asked to tune the best noise they can achieve by proportioning the near-field recordings among each other. Total sound pressure level is justified at same value to avoid other complexities. The process is summarized below:

- Placing the subject in the appropriate environment
- Presenting the subject via a single high quality audio channel with the result of mixing a set of sounds, each of which contains one dominant characteristic.
- Providing the subject with a means of altering the proportion of each characteristic in the sound mix

- Inviting the subject to change the mix of sound characteristics to achieve the sound which is most acceptable.

- Automatically increasing the overall level of the sound to compensate, in any chosen ratio, for the reduction in any of the sound characterstics by the subject. Choosing the ratio of automatic level change for each sound characteristic until (experienced) subjects cannot find any optimum mix.

- Averaging these results over a jury of subjects.

Results of this pilot experiment with diesel engine noise in cold idle conditions show that most subjects found the impulsive characteristic and high frequency content to be least acceptable components in diesel noise.

Shiffbanker et al. (1991) and Hussain et al. (1991) develops an annoyance index to assess diesel engine sounds. Several sound quality metrics and filtered sound pressure levels have been used to find a correlation between subjective ratings and objective measurements. The measurables are listed in Table 3.1. According to this investigation, it has been found out that loudness, preferred periodicity (a periodicity measure), kurtosis (reflecting impulsiveness) and sharpness are the physical parameters that significantly influence the subjective perception of annoyance of engine noises. These parameters have been linearly combined to form a unique annoyance index to rate the noise of an engine without having to rely on subjective judgement. For this reason, 60 different engine noises have been correlated with subjective ratings. This has prepared a basis for optimizing the perceived noise character of an engine. Besides, application examples demonstrate that measures to reduce the engine noise level in dB(A) only, do not necessarily imply an improved noise quality and it can even result in a detoriation of the subjective noise character.

In this research, multidimensonal scaling of the ratings of numerous test persons indicates the number and contribution of single physical components to the subjective impression. Regression analysis together with a stepwise selection method, offered a means to achieve a solution for the description of the noise character of engines.

Hashimoto et al. (1995) uses paired comparison technique for real and artificial diesel exterior idling noises. For the confirmation of findings, engine compartment is enclosed in a real vehicle and it has been proved that pleasant

sound quality was over-achieved. Sharpness, loudness, roughness and fluctuation strength highly correlated with subjective impressions in this study.

Table 3.1 : Metrics to Compute AVL Annoyance Index

Categories	Definition	Notation
Sound Pressure Level	Linear	LIN
	A-Weighted	A
	B-Weighted	B
	C-Weighted	C
	D-Weighted	D
	AD-Weighted	AD
Combined Level Quantities	High Frequency Level	HF
	Speech Interference Level	SIL
	Composite Rating of Preference	CRP
Periodicity Measures	Engine Speed	RpM
	Preferred Periodicity	PrePer
	Firing Frequency	FiFreq
Psychoacoustic Loudness	Loudness Level Sone	soneG
	Sone > 900 Hz	soneT
	Loudness Level Phon	phonG
	Phon > 900 Hz	phonT
Psychoacoustic Sharpness	Unweighted sharpness	barkG
	Unweighted sharpness > 900 Hz	barkT
	Sharpness	acumG
	Sharpness > 900 Hz	acumT
Roughness	Weighted Modulation Level	TOTW
	Weighted Modulation - 125 Hz Oct	MOD1
	Weighted Modulation - 250 Hz Oct	MOD2
	Weighted Modulation - 500 Hz Oct	MOD3
	Weighted Modulation - 1 kHz Oct	MOD4
	Weighted Modulation - 2 kHz Oct	MOD5
	Weighted Modulation - 4 kHz Oct	MOD6
	Avg. Modulation 80 Hz - 5.7 kHz	SMOD
	AVL - Modulation - 125 Hz Oct	MAVL1
	AVL - Modulation - 250 Hz Oct	MAVL2
	AVL - Modulation - 500 Hz Oct	MAVL3
	AVL - Modulation - 1 kHz Oct	MAVL4
	AVL - Modulation - 2 kHz Oct	MAVL5
	AVL - Modulation - 4 kHz Oct	MAVL6
	AVL - Modulation Sum	SMAVL
Sound Pressure Distribution	Mean Value - linear	MEANl
	Mean Value - A-Weighted	MEANa
	Mean Value (0.8-3 kHz)	MEANf
	Standard Deviation - linear	STDEVl
	Standard Deviation - A-Weighted	STDEVa
	Standard Deviation (0.8-3 kHz)	STDEVf
	Skewness - linear	SKEWl
	Skewness - A-Weighted	SKEWa
	Skewness (0.8-3 kHz)	SKEWf
Impulsiveness	Kurtosis - linear	CURTl
	Kurtosis - A-Weighted	CURTa
	Kurtosis (0.8-3 kHz)	CURTf
	Cumulated Power	CUMPOW

Champagne and Shiau (1997) investigates idle sound quality again, but this time focusing on semantic differences between US and UK participants. According to this

study, the US annoyance is more related to impulsive/not impulsive and loud/quiet adjective descriptors. On the other hand, UK participants' annoyance results best correlates with loud/quiet and pulsating/not pulsating adjective descriptors. For this reason, the authors propose experiments to have training sessions which include example of sounds to illustrate the meaning of adjectives. Ingham et al. (1999) includes wide open throttle sounds besides the steady speed diesel engine sound. Sharpness and loudness values are found to be more dominant parameters for wide open throttle conditions.

Hastings (2004) creates a model simulating the noise generated from a diesel engine. This model includes combustion pressure profiles, cycle-to-cycle and cylinder-to-cylinder variations combined with an impulse train. Also, other components, such as pumps and fans have been added as sine waves. Thus, a complete artificial sound was generated, including all the noise source variables in a diesel engine. The subjects gave ratings for several generated noises. After the subjective evaluation, the objective and subjective results have been correlated. The investigation showed that timing variation has a considerable effect over subjective annoyance. Moreover, noises with high level of sharpness values can affect the perception of impulsiveness, leading to a wrong judgement of combustion noise.

3.4.3 Frequency Modulation Analysis

The time frequency analysis and psychoacoustic metrics are not able to uniquely predict the diesel knocking perception of customer. On the other hand, visualizing the diesel knocking performance of a vehicle and deliver crucial hints about the diesel knocking root cause is needed to develop solutions for these issues. Also, noise path analysis should be included for preventing the noise on the path and setting targets for both source and transmission loss on the path is not possible with the methods mentioned before. Modulation analysis is used to overcome these issues with noises having impulsive content (Heinrichs, 2004).

The modulation index gives information about how the noise level is oscillating in a frequency range. The depth of this modulating wave gives the index. In order to provide better information of modulation characteristics, double FFT is applied to the acquired noise data. The algorithm detects the peaks and their repetition and applies weightings according to the human perception. As a result, amplitude modulations are visualized in a plot where the axes consisting of modulation

frequency and carrier frequency. The third dimension is the modulation index. Figure 3.9 illustrates the modulation index calculation.

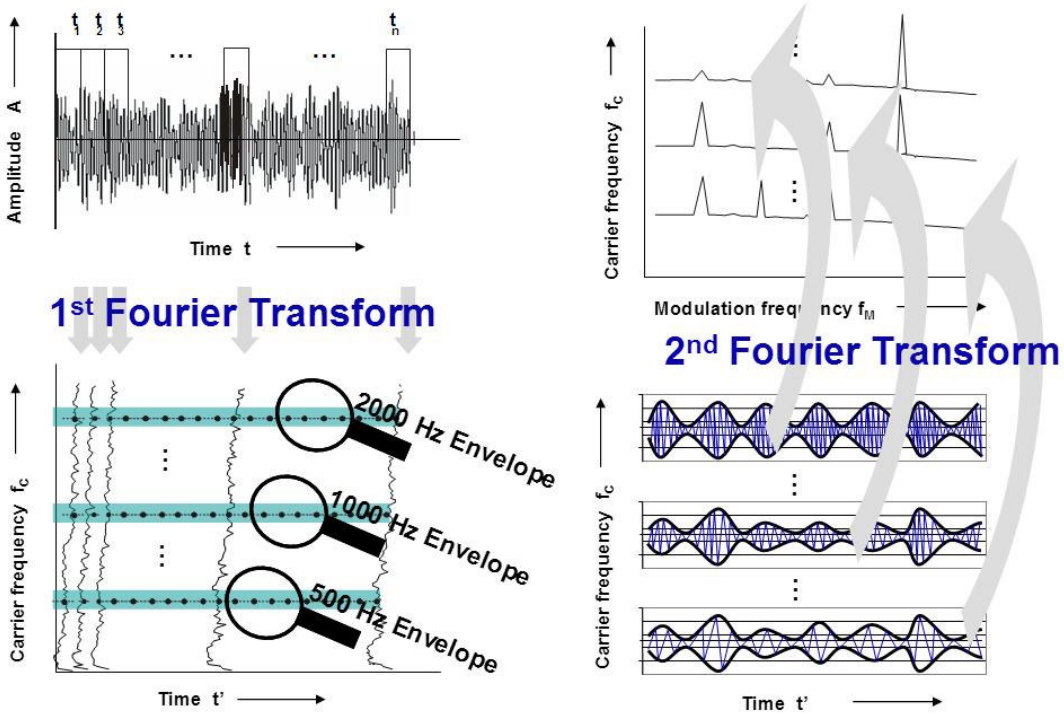

Figure 3.9 : Determination of modulation index of a signal

This method can also be used to filter the impulsive content as mentioned before. The Ford internal program ModFil is capable of this function. Moreover, a weighting for modulations in harmonics of engine order content can be applied in this three dimensional plot to correlate with subjective evaluations. The metric derived from this secondary calculation is called Diesel Knocking Index. Formulation of this index is shown in equation 3.2. In this secondary index, the level of the signal is also included.

$$DKI = \sum_{o=0.5}^{O(step=0.5)} \sum_{f_m=f_{m,o}-b*\Delta f_m}^{f_{m,o}+b*\Delta f_m} w_m(f_m) \sum_{f=f_u}^{f_o} P_{mi}(f, f_m) + L \qquad \textbf{(3.2)}$$

4. CASE STUDY OF INTERIOR SOUND QUALITY IN A VEHICLE WITH COMMON-RAIL DIESEL ENGINE

In previous chapters, fundamentals of acoustic signal processing and diesel sound quality are summarized. In this study, impact of diesel combustion process over interior sound quality is investigated for a light commercial vehicle development process. The test vehicles are powered with a 5 cylinder 3.2L diesel engine having common-rail fuel injection which is able to deliver 200PS peak power and 470 Nm peak torque. The intake system includes turbocharger and intercooler for higher performance. The steps of this study are listed below:

- Identification of diesel impulsiveness in passenger compartment with sound quality metrics and time-frequency analyses
- Analyzing Simulink generated artificial engine sound files to find out possible error states that may cause the issue
- Examination of direct combustion noise by comparing simultaneously recorded cylinder pressure levels and near-field sound pressure levels
- Detailed examination of cylinder pressure measurements for a better understanding about the sound generation mechanism

Details of these steps will be presented in the following sections. As a final step, possible root causes of the issue will be listed with the outcome of findings.

4.1 Identification of Diesel Impulsiveness

For the identification of diesel impulsiveness, interior sound pressure levels are measured. The measurements are repeated with two different engine control units installed to the vehicle. Even though the calibration settings remain the same, in the first setting there is no perceptible diesel impulsiveness issue whereas in the second version diesel clatter is audible inside the passenger comparment for certain

operating conditions. The diesel clatter is characterized by discrete, constant frequency peaks giving the impression of typical diesel noise.

4.1.1 Test Conditions and Measurement Setup

For binaural recording, the test vehicle is instrumented with Head Acoustics Artificial Head HMS III in passenger seat and SQLab III Data Acquisition Front End. An IBM Thinkpad laptop is used for storing and analysing acquired data. The interior noise is acquired on smooth surface road with 48k sampling rate for two different maneuvers:

- First step is to monitor the oveall Powertrain NVH performance through 3rd Gear Wide Open Throttle aceleration starting from creep rpm and finishing with maximum allowed engine speed.

- In the second step, interior sound is recorded for a constant point in load-engine speed map. Subjective evaluation is used to determine this engine operation point. In other words, the point in which diesel clatter is dominant and clearly audible is chosen. During the data acquisition, throttle position and engine speed is monitored through CAN-Bus. Three samples are recorded from both conditions. The details for this operating condition is shown in Table 4.1

Table 4.1 : Engine Operating Parameters for 1500 rpm Constant Engine Speed-Load Interior Noise Recording.

Engine Speed	1500 rpm
Throttle Position	40%
Main Injection Quantity	42,5 mm^3/stroke
Main Start of Injection	2.2° BTDC
Pilot Injection Volume	1,5 mm^3/stroke
Pilot Injection Seperation	11.3° CA
Rail Pressure	101 MPa
EGR Rate	0%

4.1.2 Analysis of the Results

The comparison of overall sound pressure level and articulation index in 3rd Gear WOT showed clear degradation with the second engine control unit. In figure 4.1 the degradation below 2500 rpm is visible for both metrics. The articulation index drops 5% and the interior sound pressure level is 1.5 dB(A) higher than the first ECU.

These results indicates a combustion related problem since the combustion noise contribution is higher for lower engine speed as mentioned in Chapter 3.

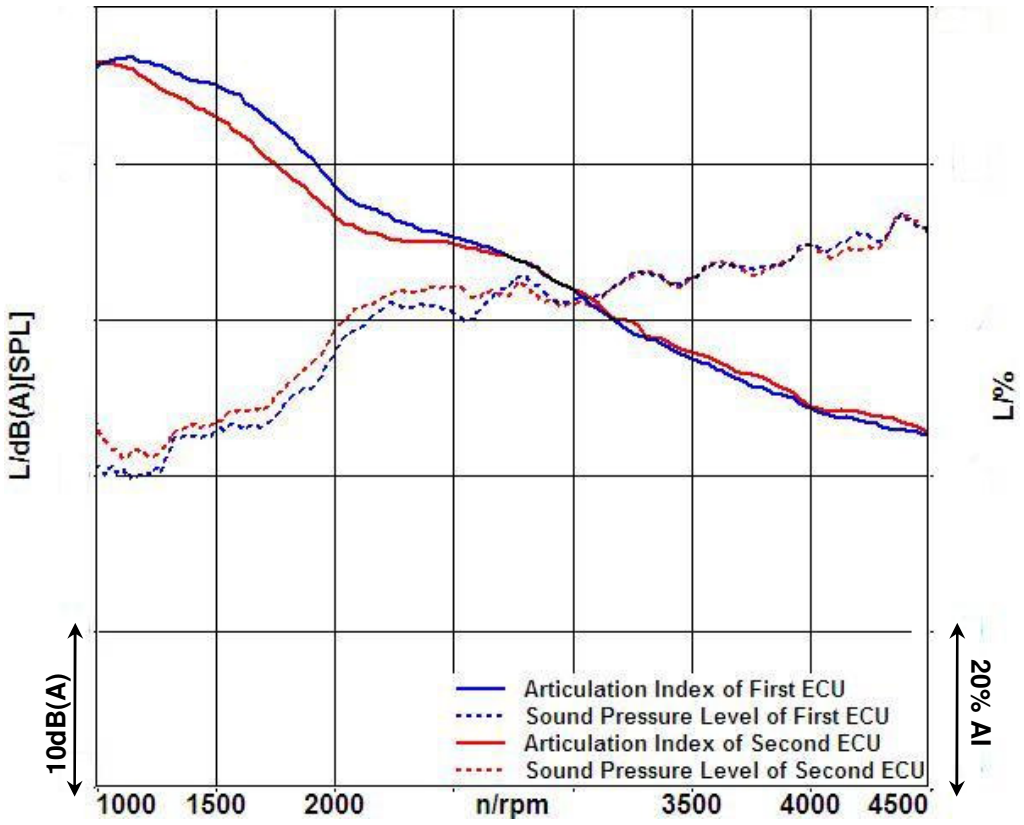

Figure 4.1: The comparison of sound pressure levels and articulation index of interior noise recordings with two different engine control units.

On the other hand, 3rd Gear WOT measurements have notable disadvantages for investigating diesel impulsiveness. Basically, higher engine speeds are included and lower engine speeds are swept very rapidly preventing a proper study. Therefore, constant engine speed-load measurements are investigated in details.

FFT vs Time analysis is preferred for a better understanding of impulsive nature of the diesel clatter. The spectrum size is chosen as 1024, so the time resolution is:

$$\left(\frac{Sampling\ \ Rate}{Spectrum\ \ Size}\right)^{-1} = 1/\left(\frac{48000\ sample/s}{1024\ samples}\right) = 0.021\bar{3}\ s \qquad \textbf{(4.1)}$$

Accordingly, the frequency resolution will be:

$$\frac{Sampling\ \ Rate}{Spectrum\ \ Size} = \left(\frac{48000\ sample/s}{1024\ samples}\right) \cong 47\ Hz \qquad \textbf{(4.2)}$$

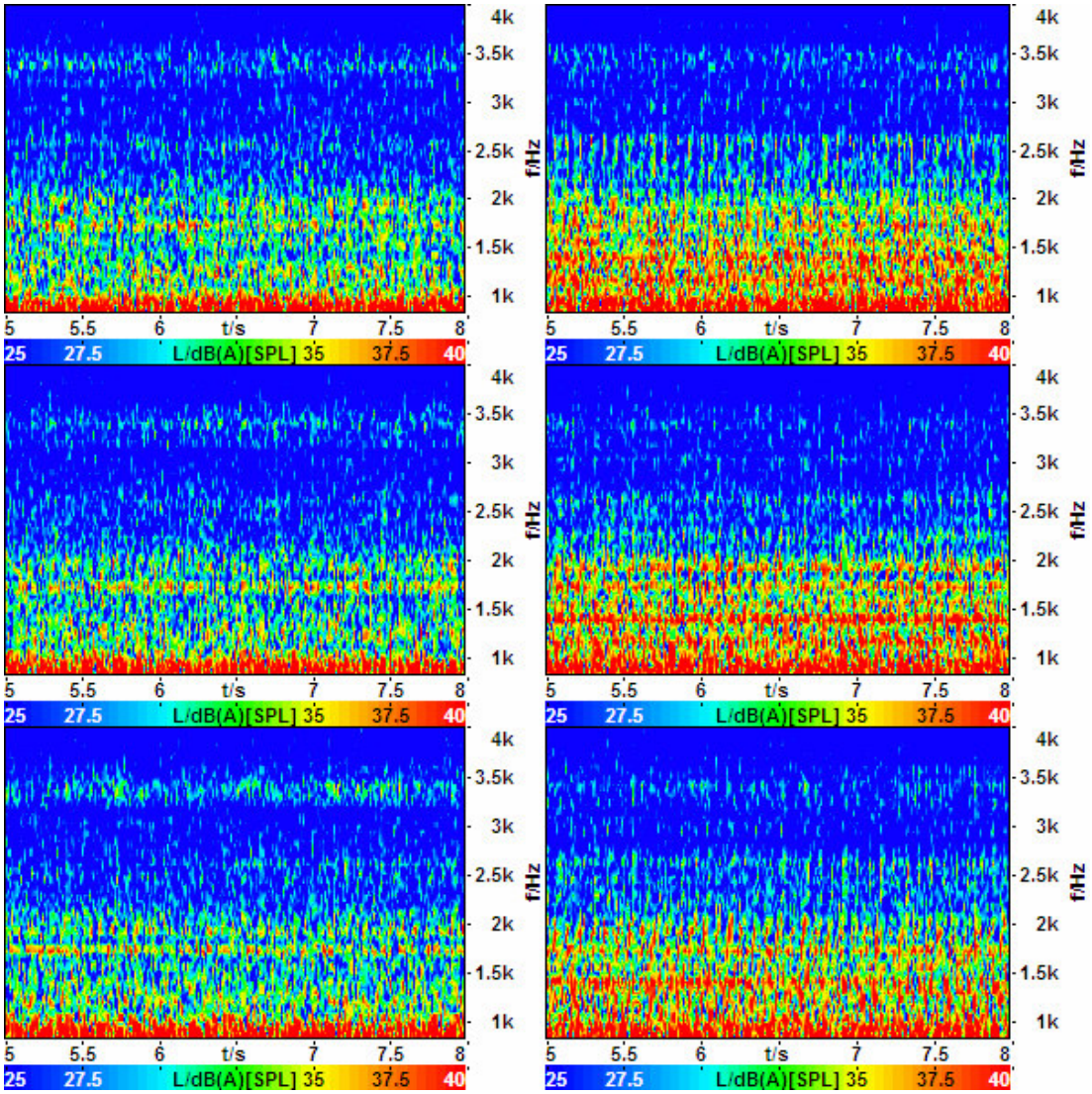

(a) (b)

Figure 4.2: FFT vs time analyses of (a) 3 sample recordings of first engine control unit and (b) 3 sample recordings of second engine control unit

The waterfall diagrams show a noticable increase of sound pressure levels from 1 to 4 kHz. The impulsive character of the noise is identified from the discrete peaks in these frequency range. The samples with first engine control unit have slight peaks around 1750 Hz. However, 1 to 2.2 kHz region is dominated by this impulsive noise in the samples with second engine control. Moreover, the higher frequency range also includes traces of repeating noise, unlike the plots on the left. These samples are analyzed with various sound quality metrics to have more clue about the issue. Bandpass filters are applied to emphasize the diesel clatter issue for better differentiation. Table 4.2 summarizes the results for each sample and the average values of three samples.

Table 4.2 : Results of Analyses Applied to Samples with Different ECUs

		Old Level Control Unit				New Level Control Unit			
Metric	Unit	Sample 1	Sample 2	Sample 3	Average	Sample 1	Sample 2	Sample 3	Average
Sound Pressure Level	dB	93,3	93,1	92,9	93,1	90,9	92,9	92,3	92,0
500-10k Hz SPL	dB	55,6	55,4	55,6	55,5	55,8	57,3	55,2	56,1
800-4k Hz SPL	dB	50,4	50,4	51,1	50,6	51,5	53,5	51,1	52,0
Sound Pressure Level (A-Weighted)	dB(A)	61,7	61,1	61,0	61,3	61,0	61,4	61,1	61,2
500-10k Hz SPL (A-Weighted)	dB(A)	53,9	53,7	53,3	53,6	54,3	54,4	53,9	54,2
800-4k Hz SPL (A-Weighted)	dB(A)	50,0	49,9	49,7	49,9	51,3	51,4	51,0	51,2
Loudness	sone	15,0	14,7	14,6	14,8	14,7	15,0	14,9	14,9
500-10k Hz Loudness	sone	7,27	7,21	7,21	7,23	7,63	7,63	7,42	7,56
800-4k Hz Loudness	sone	5,04	5,01	5,03	5,03	5,46	5,45	5,31	5,41
Roughness	asper	0,32	0,29	0,32	0,31	0,30	0,29	0,32	0,30
Sharpness	acum	1,29	1,29	1,31	1,30	1,33	1,31	1,31	1,32
500-10k Hz Sharpness	acum	1,86	1,86	1,88	1,87	1,85	1,84	1,87	1,85
800-4k Hz Sharpness	acum	1,53	1,53	1,55	1,54	1,54	1,52	1,54	1,53
Kurtosis		2,96	3,04	2,93	2,98	3,13	3,07	3,03	3,08
Modulation Index 400-4k Hz		0,49	0,50	0,50	0,50	0,54	0,53	0,53	0,53

The weighted and unweighted overall sound pressure levels do not give good indications of diesel clatter presence. This result can be confusing, however the answer for equivalent performance is averaging. When all the data is averaged over time domain, the peaks converge to the average value so that the differences between impulsive and constant noises vanish.

Application of sound quality metrics to these data gives some clues about the differences between two control units. Sharpness values are identical for all sample recordings in a parallel manner with overall sound level. This result is reasonable since sharpness method considers a value averaged over time domain. Similar results are attained with roughness metrics since this analysis focuses on high frequency modulation. However, filtered loudness levels, kurtosis and modulation index of filtered noise shows an indication of degradation in interior sound quality with diesel clatter presence. The change in modulation index may look negligible, but the 0.03 difference is quite high for this metric. For instance, a change of 0.1 modulation index stands for the difference between a gasoline engine and an agricultural diesel engine.

4.1.3 Frequency Modulation Analysis

The modulation index analysis is capable of addressing the issue in more details. With this analysis, it is possible to examine the modulation frequencies and the carrier frequency. As a rule of thumb, the half engine order harmonics will be dominant in modulation frequencies. A well designed engine should only have

modulations around its main firing order frequency. Different results indicate a combustion instability problem between cylinders and/or firing cycles.

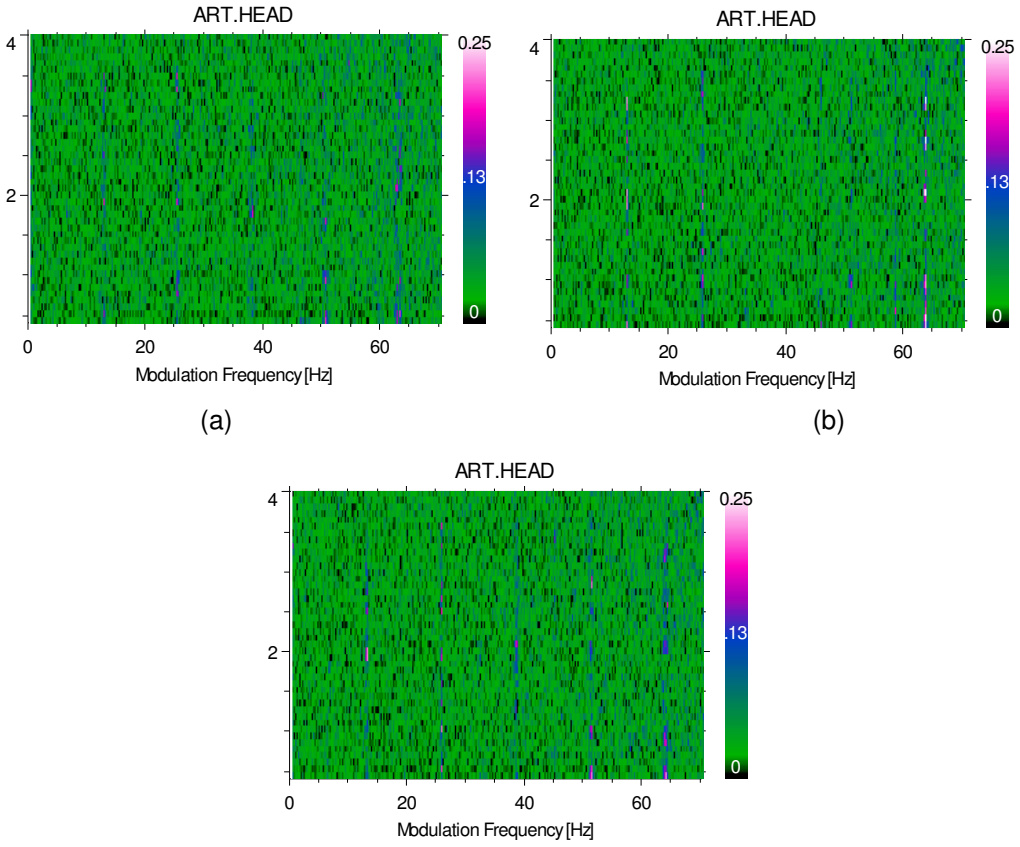

Figure 4.3: The frequency modulation analysis for the three sample recordings (a), (b) and (c) with first engine control unit.

The results for modulation analysis of first three samples are shown in Figure 4.3. The presence of half engine orders are indistinct in the plots except the second sample. The second sample has relatively high 2.5 engine order modulation than the others.

The modulation analysis is also performed for the remaining three samples as well. In Figure 4.4, it is clearly visible that the modulations around half engine orders increase. Especially 0.5 and 1.0 engine order modulations are highly pronounced in the recordings with second engine control unit. The carrier frequency, in other words the frequency that has been modulated, is between 800-4000 Hz. A slight increase in 2.5 engine order modulation is also present, however it is not as clear as it is for 0.5 and 1.0 engine order modulation.

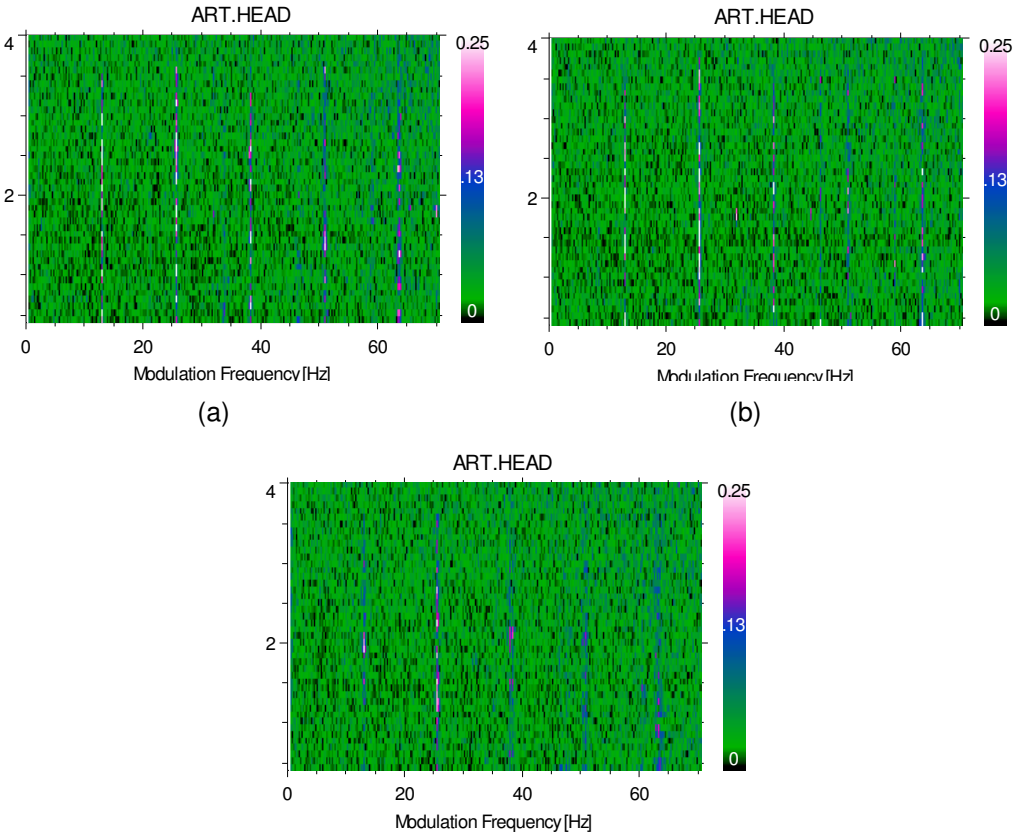

Figure 4.4: The frequency modulation analysis for the three sample recordings (a), (b) and (c) with second engine control unit.

The difference can also be displayed by only taking the modulations at engine order frequencies into account. The result will be a two dimensional plot and it can be presented as a bar graph as shown in Figure 4.5.

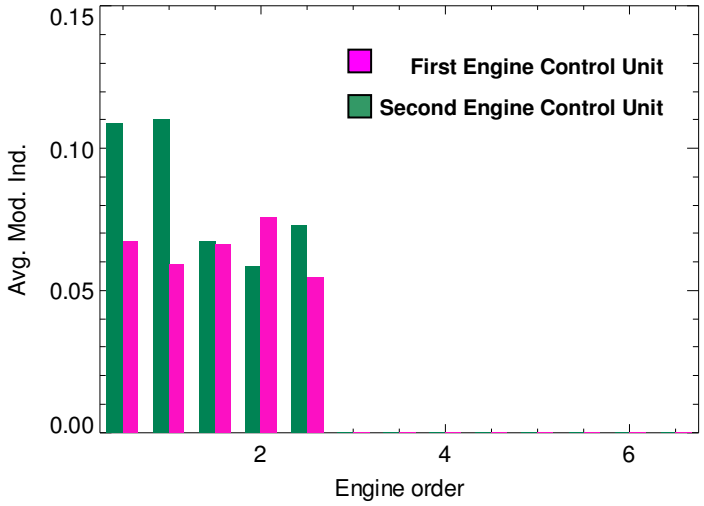

Figure 4.5: Average modulation index analysis for engine order harmonics. Second recording samples are used for each case.

As the final part of the frequency modulation analysis, listening studies have been performed. For this reason, with ModFil software, each engine order modulation has seperately been removed from the sound file and the changes in subjective perception is evaluated. The best result is achieved with the removal of 0.5, 1.0 and 2.5 engine order modulation. However, only cancelling 0.5 and 1.0 engine order modulations gave satisfactory sound quality as well. The listening study chart is shown below:

Table 4.3 : Listening Study Chart for Engine Order Modulation Removal

	0.5 Order	1.0 Order	1.5 Order	2.0 Order	2.5 Order
Base	-	-	-	-	-
Iter 1	-	*	-	-	-
Iter 2	-	*	-	-	*
Iter 3	*	-	-	-	-
Iter 4	*	-	-	-	*
Iter 5	*	*	-	-	-
Iter 6	*	*	-	-	*
Iter 7	*	*	-	*	*
Iter 8	*	*	*	*	*

As an example of modulation removal, “Iter 5” sound is compared with base sound in Figure 4.6. 0.5 and 1.0 engine order modulations completely vanishes.

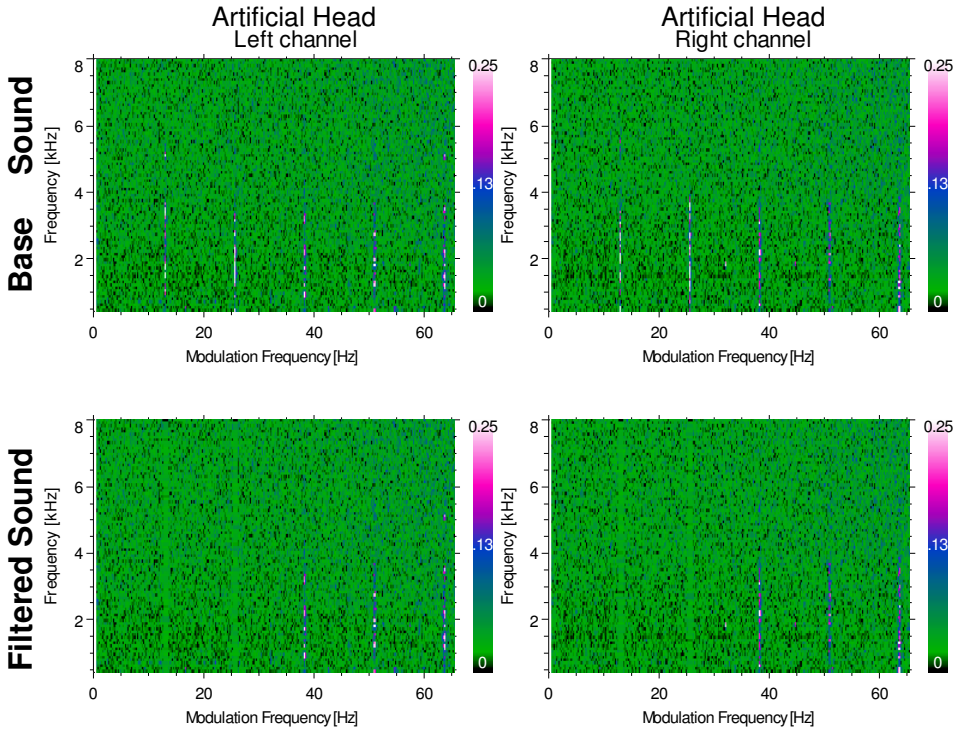

Figure 4.6: Plots showing base sound frequency modulation and the frequency modulation after the removal of 0.5 / 1.0 EO modulations.

4.2 Sound Generation for Combustion Noise Related Issue Detection

In the previous section, it has been concluded that half and first engine order modulation causes diesel clatter in the case study. However, the physics behind these symptoms are not very clear at this phase of study. For engines having four cylinders, previous studies of Heinrichs (2006) enlighten these modulations and propose possible combustion instabilities as a root cause. But lack of frequency modulation analysis experience with five cylinder engines prevents a conclusion with only frequency modulation analysis of interior sound.

In order to predict the extent of combustion instability, a basic five cylinder engine model is developed to simulate numerous variations of cylinder combustion pressure amplitudes and timing. For this reason, each cylinder is treated as a unique impulse signal generator.

During the combustion process in one cylinder cycle-to-cycle fluctuations occur. The degree of these fluctuations defines the cycle-to-cycle stability of the combustion process. In the model, the impulse generators are fed by a counter triggered every 0,05 ms of the simulation time. As a result, the audio sampling frequency is set to 20 kHz.

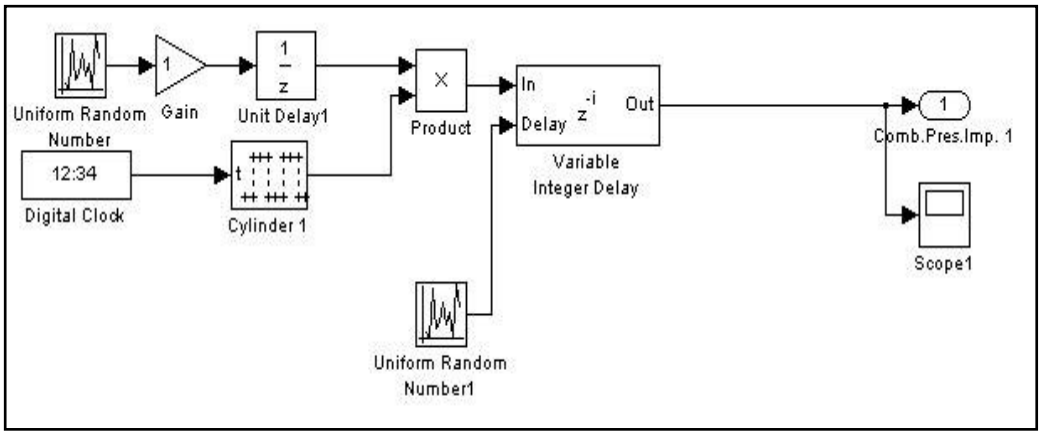

Figure 4.7: Scheme showing the combustion pressure signal generation from a cylinder.

The signal generator produces a periodic impulse signal aligned to the firing period of a single cylinder revoluting at 1500 rpm. In other words, for every 1600 samples, the signal generator produces an impulse input. The width of the impulse signal is set to 130 samples, which corresponds to 55^{o} of crankshaft angle. The combustion amplitude and timing variation is added to the signal generator with the help of

uniform random number generators. One of the random generator is multiplied with impulse generator signal to differentiate amplitude from cycle to cycle. Another random number generator defines the delay of the impulse signal by giving an input to the variable integer delay block. Thus, the block gives random sample delays which is defined by random number generator. A scheme of signal generator from one particular cylinder is shown in Figure 4.7.

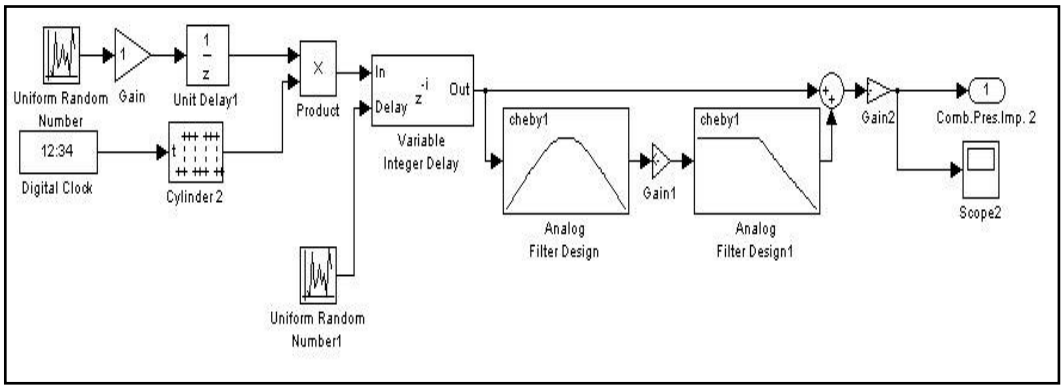

Figure 4.8: Cylinder combustion signal generator with parallel filters

Beside the sound generation with impulse signal generators, it is possible to manipulate signal with additional filters. In this manner, any variations in combustion pressure spectrum can be given as an input to the generated sound. The aim for adding filters is to create a similar frequency modulation analysis plot with the measured data.

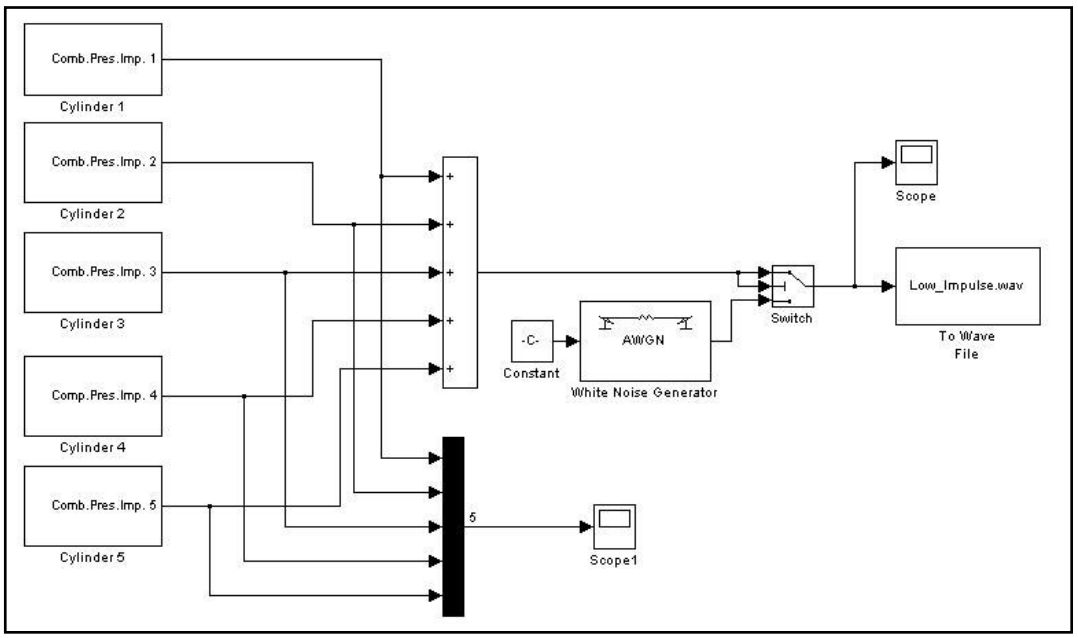

Figure 4.9: Overall five cylinder engine model for combustion noise generation

Finally, all generated signals from five cylinder subsystems is added together as an engine system. A white noise is inserted to the engine model, which stands for the flow noise and accessory noise. The presence of white noise contributes to the realistic visualization of frequency modulation analysis of generated noise files. The amplitude of white noise is aligned to have identical plot with the first engine control unit data. However, a better simulation can be produced with adding tonal components as sine signal generators. The frequency of these signal generators can be aligned to the pumps in the accessory components. But the scope of this study does not cover these aspects of sound generation.

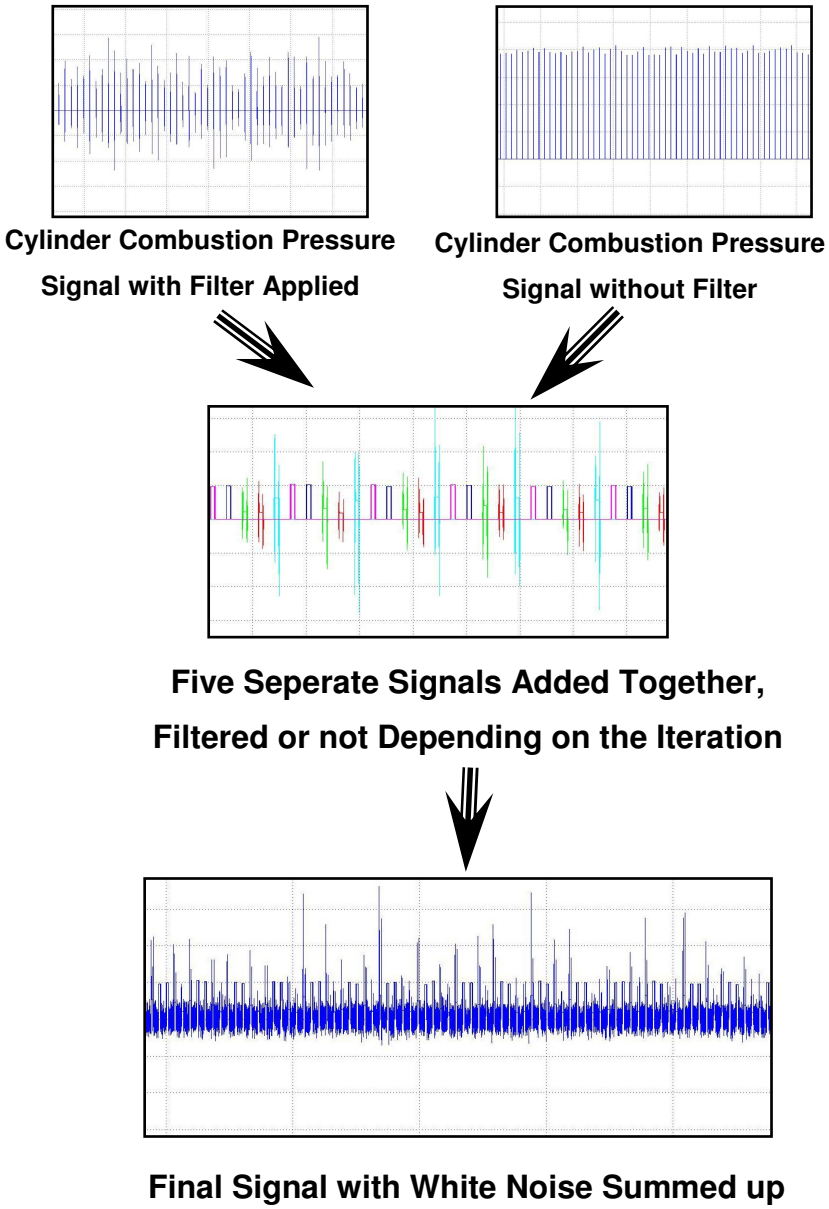

Figure 4.10: Scheme showing the principle and operations of direct combustion noise generation model

The model is used to generate combustion noises with different settings of combustion pressure amplitude, combustion timing and combustion pressure spectrum. For the base sound file, 5% cycle-to-cycle amplitude and ±2 ms ignition timing variation is preferred. On the other hand, no cylinder-to-cylinder variation is present in this file. These values are derived from the investigation of Hastings (2004) on several diesel engines. Combustion pressure spectrum is manipulated between 800 and 4000 Hz in order to get similar results with real life measurements. The iterations used in this study are listed in Table 4.4.

Table 4.4 : Iterations for Simulink Combustion Noise Generation

		Cyl 1				Cyl 2				Cyl 3				Cyl 4				Cyl 5			
Iter No	File Name	Ampl.	Cy-to-Cy Ampl.Var.	Cy-to-Cy Time Var.	Pres. Spect.Var	Ampl.	Cy-to-Cy Ampl.Var.	Cy-to-Cy Time Var.	Pres. Spect.Var	Ampl.	Cy-to-Cy Ampl.Var.	Cy-to-Cy Time Var.	Pres. Spect.Var	Ampl.	Cy-to-Cy Ampl.Var.	Cy-to-Cy Time Var.	Pres. Spect.Var	Ampl.	Cy-to-Cy Ampl.Var.	Cy-to-Cy Time Var.	Pres. Spect.Var
1	Baseline	0,2	0,95-1,05	2ms	-	0,2	0,95-1,05	2ms	-	0,2	0,95-1,05	2ms	-	0,2	0,95-1,05	2ms	-	0,2	0,95-1,05	2ms	-
2	Cyl4 High	0,2	0,95-1,05	2ms	-	0,2	0,95-1,05	2ms	-	0,2	0,95-1,05	2ms	-	0,3	0,95-1,05	2ms	-	0,2	0,95-1,05	2ms	-
3	Cyl4 Random High	0,2	0,95-1,05	2ms	-	0,2	0,95-1,05	2ms	-	0,2	0,95-1,05	2ms	-	0,3	0,80-1,20	2ms	-	0,2	0,95-1,05	2ms	-
4	Cyl3&4 High	0,2	0,95-1,05	2ms	-	0,2	0,95-1,05	2ms	-	0,3	0,95-1,05	2ms	-	0,3	0,95-1,05	2ms	-	0,2	0,95-1,05	2ms	-
5	Cyl3&4 Random High	0,2	0,95-1,05	2ms	-	0,2	0,95-1,05	2ms	-	0,3	0,80-1,20	2ms	-	0,3	0,80-1,20	2ms	-	0,2	0,95-1,05	2ms	-
6	Cyl2&4 High	0,2	0,95-1,05	2ms	-	0,3	0,95-1,05	2ms	-	0,2	0,95-1,05	2ms	-	0,3	0,95-1,05	2ms	-	0,2	0,95-1,05	2ms	-
7	Cyl2&4 Random High	0,2	0,95-1,05	2ms	-	0,3	0,80-1,20	2ms	-	0,2	0,95-1,05	2ms	-	0,3	0,80-1,20	2ms	-	0,2	0,95-1,05	2ms	-
8	Cyl4 Filtered	0,2	0,95-1,05	2ms	-	0,2	0,95-1,05	2ms	-	0,2	0,95-1,05	2ms	-	0,2*	0,90-1,10	2ms	Filter 1	0,2	0,95-1,05	2ms	-
9	Cyl4 Filtered High	0,2	0,95-1,05	2ms	-	0,2	0,95-1,05	2ms	-	0,2	0,95-1,05	2ms	-	0,3*	0,90-1,10	2ms	Filter 2	0,2	0,95-1,05	2ms	-
10	All Random Amp Cyl 4 Flt.	0,2	0,50-1,50	2ms	-	0,2	0,50-1,50	2ms	-	0,2	0,50-1,50	2ms	-	0,2*	0,50-1,50	2ms	Filter 3	0,2	0,50-1,50	2ms	-
11	Cyl 3 4 Random Filtered	0,2	0,95-1,05	2ms	-	0,2	0,95-1,05	2ms	-	0,2*	0,50-1,50	2ms	Filter 3	0,2*	0,50-1,50	2ms	Filter 3	0,2	0,95-1,05	2ms	-
12	Cyl 2 4 Random Filtered	0,2	0,95-1,05	2ms	-	0,2*	0,50-1,50	2ms	Filter 3	0,2	0,95-1,05	2ms	-	0,2*	0,50-1,50	2ms	Filter 3	0,2	0,95-1,05	2ms	-

Filter 1: (BP 1400-3500)*3+LP 3500
Filter 2: (BP 1400-3500)*1.5+LP 3500
Filter 3: Output Signal scaled to 0.3
*: Filters increase the amplitude level of the signal

Frequency modulation analysis is applied to each generated sound file and the plots have been compared with the vehicle passenger compartment measurements. Two of the generated sound files showed similar engine order frequency modulation with the second engine control unit:

- Iteration 8: In this sound, one of the cylinders is set to a higher combustion pressure amplitude and an increase in middle frequency region is introduced.

- Iteration 12; The manipulation of combustion pressure is similar to Iteration 8, but this time it is applied to two cylinders. These two cylinders are not directly after one on the other in the firing sequence. For example, if the firing sequence is 1-2-4-5-3, then the cylinders with different combustion pressure spectrum can be 1-4, 2-5 i.e.

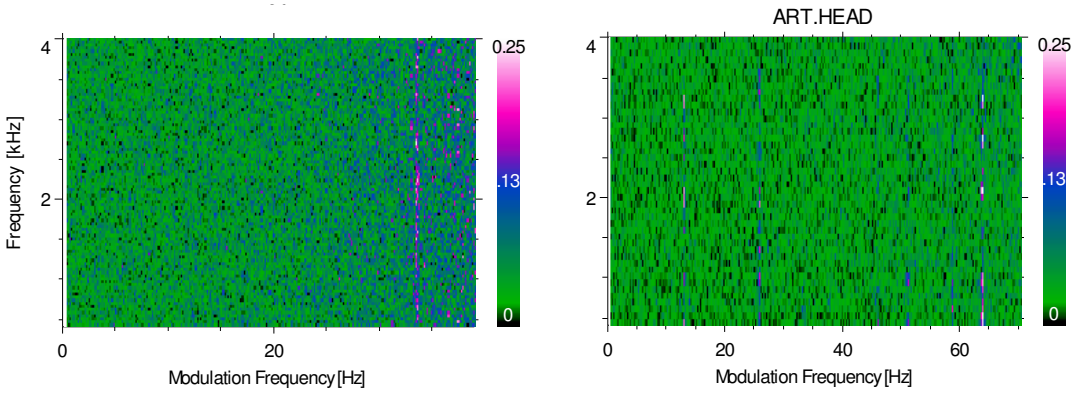

(a)

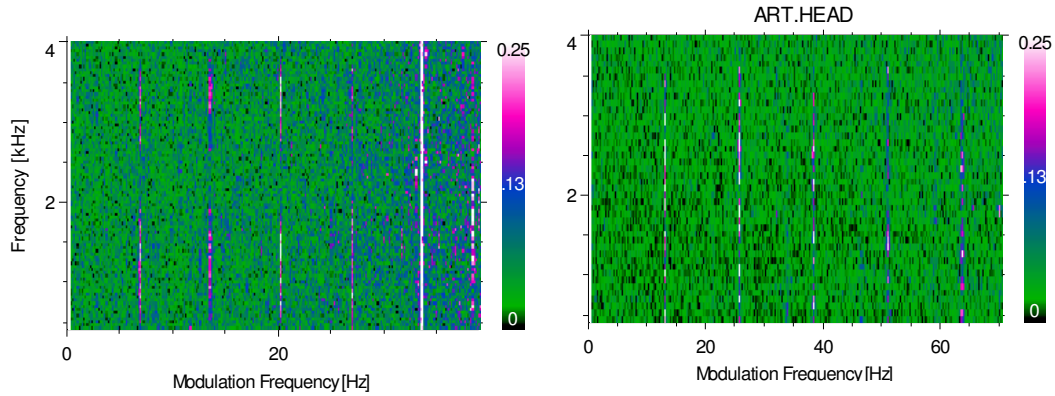

(b)

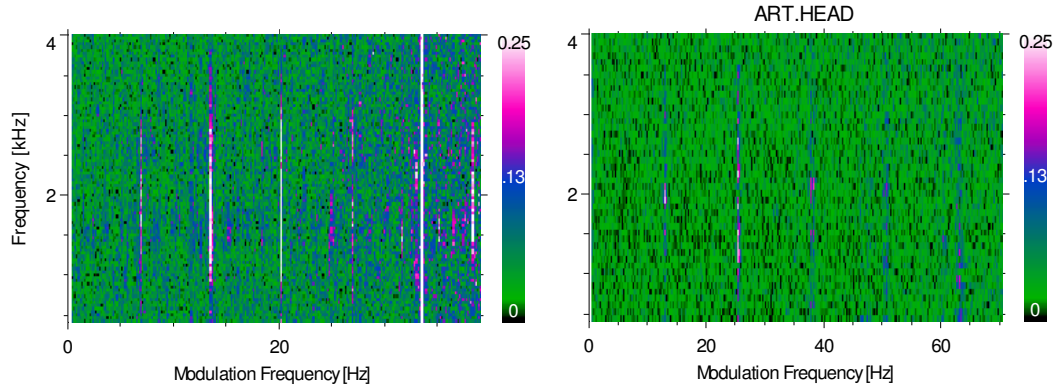

(c)

Figure 4.11: Plots showing the comparison of a) base generated sound file (on the left) with the measurrement with the first engine control unit (on the right) b) Sound file of Iteration 8 (on the left) and second sample measurement with second engine control unit (on the right) and c) Sound file of Iteration 12 (on the left) and third sample measurement with second engine control unit (on the right).

The frequency modulation analyses of generated sound files show a fine correlation with half and first engine order modulations in real life measurements. However, 2.5 engine order modulation is very dominant in the generated sound files. The reason of this high estimation can be because of high disturbance of higher frequency modulations in the passenger compartment. As the repeating sequence of sound increases, the harder it gets for the ModFil to seperate the combustion related noise from other sound sources.

Combustion pressure measurements have been performed to correlate the findings of this study. This next investigation will be explained in details in next chapter. Frequency modulation analysis diagrams of other iterations are presented in Appendix A.

4.3 Examination of Direct Combustion Noise Excitation Mechanism

In Chapter 3, the relationship between cylinder combustion pressure and radiated noise is summarized. Briefly, the source of the combustion noise excitation mechanism is the combustion pressure inside the chamber. The engine block attenuates this excitation by acting as a high-pass filter. Then this excitation transforms into surface vibration and it radiates through the surface of the engine. The noise is transferred to the passenger compartment through various paths, structureborne or airborne. But this time, higher frequencies are attenuated very well, with sufficient body noise reduction.

In order to correlate the findings in previous section, another test vehicle is instrumented with pressure sensors and a near-field microphone. Thus, combustion pressure and radiated noise data is acquired simultaneously.

4.3.1 Test Conditions and Measurement Setup

The vehicle is subjectively evaluated before the acquisition of cylinder pressure and noise signals. The reason for this evaluation is to detect the best engine operation point on the engine speed-load map where diesel clatter is clearly audible. With the information gained from this evaluation, the data acquisition is performed at two different engine speed-load operating points. The first operating point is chosen as 1350 rpm / 40% throttle position, since it is nearer to the initial torso measurement. Other point is determined as 2100 rpm / 65% throttle position. This engine operating condition is useful to simulate tip-in maneuver during high speed cruising, take-over

another vehicle or driveaway acceleration to join a highway. The values of main parameters affecting the combustion process are listed in Table 4.5.

Table 4.5 : Engine Operating Parameters for Constant Engine Speed-Load Interior Noise Recordings.

	Condition 1	**Condition 2**
Engine Speed	1350 rpm	2100 rpm
Throttle Position	40%	65%
Main Injection Quantity	38,2 mm^3/stroke	42,5 mm^3/stroke
Main Start of Injection	1.95° BTDC	2.2° BTDC
Pilot Injection Volume	1,5 mm^3/stroke	1,5 mm^3/stroke
Pilot Injection Seperation	12.2° CA	10.1° CA
Rail Pressure	100 MPa	135 MPa
EGR Rate	0%	0%

For the measurement setup, five GU12P type pressure measuring probes are installed to the engine with a glow plug adapter. The detailed sketches of pressure sensor installation and other specifications about the sensors are available in Appendix B. The pressure sensors are connected to the SQLab III frontend via an AVL preamplifier, which is fed by the vehicle batteries.

Beside the pressure sensor installation, a B&K 4189 type microphone is located to the near-field of powerplant. The air intake manifold side is preferred in order to avoid turbocharger related noises on the exhaust manifold side. Moreover, components of fuel injection system is on the intake manifold side which acts as one of the impulsiveness sources. Finally, the data acquisition and storage is performed with an IBM Thinkpad laptop.

4.3.2 Analysis of the Measured Data

First aim of this analysis is to correlate the findings in previous chapter with the real life data. Secondly the time history of cylinder pressure data are inspected in order to find relationship between the pressure traces, frequency spectrum and radiated noise data. Finally, pressure data is investigated in details to determine the cylinder-to-cylinder and cycle-to cycle variations.

4.3.2.1 Frequency Modulation Analysis Correlation with Measured Data

Frequency modulation analysis of measured near-field microphone sound pressure data shows strong similarity with the previously measured artificial head data. The half engine order content between 1500-4000 Hz shows up in the engine bay

measurements as well. On the other hand, the main firing order modulation is more pronounced near to the engine. This symptom is normal since inside the passenger cabin, masking of other noises such as panel resonances or wind noise will reduce the emphasizing of this modulation. Figure 4.12 shows the result of this analysis.

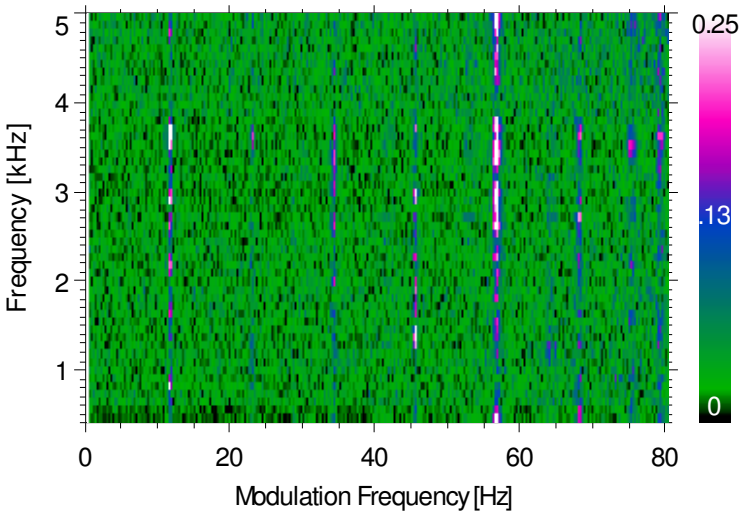

Figure 4.12: Modulation analysis of engine bay near field microphone

The assumption derived from the sound generation study was the presence of one or two cylinders with higher amplitude pressure spectrum in the complained frequency range. Therefore, the combustion pressure spectrums and level traces are compared with the modulation analysis shown above (Figure 4.13 & 4.14).

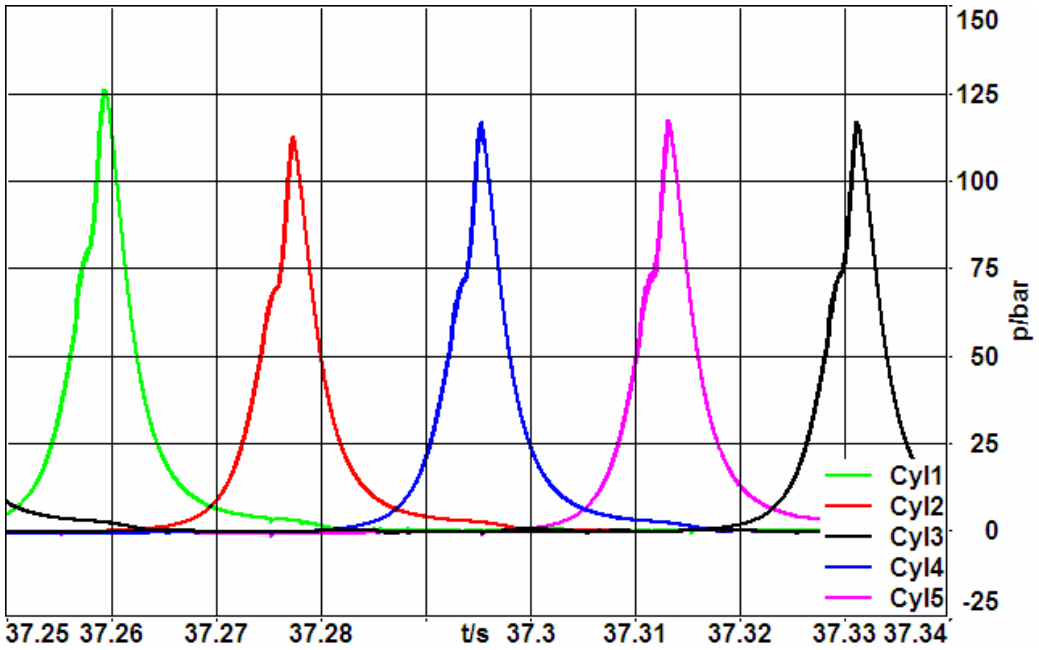

Figure 4.13: Combustion pressure levels of all five cylinders

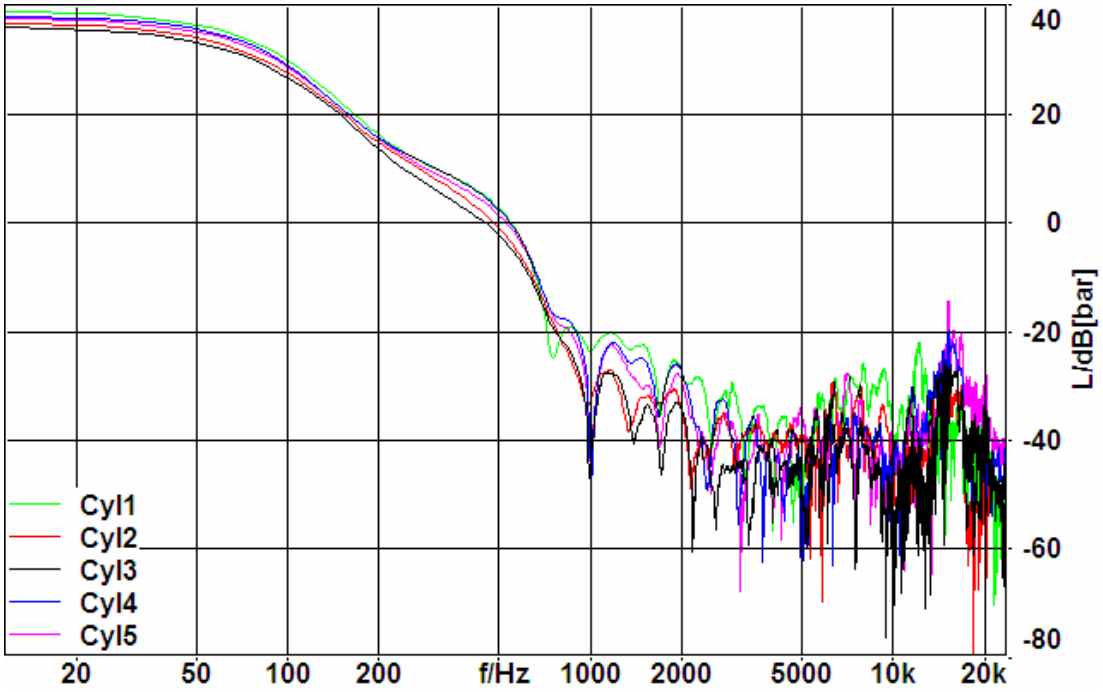

Figure 4.14: Combustion pressure spectrum of all five cylinders

The data shown on these plots are acquired during two revolutions of crankshaft. The firing sequence starts with first cylinder and follows up in the order of second, fourth, fifth and third. The pressure frequency spectrums are the result of post-processing this complete one firing cycle of the engine.

The overall combustion pressure level of first cylinder is significantly higher than the remaining cylinders. Besides, this higher level of combustion pressure has a major affect over the frequency spectrum in frequencies over 1 kHz. On the other hand, fourth and fifth cylinders; and second and third cylinders exhibit similar frequency spectrum contents in this frequency range. The spectrum tends to increase again after 10kHz, due to the combustion chamber cavity modes. All the findings above are strongly correlated with the expectations from previous studies. The next step is to show the relationship between the noise radiation and the cylinder pressure traces.

4.3.2.2 Relationship between Impulsive Noise and Combustion Pressures

When the engine is running at 1350 rpm, one cycle to complete combustion in all five cylinders take two revolutions of the crankshaft, which means 90 ms in time domain. In other words, a combustion and consequently impulsive noise will be radiated for every 18 ms. As a result; FFT analysis will be limited to examine these

rapid changes in time domain because of the decreasing resolution in frequency domain. For this reason, wavelet analysis is performed in the time segment analysed for modulation analysis correlation. The close-up of the pressure traces will provide some information about the frequency content of the combustion according to the Föller estimation. In Figure 4.15, the combustion pressure traces of five cylinders are shown. The fifth cylinder exhibits higher oscillations with respect to other cylinders. This is reflected to the frequency spectrum as an increase over 10kHz content. On the other hand, oscillation in the first cylinder has a lower amplitude and the period is slightly higher. These findings are hardly differentiated in inspection with eye. But, the frequency spectrum clearly shows a higher content in 1-5kHz range.

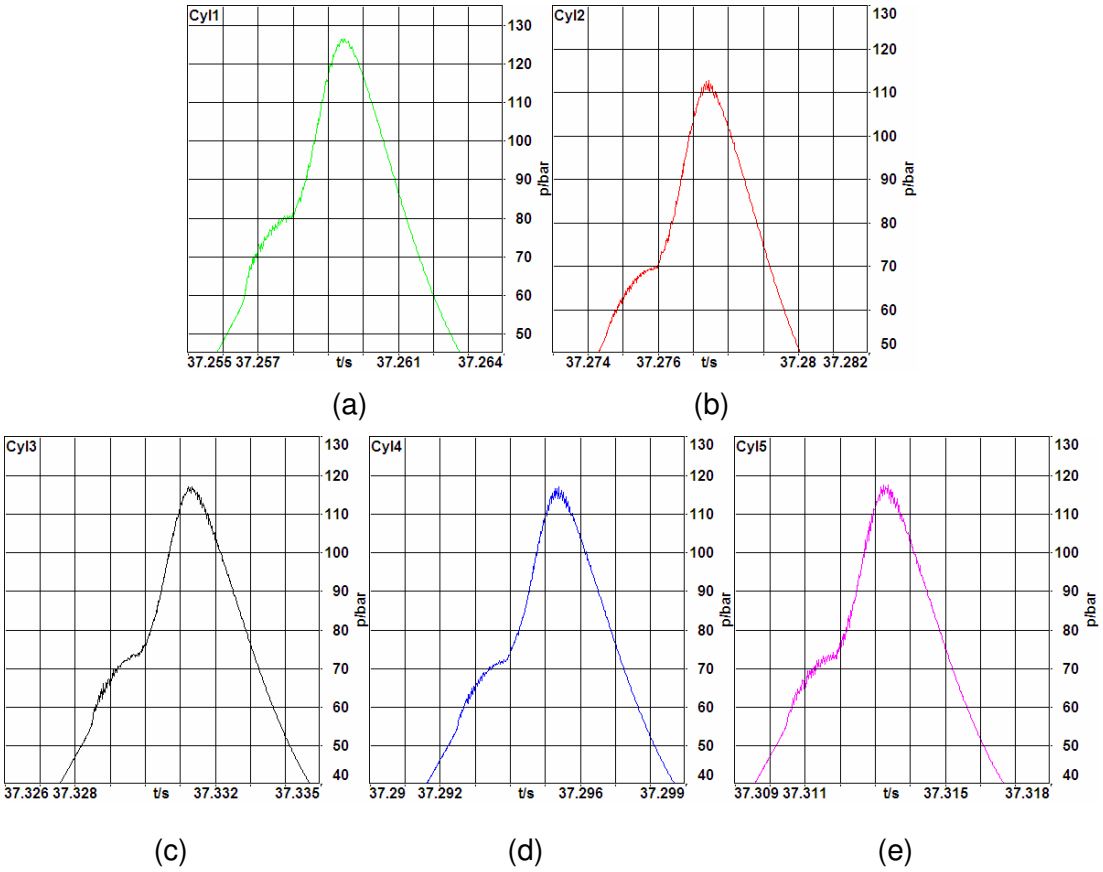

Figure 4.15: Close-up plots for the cylinder pressure traces

Wavelet transform is applied to cylinder pressure and radiated noise data in order to compare the radiated noises of these cylinders having different frequency spectrum. First, second and fifth cylinders are chosen since they exhibit different characteristics. For the same time segment, the near-field microphone data and pressure spectrums are shown in Figure 4.16 (a), (b) and (c).

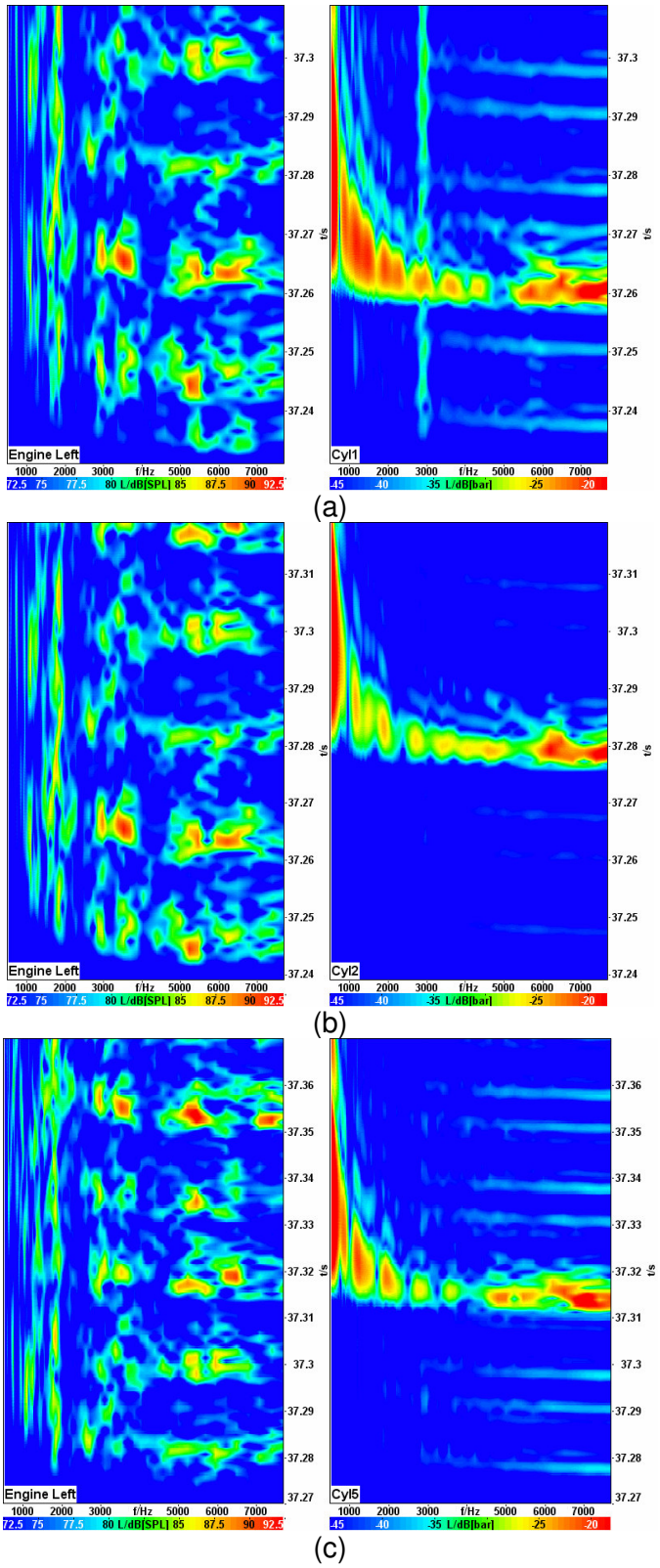

Figure 4.16: Comparison of radiated noise and combustion pressure spectrum. (a) first cylinder (b) second cylinder and (c) fifth cylinder. The diagram on the left shows the wavelet analysis of radiated noise whereas the diagram on the right shows the frequency spectrum of combustion pressure wavelet analysis of corresponding cylinder.

The examination of radiated noise plots points out resonance frequencies, or structural attenuation weakness of engine block around certain frequencies. These frequency ranges are 1800, 3000, 3500, 5300 and 6250 Hz. At these frequencies, higher radiated impulsive noise levels are measured when the combustion happens in any of the cylinders. However, variance can be seen in the structural attenuation behaviour of the engine from cylinder to cylinder. For instance, at 6kHz region, even though the combustion pressure excitation of first cylinder is similar to second one, the radiated noise levels of second cylinder is far below than the other. The reason for this different behaviour between cylinders can be the proximity of first cylinder to the front side of the engine. Russell (1987) proposes the weakness of side and front covers as the main drop in structural attenuation in 1-5 kHz region. But for the lower frequency range, the structural response to the excitation of cylinder pressure is similar: higher for first, moderate for fifth and least for second cylinder.

4.3.2.3 Body Noise Reduction

Body attenuation should be kept in mind when investigating the affect of engine radiated impulsive noise over the interior sound quality. The radiated noise are transfered to the passenger compartment in two ways: structureborne and airborne. In the case study of diesel impulsiveness, the presence of the noise is between 1kHz and 4 kHz. For this reason, it can be concluded that the main transfer path is the airborne.

The analysis of engine bay near-field microphone shows impulsive noise content between 1.5 and 6.5 kHz. However, in the definition phase, the impulsive content in passenger compartment is addressed at 1-4 kHz region. These numbers point out a better acoustic attenuation of body in higher frequency range. In order to confirm these assumptions, the noise reduction values of body acoustic pack of the test vehicle with longitudinal powertrain is measured.

Test has been conducted with an ISVR high frequency sound source and two B&K 4188 type microphones. The noise reduction is measured reciprocally: sound source in passenger compartment and microphones in engine bay. The results are shown in Figure 4.17. The noise reduction values are presented with two different plots: one point nearer to the front of the engine (first cylinder) and the other closer to the rear (fifth cylinder). The body attenuation of both curves tends to increase after 4kHz. In the concern frequency range, the curves increase in a linear manner.

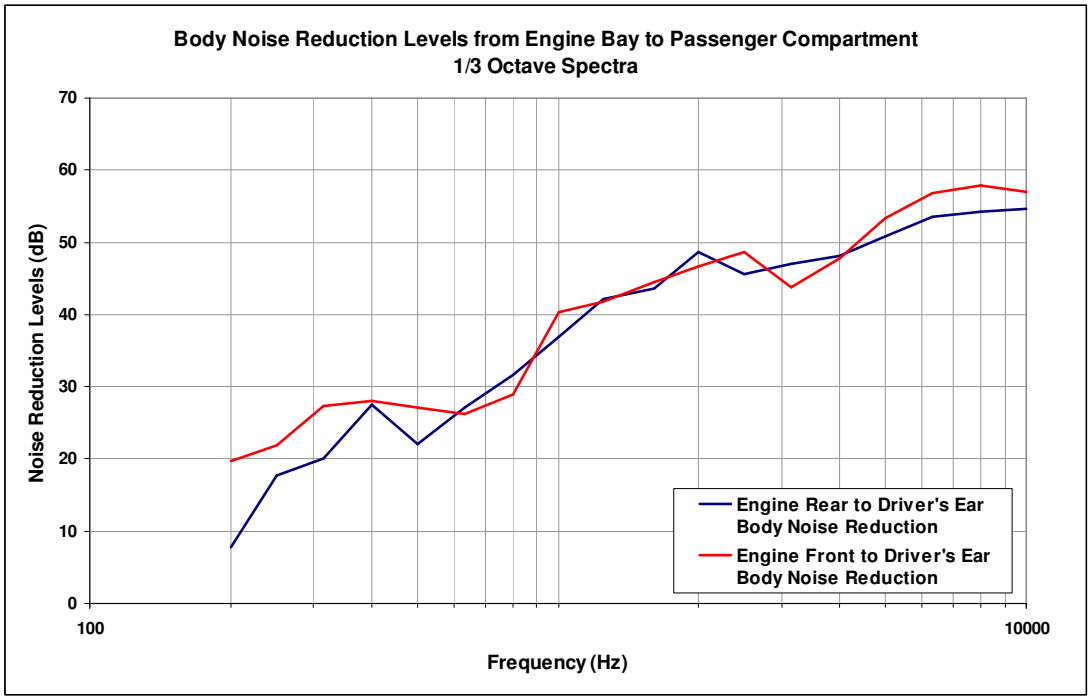

Figure 4.17: Noise Reduction Levels from Engine Bay to Driver's Ear

The figures indicate lower noise reduction in 1600 Hz center frequency in the 1/3 octave band in the rear side of the engine. This would explain the presence of higher impulsive noise content in 1800Hz region in passenger compartment. So, it is obligatory to emphasize over this frequency range when investigating the near-field microphone findings and cylinder pressure data.

Investigation of lower frequency range spectrum of near-field microphone includes similar results with the higher frequency analysis. First cylinder has higher content around 1800 Hz and this excitation is transmitted through the engine block and radiated as the impulsive noise. Figure 4.18 summarizes the findings above, as the wavelet transforms of cylinder pressure spectrum and corresponding radiated noise spectrum for the same time segment.

In the wavelet analysis, the content around 1800 Hz is highest in first and fourth cylinder. In the noise spectrum, this impulses from two cylinerds can be differentiated. Less amount of noise is radiated with the combustion happening in third cylinder. On the other hand, the remaining second and fifth cylinders do not have significant contribution to the issue. The higher excitation of first and fourth cylinder is also confirming the findings from sound generation study, as they have another cylinder in between during the firing sequence.

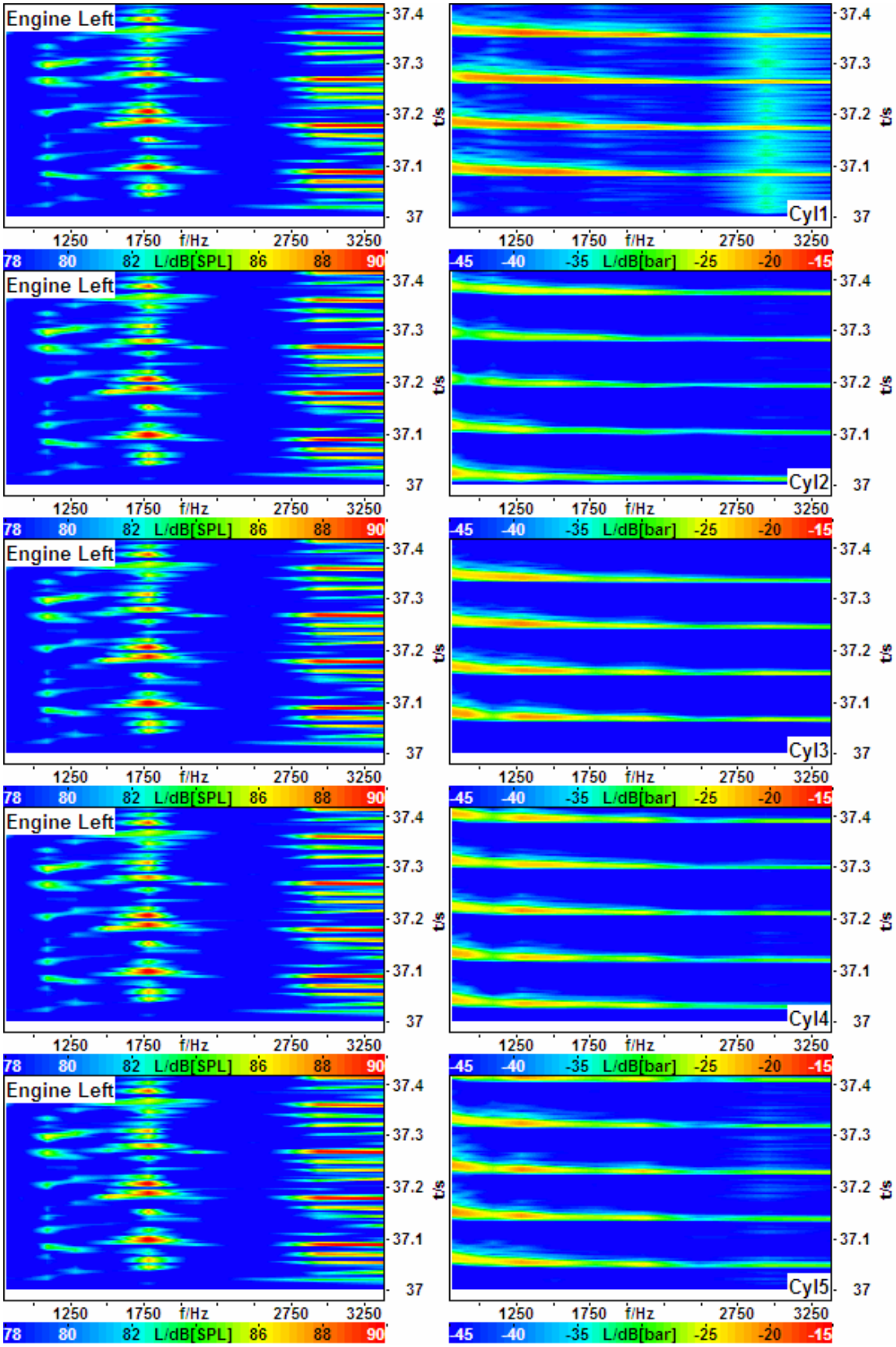

Figure 4.18: Diagrams comparing wavelet analysis of cylinder pressures and interior noise data. Diagrams on the left side presents the near-field microphone frequency spectrum for a time period. Right side diagrams are the corresponding cylinder pressure spectrums for the same time segment.

4.3.2.4 Analysis in Second Engine Operating Point

Investigation of frequency modulation analysis, cylinder pressure levels, frequency spectrum of the combustion pressure and wavelet analysis of corresponding microphone recordings are repeated for this condition as well.

Frequency modulation analysis shows a high 0.5 engine order modulation for the 1-4 kHz region, which is the case for interior noise recordings. As stated in previous chapters, this is assumed to be the result of error states in two cylinders having another cylinder in between in the firing sequence.

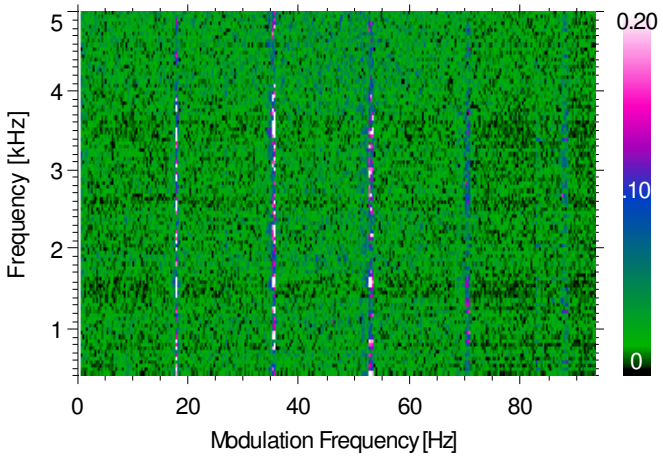

Figure 4.19: Frequency modulation analysis of engine near-field microphone recordings in second operating point.

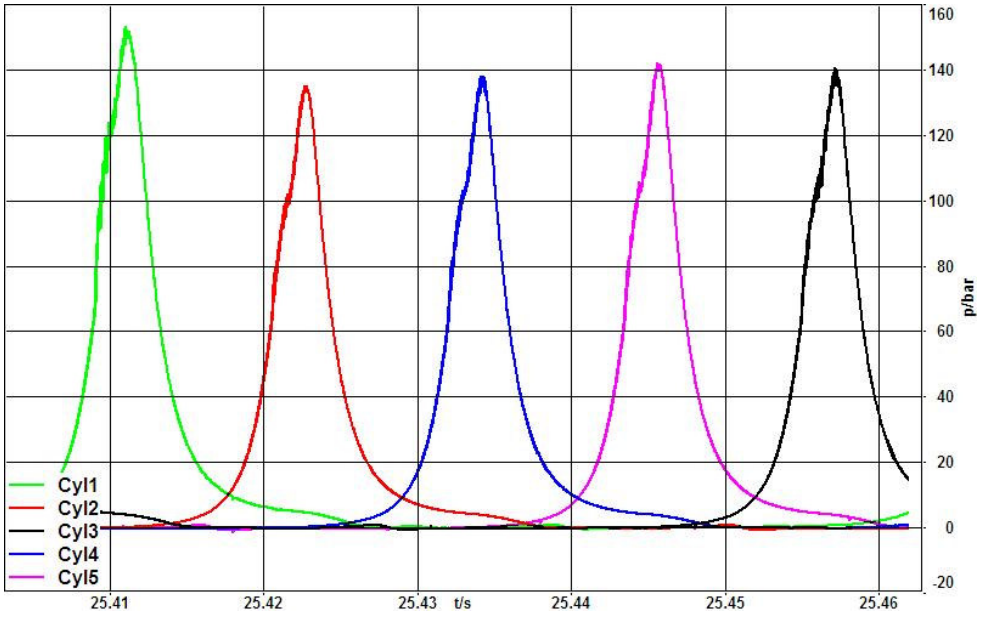

Figure 4.20: Combustion pressure levels for the sample time segment

Combustion pressure levels of first cylinder is higher than the others again for this operating condition (Figure 4.20). High frequency oscillations are the highest for first cylinder. Also considerable oscillations exist in third and fourth cylinders. Combustion pressure trace of second cylinder is the smoothest curve among the others. Effect of these differences in combustion pressure traces are also investigated with FFT analysis of the acquired data.

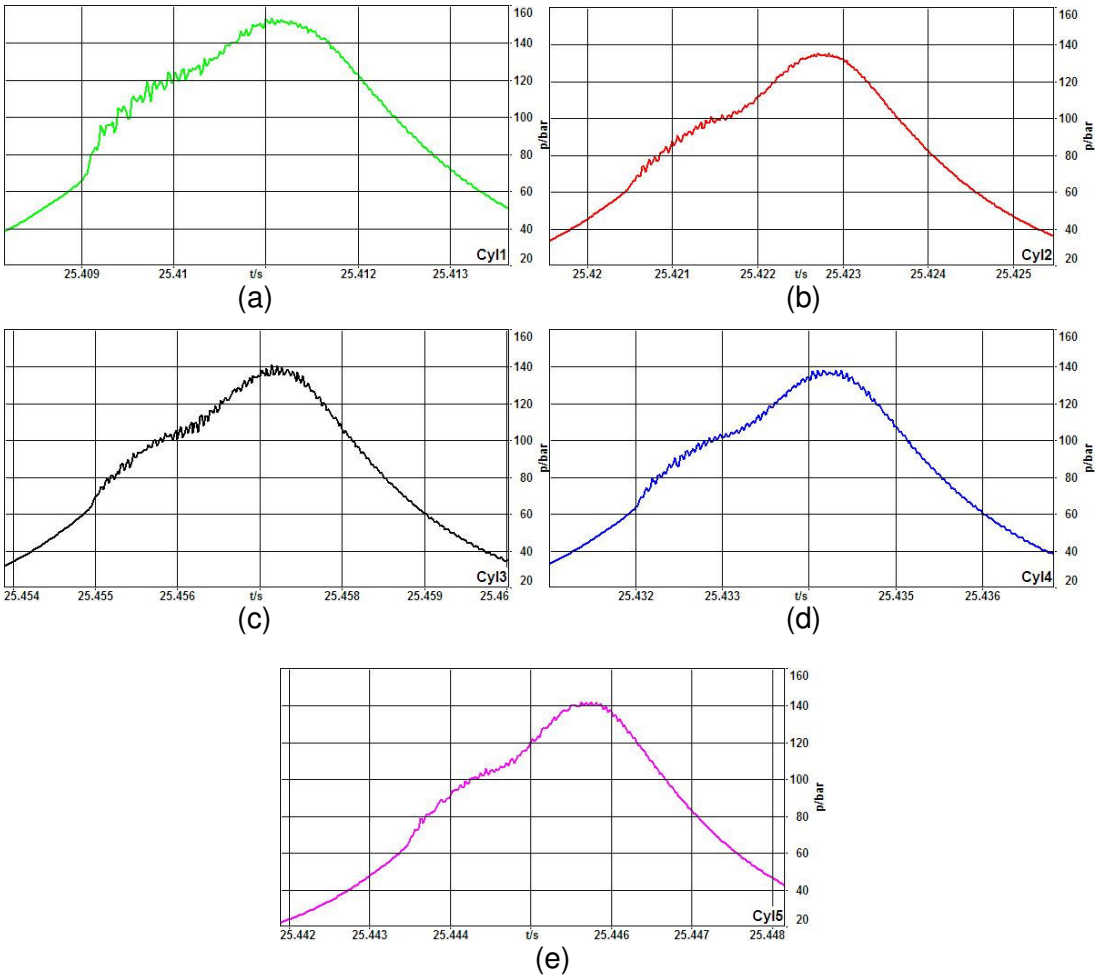

Figure 4.21: Close-up of combustion pressure traces of five cylinders in the sample time segment.

Frequency spectrum of the pressure traces is presented in Figure 4.22. The first cylinder dominates the excitation levels over all the frequency range. On the other hand, third and fourth cylinders give sharp peaks after 10 kHz, explaining the oscillations detected in the examination of pressure traces. Second cylinder excitation remains the lowest, again similar to what has been observed. But it can be concluded that, examination of the oscillations in cylinder combustion pressures do not clearly address the issue. This is mainly due to the masking effect of high frequency content which prevents making an explicit comment about the mid-frequency range.

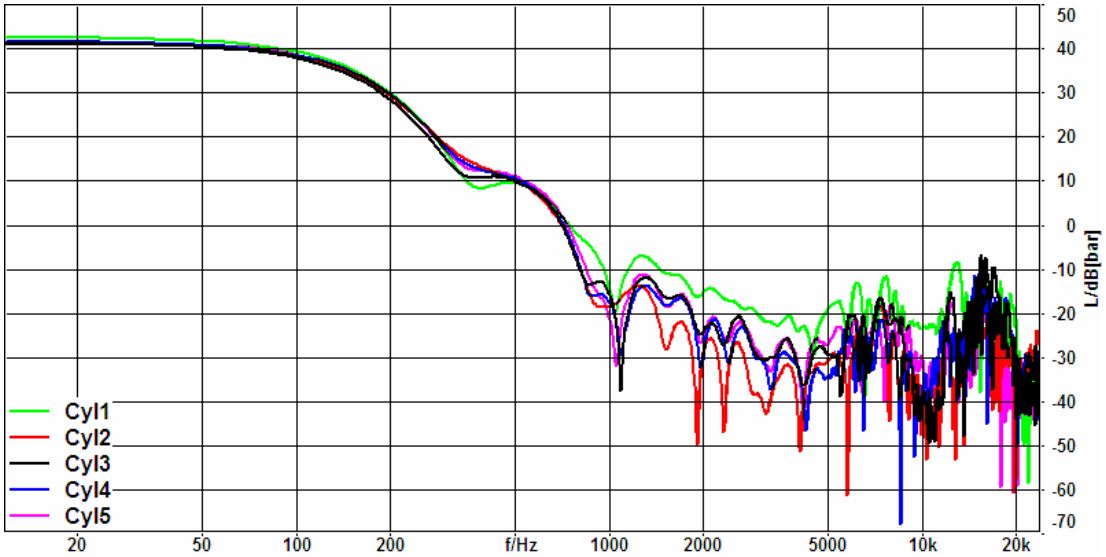

Figure 4.22: FFT analysis of cylinder combustion pressures in the second operation point.

For the final examination of acquired data, wavelet analysis of combustion pressure and corresponding near-field microphone recordings are presented (Figure 4.23). Similar to the previous plots, five diagrams on the left side shows the recordings from microphone data for the same sample time segment. On the right hand side, the diagrams of cylinder pressure wavelet analysis for each cylinder are presented. Thus, a comparison of radiated noise and combustion pressure can be matched in time domain.

For the investigation, frequency content is again divided into three segments: 1800 Hz region, 2.5-3.5 kHz region and the frequency band over 4kHz. For all the three segments, first cylinder produces high level of noise, differentiated by the red zones in the diagrams. For the lower frequencies, other cylinders except second cylinder also contribute to the noise radiation. On the other hand, second cylinder is able to excite as well, but slightly less than the others.

The mid-frequency range is completely excited by first cylinder combustion pressure. All other cylinders have barely perceptible traces in the concern frequencies. This is identical with the FFT analysis of combustion pressures.

In the higher frequencies, some cylinders accompany the first cylinder in noise generation. Fifth cylinder firing at 25.45th second, fourth cylinder just before 25.44th second and third cylinder at 25.4th second are some examples of this. The radiated noise spectrum correlates very well with the combustion pressure excitation spectra derived from each cylinder.

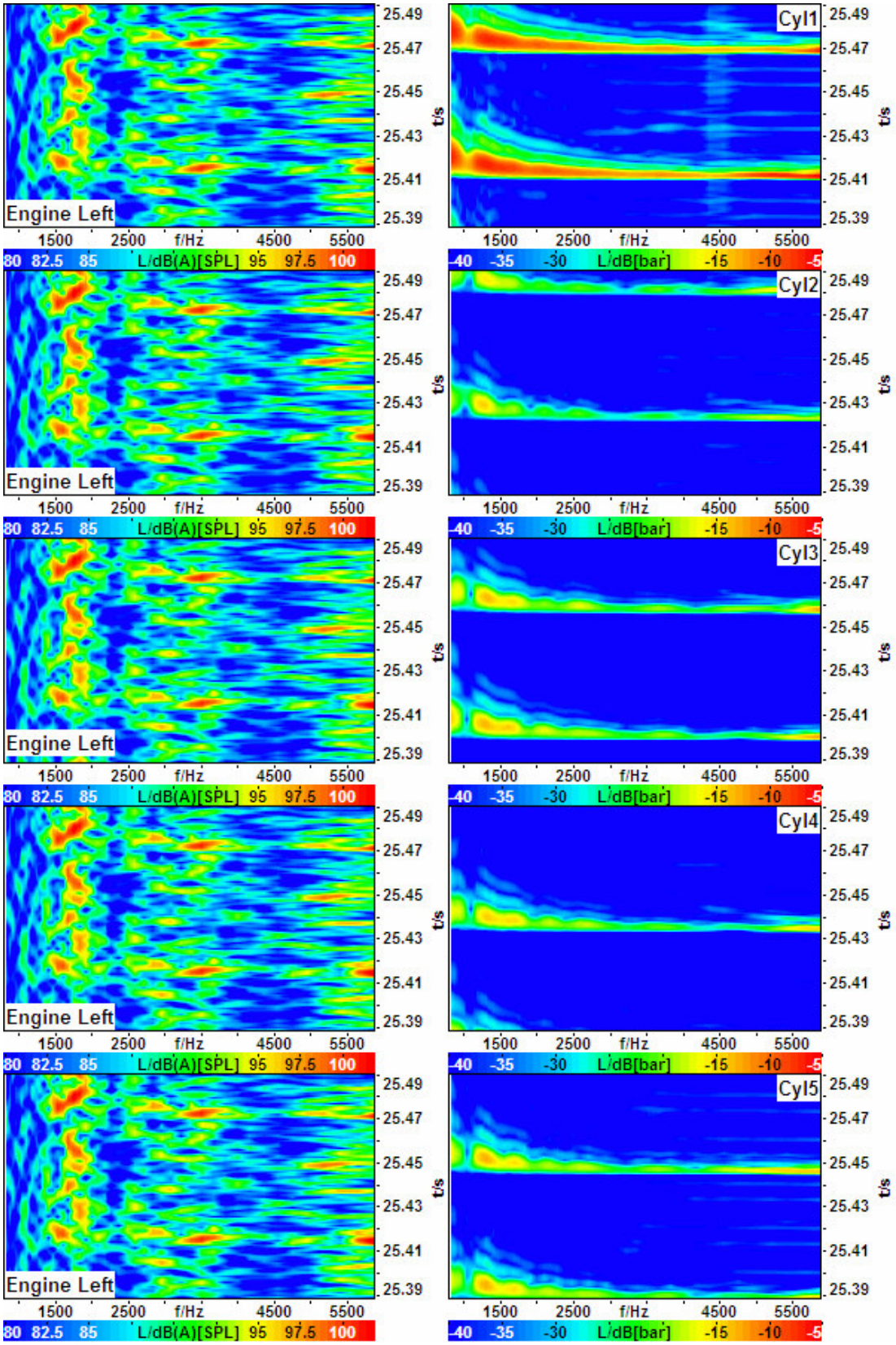

Figure 4.23: Wavelet analysis of acquired combustion pressure and near-field microphone data. The diagrams on the left present the analysis of radiated noise for the same time segment whereas diagrams on the right shows corresponding cylinder pressure diagrams.

4.3.3 Analysis of Pressure First and Second Derivatives

In the previous studies, Kondo et al. (2000) and Alt et al. (2004) proposes a direct relationship between first derivative of pressure time-signal. Additionally, Alt et al. (2000) proposes an estimation for the effect of time signal of combustion pressure on the frequency spectrum.

According to this assumption, the level of lower frequency range is dominated by the area that the cylinder pressure trace sweeps. Around 50 Hz, the peak level of the combustion pressure defines the shape of the curve. Then, the trend of the curve is determined by the first derivative and second derivative of combustion pressure. These variables affect relatively higher frequencies of the frequency spectrum: 250 Hz and higher content in order. Latter is currently the case for investigating the diesel clatter impulsive noise because of the frequency content in 1500-6500 Hz.

The frequency spectrum of combustion pressure and corresponding combustion pressure trace, first and second derivatives are investigated in this part. For both operating conditions, two cylinders with the most distinct combustion pressure frequency spectrum are chosen as samples since they would visualize the differences in a better way.

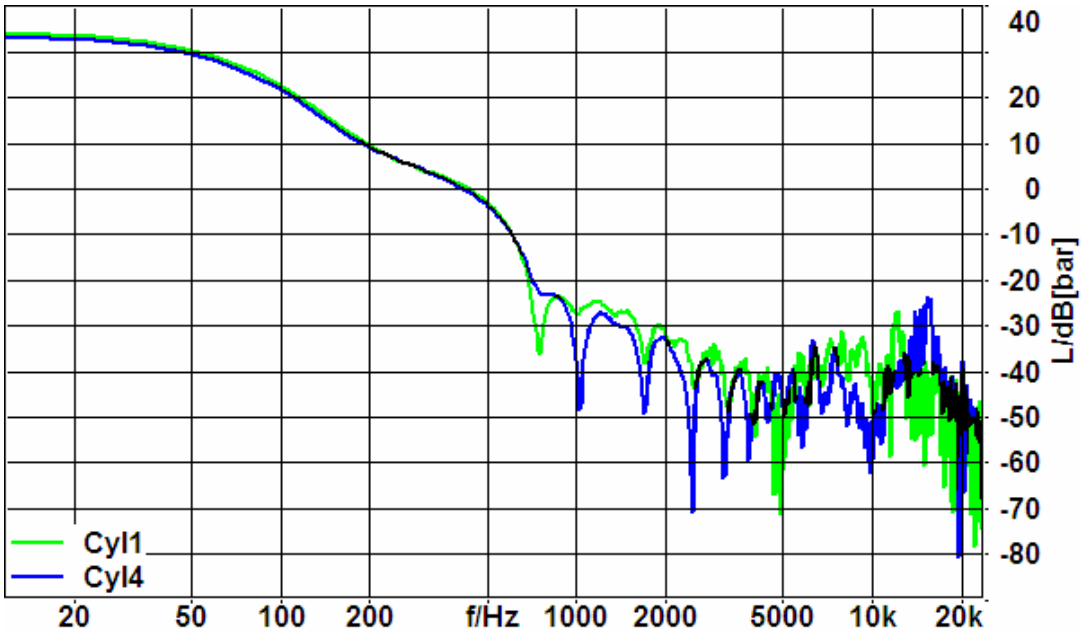

Figure 4.24: Combustion pressure spectrum for cylinder 1 and 4 at 1350rpm, %40 throttle position.

The combustion pressure spectra of first and fourth cylinder is investigated for the first engine operating point. As mentioned before, the first cylinder excitation is

higher than fourth cylinder for all frequency range except the peak at 15kHz (Figure 4.24). This peak can be related to combustion chamber resonances around this frequency range.

The time signal of combustion pressure and its first and second derivatives are presented in Figure 4.25. The overall area below the curve and the peak pressure level is higher for the first cylinder. This difference is also visible in the lower frequency spectrum of two cylinders. However, first derivative is calculated higher for the fourth cylinder. On the other hand, foruth cylinder has a higher excitation only around 750Hz in the frequency spectrum. Moreover, second derivative of fourth cylinder is significantly higher than the other, but in the frequency spectrum, this change is only reflected at around 15 kHz. Therefore, a filter application can give more realistic results of the combustion pressure spectra by eliminating the effect of combustion chamber resonances.

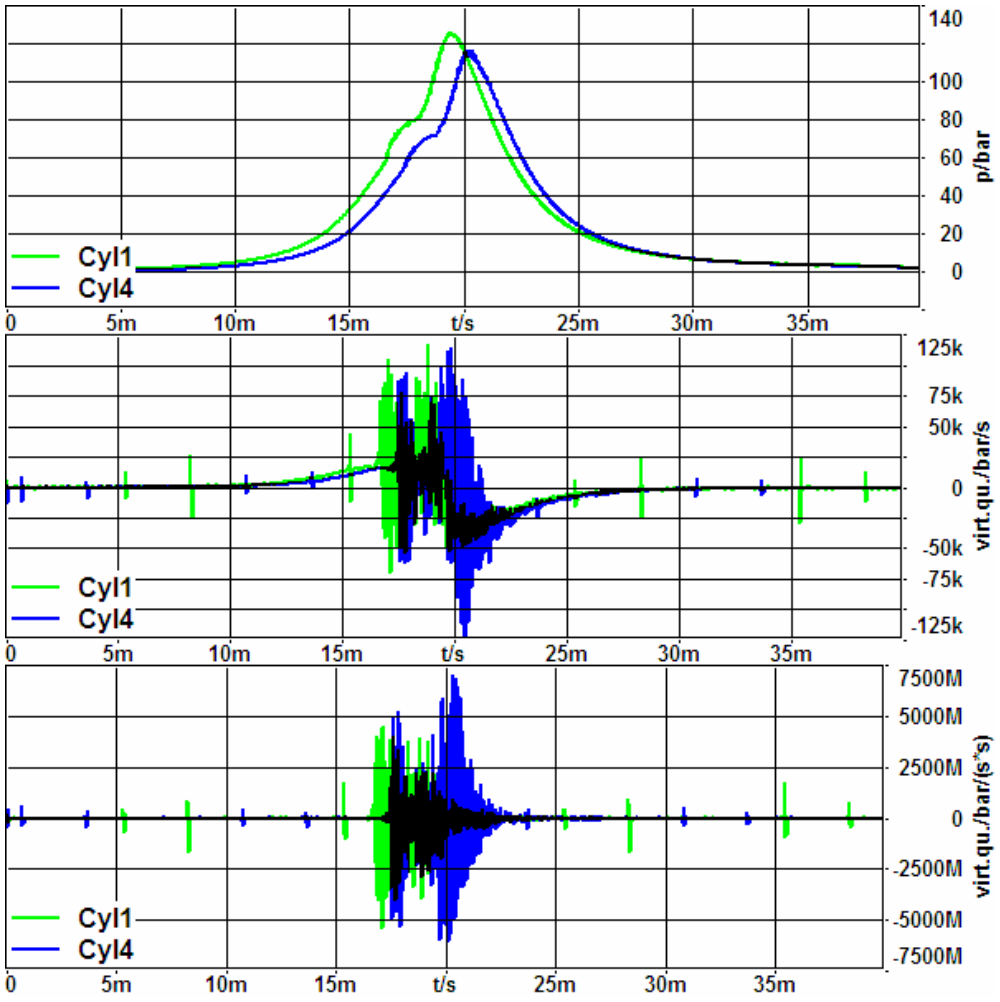

Figure 4.25: Comparing the level (upper diagram), first derivative (middle diagram) and second derivative (lower diagram) of combustion pressure in first and fourth cylinder without filter in the first operating condition.

The differences between the derivatives converge to the results of mid-range frequency spectrum when a low-pass 10kHz filter is applied to the signal (Figure 4.26). The drop of derivative curve levels also indicate high input of higher frequency range in the previous diagrams.

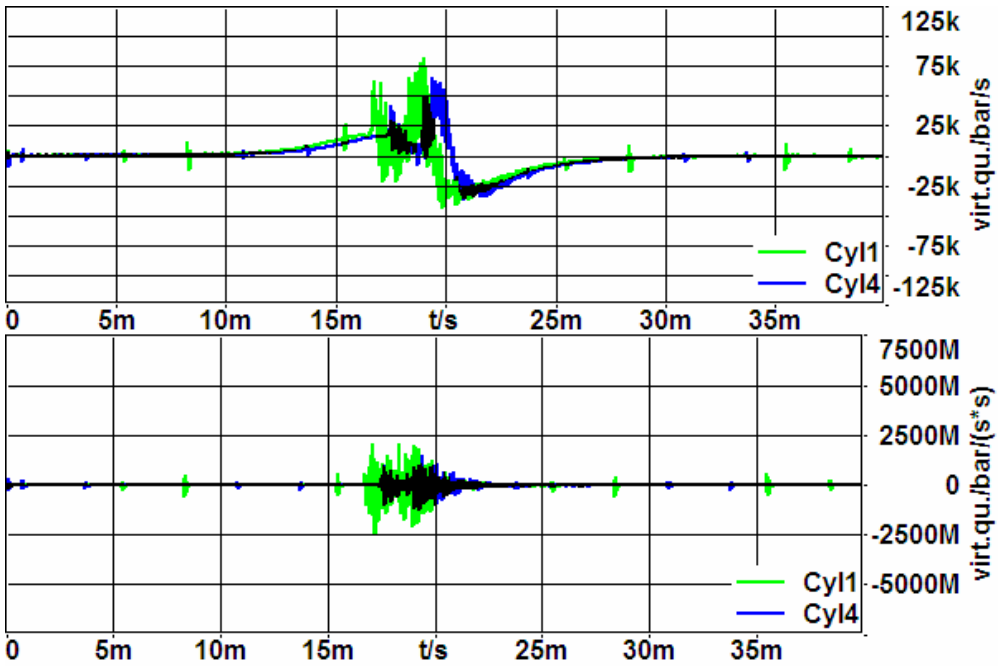

Figure 4.26: Comparing the first derivative (upper diagram) and second derivative (lower diagram) of combustion pressure in first and fourth cylinder with 10kHz low-pass filter.

The same analysis is performed in second operation point comparing the excitation of first and second cylinders. First cylinder excitation is considerably higher than the second over all the frequency range in this example (Figure 4.27). The gap between two frequency spectra decreases as the frequency increases, however especially between 1-12kHz, first cylinder excitation is around 10 dB (dB ref: 1 bar) higher than the other spectrum.

Unlike the first example in first operating condition, the differences between the pressure derivatives confirm the results of frequency spectrum. These findings show that, the effect of higher frequency oscillations are able to dominate the results from pressure derivatives. In conclusion, only checking the pressure derivatives may yield to undesired results which will point out a completely different direction instead of what should be. In order to avoid these kind of errors, filtering should be applied to emphasize the concern range, or directly frequency spectra must be investigated. In other words, compared to the radiated noise diagrams, analysis in frequency domain gives accurate results.

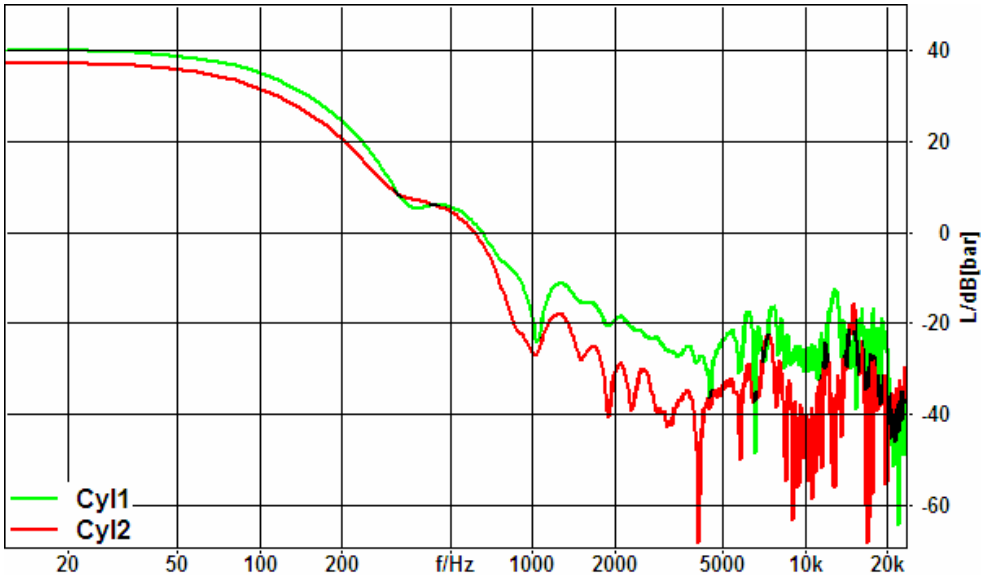

Figure 4.27: Combustion pressure spectrum for cylinder 1 and 2 at 2100rpm, %65 throttle position.

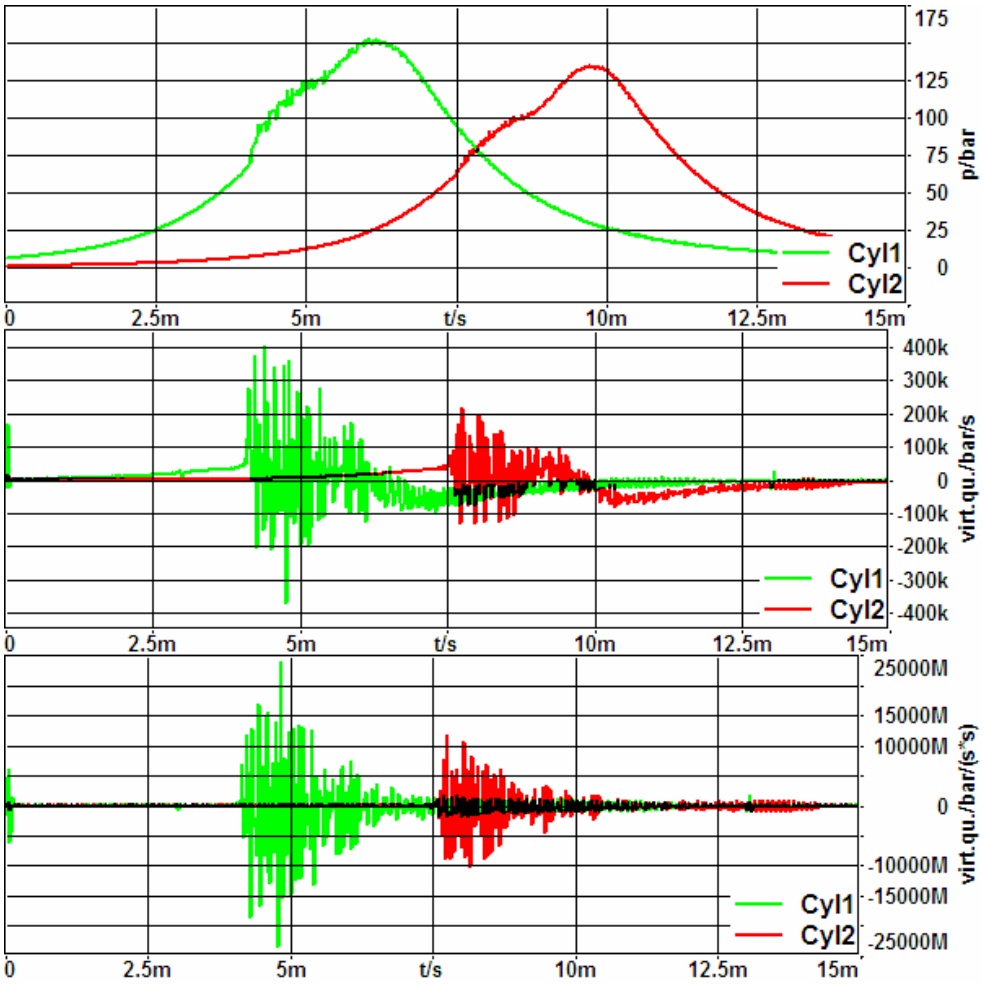

Figure 4.28: Comparing the level (upper diagram), first derivative (middle diagram) and second derivative (lower diagram) of combustion pressure in first and second cylinder without filter in the second operating condition.

4.3.4 Possible Root Causes of the Issue

The acquired data has been investigated so far indicates a different combustion pressure spectrum between the cylinders. It can be hard to define the root cause since numerous variables have an influence over the combustion process. Besides, not only one particular variable, but also a bunch of variables may result in this difference. Therefore a more detailed investigation is needed to have a direct conclusion for the root cause of the issue. A complete measurement setup should include the acquisition of inlet air temperature, wall temperature for each cylinder, electric signals for injectors, throttle position and crankshaft angle positioning sensor.

The difference between the cylinder spectrums can be mainly affected by three parameters: fuel injection, temperature and the air charge.

Fuel injection variances happen due to production variances between injectors and the pulsation in the rail pressure. In case of a failure in controlling these two variables, higher than expected fuel could be injected inside the chamber prior to the combustion, producing a higher excitation level over all the frequency range. A drop in injected fuel quantity can also be expected as well for the rail pressure pulsation.

Temperature variance can increase the ignition delay which produces a sharper combustion pressure rise. Therefore the colder charge air and/or chamber wall temperature will lead to a combustion process with sharper oscillations.

Unequal charge of intake air also creates variances between cylinders, since the rate of fresh air will change from cylinder-to-cylinder. The cylinder which is fed easier than the others will have more fresh air, and therefore combustions with higher amplitude will happen.

5. CONCLUSIONS AND DISCUSSION

Objective of this study was to identify diesel impulsiveness and its effect over interior sound quality. Further studies were focused on using frequency modulation analysis more comprehensive in a case study with a 5 cylinder engine and generating sound files to determine the root cause of the issue. In the following sections, the findings of artificial sound generation study has been correlated with the measurement of cylinder pressures simultaneously with the near-field microphones.

First step of the studies indicate that frequency modulation analysis is the most proper method for quantifying diesel impulsiveness. Other metrics fail to differentiate subjective differences between good and bad conditions. Moreover, frequency modulation analysis is also useful to make assumptions for finding the error state that may trigger the issue.

In the second step, the sound generation study is performed to utilize the frequency modulation analysis for determining the error state in the engine. For this reason, a basic simulink model is created, in which each cylinder parameters can be independently adjusted. In order to confirm the findings, real life cylinder pressure measurements have been performed.

Final step includes the confirmation of second step with the analysis of cylinder pressures and further examination of the acquired data. In conclusion, the higher excitation of first cylinder is pointed out as the root cause in the case study.

In this study, the opportunities with artificial sound generation is highlighted. The sound generation with an improved engine model will be a useful tool for engineers for checking possible error states in the noise source as it is in this case. Furthermore, in the design phase, implementation of calculated pressure traces into the model as an input will help to optimise the sound quality and radiated noise levels.

REFERENCES

Alt, N. Heuer, S. Thiele, S. Schwaderlapp M., 2004. Optimisation of Diesel Cold Start Noise, Ford NVH Conference 2004, İstanbul.

Aures, W., 1984. Berechnungsverfahren für den Wohlklang beliebiger Schallsignale, ein Beitrag zur Gehörbezogenen Schallanalyse, Dissertation am Lehrstuhl für Elektroakustik der Technischen Universität München, 1984

Badami, M. Mallamo, F. Millo, F. and Rossi, E.E., 2002. Influence of Multiple Injection Strategies on Emissions, Combustion Noise and BSFC of a DI Common Rail Diesel Engine, SAE 2002 World Congress, Detroit, Michigan, March 4-7.

Blommer, M. Otto, N. Wakefield, G. Feng, B. J. Jones, C., 1996. Calculating the Loudness of Impulsive Sounds, SAE Transactions 104/6, Pt2, pp. 2302-2308.

BS ISO 226, 2003. Acoustics - Normal Equal Loudness Level Contours.

Champagne, A.J. and Shiau, N., 1997. Commercial Van Diesel Idle Sound Quality, SAE 2002 World Congress, Detroit, Michigan, March 4-7.

Chiatti, G. and Chiavola, O., 2004. Combustion Induced Noise in Single Cylinder Diesel Engines, 2004 Small Engine Technology Conference, Graz, Austria, September 27-30.

Desantes, J.M. Torregrosa, A.J. Broatch, A., 2001. Wavelet Transform applied to Combustion Noise Analysis in High-speed DI Diesel Engines, SAE Paper 2001-01-1545.

Flaig, U. Polach, W. Ziegler, G., 1999. Common Rail System (CR-System) for Passenger Car DI Diesel Engines; Experiences with Applications for Series Production Projects, SAE Paper 1999-01-0191.

Fletcher, H. and Munson, W.A., 1933. Loudness, its definition, measurement and calculation, Journal of Acoustic Society America, **5**, 82-108.

Ford Internal Documents, 2005. NVH Awareness.

Gazon, M. and Blaisot, J., 2006. Cycle-to-cycle Fluctuations of Combustion Noise in a Diesel Engine at Low Speed, Powertrain & Fluid Systems Conference & Exhibition Toronto, Canada, October 16-19.

Gowindswamy, K. Tomazic, D., 2004. Diesel Engine Development for NVH, Ford NVH Conference, May 19.

Hashimoto, T. Hatano, S. Saito, H., 1995. Improvement of Sound Quality of Exterior Idling Noise of Small Diesel Truck, SAE Paper, 951289.

Hastings, A., 2004. Sound Quality of Diesel Engines, Ph.D. Thesis, Purdue University, West Lafayette, Indiana.

HEAD Artemis Documentation, 2006.

Heinrichs, R., 2004. Diesel Sound Quality; Getting Rid of Diesel Knocking, 4th FMC P/T NVH Sound Quality Symposium, Hiroshima.

Heinrichs, R., 2006. Ford Internal Report, Confidential.

Hussain, M. Golles, J. Ronacher, A. Schiffbanker, H., 1991. Statistical Evaluation of an Annoyance Index for Engine Noise Recordings, SAE Paper, 911080.

Ingham, R. Otto, N. McCollum, T., 1999. Sound Quality Metric for Diesel Engines, SAE Paper, 1999-01-1819.

Kinsler, L. E. Frey, A. R. Coppens, A.B. Sanders, J.V., 1982. The fundamentals of acoustics (Third Edition), John Wiley & Sons, New York.

Kondo, M. Kimura, S. Hirano, I. Uraki, Y. Maeda, R., 2000. Development of noise reduction technologies for a small direct-injection diesel engine. JSAE Review, **21**, 327-333.

Mallamo, F. Badami, M. Millo, F., 2002. Analysis of Multiple Injection Strategies for the Reduction of Emissions, Noise and BSFC of a DI CR Small Displacement Non-Road Diesel Engine, Powertrain & Fluid Systems Conference & Exhibition, San Diego, California, USA, October 21-24.

March, J. Strong, G. Gregory, S. Rediers, B., 2005. Achieving Diesel Vehicle Appeal Part 1: Vehicle NVH Perspective, SAE 2005 Noise and Vibration Conference and Exhibition, Traverse City, Michigan May 16-19.

March, J. Ward, A. Bennett, C. and Towalski, C., 2005. Achieving Diesel Vehicle Appeal Part 2: Powertrain NVH Perspective, SAE 2005 Noise and Vibration Conference and Exhibition, Traverse City, Michigan May 16-19.

Nyquist, H., 1928. Certain Topics in Telegraph Transmission Theory, Winter Convention of the A. I. E. E.,New York, NY, February 13–17, Transactions of the A. I. E. E., pp. 617–644.

Payri, F. Broatch, A. Serrano, J.R. Rodríguez, L.F. and Esmoris, A., 2006. Study of the Potential of Intake Air Heating in Automotive DI Diesel Engines, 2006 SAE World Congress, Detroit, Michigan, April 3-6.

Pharr, M. Humphreys, G., 2004. Physically Base Rendering, Morgan & Kaufman, New York.

Pickles, J.O., 1988. An Introduction to the Physiology of Hearing, Academic Press Inc., London.

Randall, R.B. and Tech, B., 1979. Frequency Analysis, 3rd Edition, Bruel and Kjaer, September 1979.

Randall, R.B. and Tech, B., 1987. Bruel and Kjaer Technical Reviews No.4, September.

Rioul, O. Vetterli, M., 1991. Wavelets and Signal Processing, IEEE SP Magazine, Vol. 8, No.4, pp. 510-590.

Russell, M.F. Haworth, R., 1985. Combustion Noise from High Speed Direct Injection Diesel Engines, SAE Paper, 850973.

Russell, M.F. Worley, S.A. Young C.D., 1987. Towards an Objective Estimate of the Subjective Reaction to Diesel Engine Noise, SAE Paper, 870958.

Russell, M.F. Greeves, G. and Guerrassi, N., 2000. More Torque, Less Emissions and Less Noise, SAE 2000 World Congress, Detroit, Michigan, March 6-9.

Scholl, D. and Blommer, M., 2005. Wavelet-Based Modification of Impulsive Sound Character and Application to Diesel Sound Quality, SAE 2005 Noise and Vibration Conference and Exhibition, Traverse City, Michigan, May 16-19.

Schiffbanker, H. Brandl, F.K. Thien, G.E., 1991. Development and Application of an Evaluation Technique to Assess the Subjective Character of Engine Noise, SAE Paper, 911081.

Shu, G. Wei, H. Liang, X., 2005. Experimental Study on Combustion Noise in Transient Conditions of DI-Diesel Engine, SAE 2005 Noise and Vibration Conference and Exhibition Traverse City, Michigan, May 16-19.

Shu, G. Wei, H. Wang, Y. Yang, Z and Wei, J., 2006. Secondary Influence Factors of Combustion Noise Mechanism under Transient Conditions of DI-

Diesel Engine, 2006 SAE World Congress, Detroit, Michigan, April 3-6.

Villarroel, G.Z. and Agren, A., 1997. Wavelet Transform Analysis of Measurements of Engine Combustion Noise, SAE Paper, 972003.

Wikipedia Encyclopedia, http://en.wikipedia.org, 11.03.2007.

Yajima, Y. Nakashima, K., 1997. New measuring technique of cylinder pressure spectrum and its application to combustion noise reduction Time-frequency analysis of combustion excitation using wavelet transform analysis, Technical Notes, JSAE Review **19,** 277- 282.

Zwicker, E. and Fastl, H., 1990. Psychoacoustics, Springer-Verlag, Berlin, 1990.

Zwicker, E. and Fastl, H., 1999. Psychoacoustics: Facts and Models, Springer series in information sciences, 22. Springer, Berlin; New York.

APPENDICES

APPENDIX A: Frequency Modulation Analysis of Sound Generation Iterations

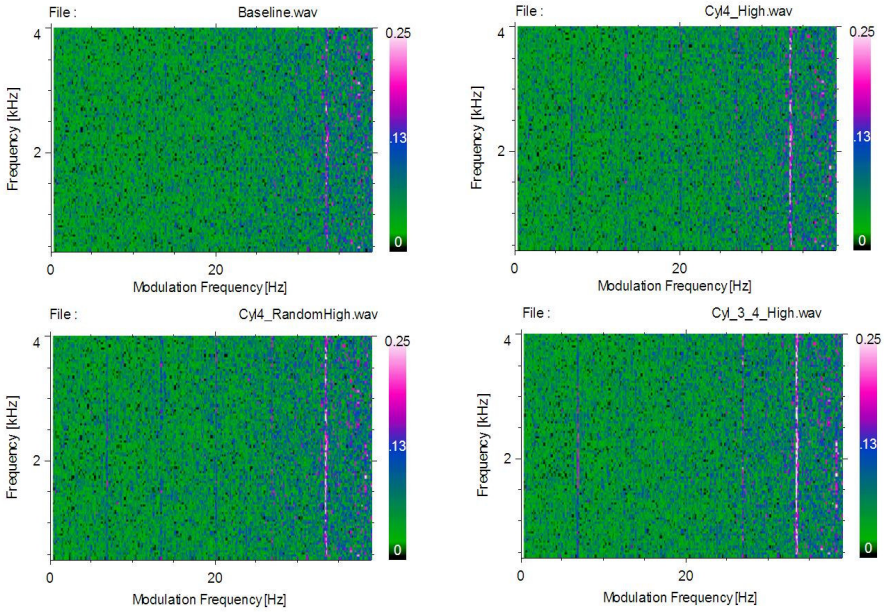

Frequency modulation analysis plots of 1st – 4th iterations

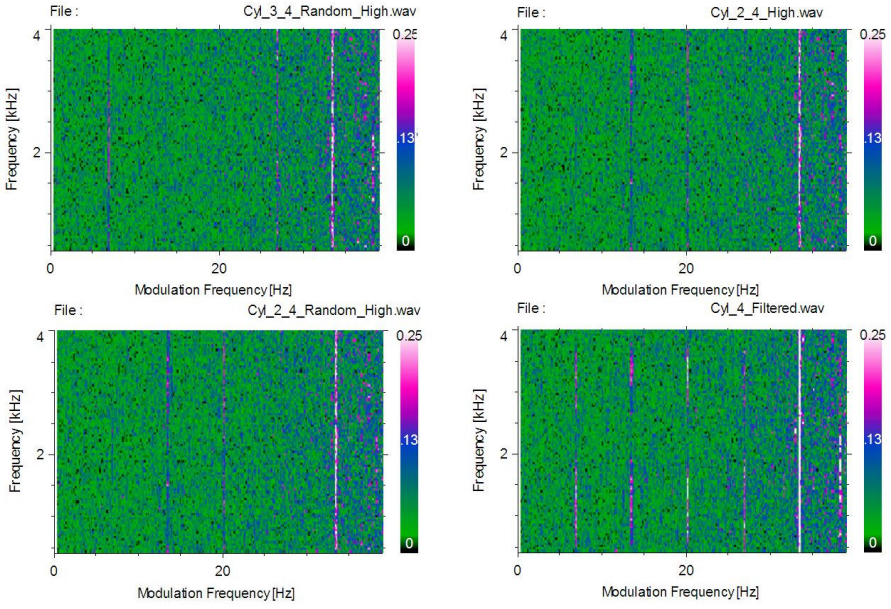

Frequency modulation analysis of 5th – 8th iterations

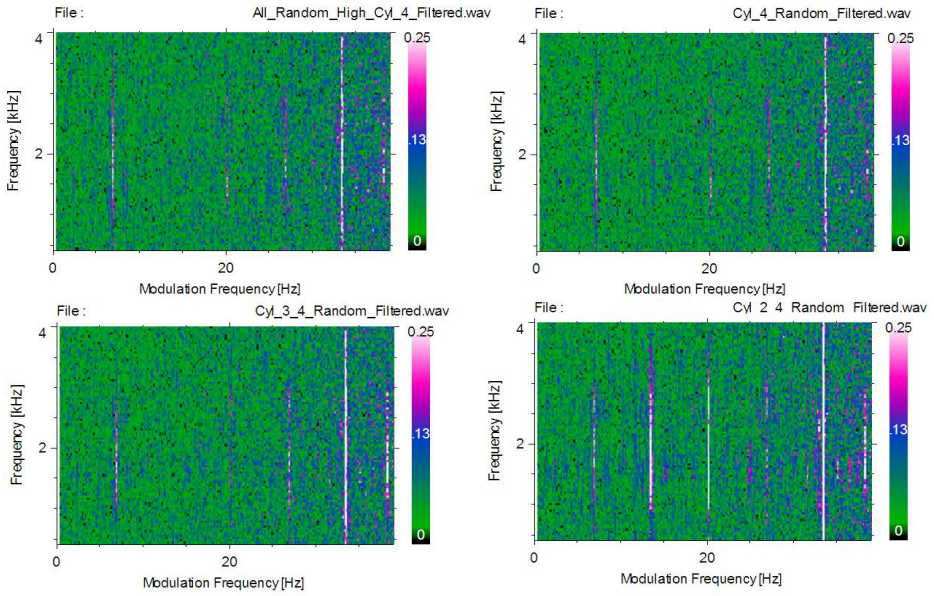

Frequency modulation analysis of 9th – 12th iterations

APPENDIX B: Test Equipment and Instrumentation

Specifications of the measurement equipment and instrumentation of the vehicle is briefly explained.

B.1 Pressure Sensors

Specifications of pressure sensors and instrumentation sketch is shown in this part.

Table B.1 : Specifications of GU12P Type Pressure Sensors

Standard Specifications	
Measuring Range	0...200 bar
Lifetime	> 10^8 load changes
Overload	250 bar
Sensitivity (nominal)	15 pC/bar
Linearity	<±0.3% FSO
Natural Frequency	130 kHz
Acceleration Sensitivity	<0.001 bar/g
Shock Resistance	>2000 g
Operating Temperature Range	up to 400°C
Thermal Sensitivity Shift	20..400°C <±2% 200...300°C <±5%
Insulation Resistance at 20C	>10^{13} Ω
Capacitance	7 pF
Mass (without cable)	5 grammes
Mounting Torque	1.5 Nm
Thermodynamic Specifications	
Cyclic Temperature Drift	< ± 0.6 bar
Load Change Drift Max. Zero-line Deviation	1.5 mbar/ms
IMEP-Stability	< 3%

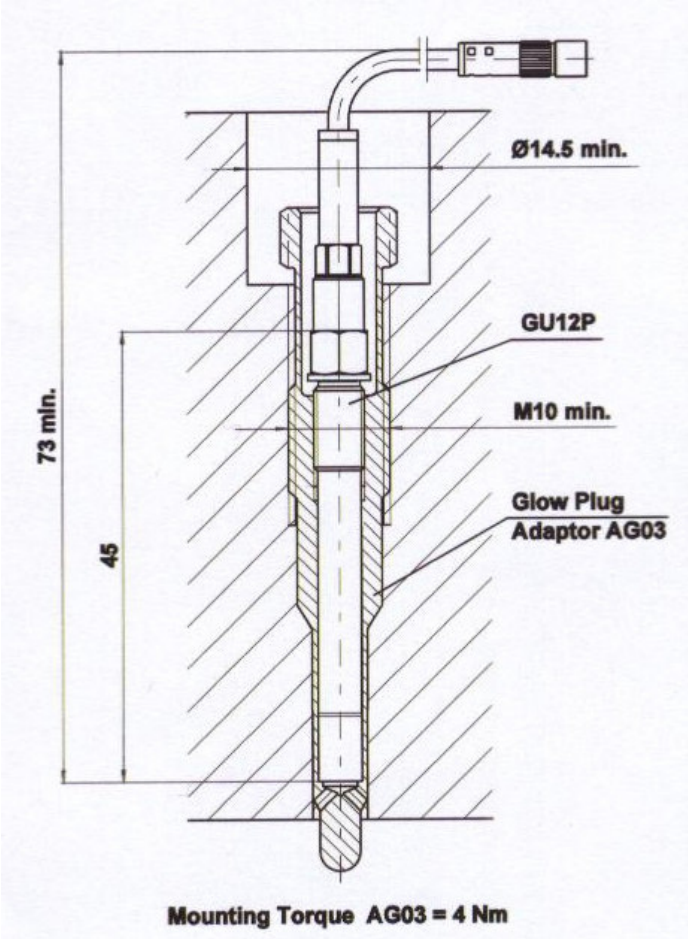

Figure B.1 : Installation of Pressure Sensor by means of glow plug adapter.

B.2 Microphone Specifications

Specifications of B&K type 4189 and 4190 microphones are presented below.

Table B.2 : Specifications of B&K Type 4189 Microphones

OPEN-CIRCUIT SENSITIVITY (250 Hz):
−26 dB ±1.5 dB re 1 V/Pa, 50 mV/Pa*
POLARIZATION VOLTAGE (external): 0 V
FREQUENCY RESPONSE*:
0° incidence free-field response:
±1 dB, 10 Hz to 8 kHz
±2 dB, 6.3 Hz to 20 kHz
In accordance with IEC 651, Type 1
LOWER LIMITING FREQUENCY (−3 dB):
2 Hz to 4 Hz (vent exposed to sound)
PRESSURE EQUALIZATION VENT:
Rear vented
DIAPHRAGM RESONANCE FREQUENCY:
14 kHz (90° phase shift)
CAPACITANCE (POLARIZED, 250 Hz): 14 pF
EQUIVALENT AIR VOLUME (101.3 kPa):
46 mm^3
CALIBRATOR LOAD VOLUME (250 Hz):
260 mm^3
PISTONPHONE TYPE 4228 CORRECTION (with DP 0776): 0.00 dB
CARTRIDGE THERMAL NOISE:
14.6 dB (A), 15.3 dB (Lin.)

* Individually calibrated

UPPER LIMIT OF DYNAMIC RANGE (3% distortion): >146 dB SPL
MAXIMUM SOUND PRESSURE LEVEL:
158 dB (peak)

Environmental

OPERATING TEMPERATURE RANGE:
−30 to +150 °C (−22 to 302 °F)
OPERATING HUMIDITY RANGE:
0 to 100 % RH (without condensation)
STORAGE TEMPERATURE:
−30 to +70 °C (−22 to 158 °F)
Data Disk: 5 to 50 °C (41 to +122 °F)
TEMPERATURE COEFFICIENT (250 Hz):
−0.001 dB/°C (for the range −10 to +50 °C (14 to 122 °F))
PRESSURE COEFFICIENT (250 Hz):
−0.010 dB/kPa
INFLUENCE OF HUMIDITY:
<0.1 dB/100 %RH
VIBRATION SENSITIVITY (<1000 Hz):
62.5 dB equivalent SPL for 1 m/s^2 axial acceleration

MAGNETIC FIELD SENSITIVITY:
6 dB SPL for 80 A/m, 50 Hz field
ESTIMATED LONG-TERM STABILITY:
>1000 years/dB (dry air at 20 °C (68 °F))
>2 hours/dB (dry air at 150 °C (302 °F))
>40 years/dB (air at 20 °C (68 °F), 90% RH)
>1 year/dB (air at 50 °C (122 °F), 90% RH)

Dimensions

Diameter: 13.2 mm (0.52″) (with grid)
12.7 mm (0.50″) (without grid)
Height: 17.6 mm (0.69″) (with grid)
16.3 mm (0.64″) (without grid)
Thread for preamplifier mounting:
11.7 mm – 60 UNS

Note: All values are typical at 23 °C (73.4 °F) 101.3 kPa and 50% RH, unless measurement uncertainty or tolerance field is specified. All uncertainty values are specified at 2σ (i.e. expanded uncertainty using a coverage factor of 2)

Table B.3 : Specifications of B&K Type 4190 Microphones

OPEN-CIRCUIT SENSITIVITY (250 Hz):
−26 dB ±1.5 dB re 1 V/Pa, 50 mV/Pa*
POLARIZATION VOLTAGE (external): 200 V
FREQUENCY RESPONSE*:
0° incidence free-field response:
±1 dB, 5 Hz to 10 kHz
±2 dB, 3.15 Hz to 20 kHz
In accordance with IEC 651, Type 0 and Type 1
LOWER LIMITING FREQUENCY (−3 dB):
1 Hz to 2 Hz (vent exposed to sound)
PRESSURE EQUALIZATION VENT:
Rear vented
DIAPHRAGM RESONANCE FREQUENCY:
14 kHz (90° phase shift)
CAPACITANCE (POLARIZED, 250 Hz)*: 16 pF
EQUIVALENT AIR VOLUME (101.3 kPa):
46 mm^3
CALIBRATOR LOAD VOLUME (250 Hz):
250 mm^3
PISTONPHONE TYPE 4228 CORRECTION (with DP 0776): 0.00 dB

* Individually calibrated

CARTRIDGE THERMAL NOISE:
14.6 dB (A), 15.3 dB (Lin.)
UPPER LIMIT OF DYNAMIC RANGE (3% distortion): >148 dB SPL
MAXIMUM SOUND PRESSURE LEVEL:
159 dB (peak)

Environmental

OPERATING TEMPERATURE RANGE:
−30 to +150 °C (−22 to +302 °F)
OPERATING HUMIDITY RANGE:
0 to 100 % RH (without condensation)
STORAGE TEMPERATURE:
−30 to +70 °C (−22 to 158 °F)
Data Disk: 5 to 50 °C (41 to +122 °F)
TEMPERATURE COEFFICIENT (250 Hz):
−0.007 dB/°C (for the range −10 to +50 °C (14 to 122 °F))
PRESSURE COEFFICIENT (250 Hz):
−0.010 dB/kPa
INFLUENCE OF HUMIDITY:
<0.1 dB/ 100 % RH

VIBRATION SENSITIVITY (<1000 Hz):
62.5 dB equivalent SPL for 1 m/s^2 axial acceleration
MAGNETIC FIELD SENSITIVITY:
4 dB SPL for 80 A/m, 50 Hz field
ESTIMATED LONG-TERM STABILITY:
>1000 years/dB at 20 °C (68 °F)
>100 hours/dB at 150 °C (302 °F)

Dimensions

Diameter: 13.2 mm (0.52″) (with grid)
12.7 mm (0.50″) (without grid)
Height: 17.6 mm (0.69″) (with grid)
16.3 mm (0.64″) (without grid)
Thread for preamplifier mounting:
11.7 mm – 60 UNS

Note: All values are typical at 23 °C (73.4 °F) 101.3 kPa and 50% RH, unless measurement uncertainty or tolerance field is specified. All uncertainty values are specified at 2σ (i.e. expanded uncertainty using a coverage factor of 2)

B.3 Artificial HEAD HMS III Specifications

Specification of HEAD Acoustics Artificial Head HMS III is presented below.

Table B.4 : Specification of HEAD Acoustics Artificial Head HMS III

Technical data - HMS III.L	
Measurement unit	
Transmission range:	20 Hz - 20 kHz: ±0.1 dB; 3 Hz - 20 kHz: -3 dB/+0.1 dB
Dynamic range (linear):	96 dB
Cross-talk attenuation:	>96 dB
Sum of harmonic equalization and noise component (THD+N)	
at 124 dB:	250 Hz: <0.008% 1 kHz: <0.007% 5 kHz: <0.009%
Inherent noise:	15 dB $(A)_{SPL}$, typ.
Nom. SPL (selectable):	94 dB_{SPL}, 104 dB_{SPL}, 114 dB_{SPL}, 124 dB_{SPL}
Headroom (electr.):	6 dB
Max. SPL:	124 dB_{SPL} (+6 dB Headroom)
Equalization modes:	linear (Lin), independent-of-direction (ID), free-field (FF), diffuse-field (DF), user-defined (USER)
Directional pattern:	corresponds to the structurally averaged directional pattern of the human outer ear to IEC 959
Analog component	
Microphone:	½″ electrostatic microphone, 200 V polarization voltage
Filters:	highpass 1st order 180 Hz (10 %), passive highpass 5th order 22 Hz (10 %), active
Digital component	
Signal processor:	Motorola DSP56309 (100 Mips)
A/D converter:	128-times oversampling
Sampling rate:	Internal 44.1 kHz, 48 kHz; externally synchronizable via AES/EBU signal 32 kHz, 44.1 kHz, 48 kHz
Data format:	AES/EBU, IEC II-Subcode adjustable. 16-bit format with noise shaping selectable
Power supply (no-break, switching between external and internal supply, incl. "smart charge" electronics)	
External power supply unit - PSH I.1	
Input voltage:	100 V - 240 V AC 47 Hz - 63 Hz
Max. input current:	1.6 A at 100 V AC
Output voltage/current:	15 V DC, 4 A
DC output:	XLR 4-pin
External DC supply:	12 V DC (9 V - 34 V e.g. vehicle circuit or power pack)
Internal DC-supply:	Rechargeable battery NiMH, 12 V, 2 Ah
Charging procedure:	Fast charge (max. 3 h), conservation charge
Op. time w. rechargeable battery:	typ. 3 h (without Remote Control RC V)
Current, Power:	Charging and operating: 2 A / 24 W
Operation:	Remote control software HUS I.1 or as option Remote Control RC V
Interfaces	
Digital I/O:	2 × AES/EBU, XLR 3-pin
RS 232:	D-SUB 9-pin
DC input:	1 × XLR 4-pin
Analog out:	Multifunction
Nominal output level:	1 V_{eff} + 6 dB headroom
Inherent noise:	90 dB under output level
Environmental conditions	
Operating temperature range:	0°C - 50°C, 32°F - 122°F
In-store temperature range:	-20°C - 70°C, -4°F - 158°F
Housing (Head-and-shoulder unit)	
Overall dimensions (WxHxD):	465 mm x 400 mm x 180 mm
Weight:	5.6 kg
Tripod socket:	UNC 3/8

AUTOBIOGRAPHY

Caner SEVGİNER was born in Bursa in 1981. He received is primary degree from Atatürk Primary School (1987-1992); and high school degree from Bursa Anatolian High School (1992-1999). He started his B.Sc. education at the Mechanical Engineering Department of the Istanbul Technical University in 1999. After receiving his B.Sc. degree in 2003; he has started his M.Sc. education at the Automotive Engineering Programme of the Mechanical Engineering Department in Istanbul Technical University. Since 2004, Sevginer has also been working in Ford – Otosan A.S. Product Development Department as an NVH Engineer.